**“The role of the glycoside hydrolase Ega3 in the biology of *Aspergillus fumigatus*”**

Caitlin Zacharias
Department of Microbiology and Immunology
McGill University, Montréal, Canada
August 2022

A thesis submitted to McGill University in partial fulfillment of the requirements of the degree of Doctor of Philosophy

## Abstract

*Aspergillus fumigatus* is a ubiquitous environmental mold. When conidia of *A. fumigatus* are inhaled by immunosuppressed individuals they can germinate to form filamentous hyphae that invade lung tissue to cause a necrotizing pneumonia which is associated with a high mortality rate. One of the major virulence factors of *A. fumigatus* is the production of the secreted cationic exopolysaccharide galactosaminogalactan (GAG), which is essential for biofilm formation. GAG is predicted to be synthesized by the products of a five gene cluster, one of which, *ega3*, is predicted to encode a glycoside hydrolase anchored to the cell membrane of *A. fumigatus*.

Through mass spectrometry studies, we established that Ega3 cleaves mature deacetylated GAG. We hypothesized that like the other proteins in the cluster, Ega3 is necessary for GAG synthesis. To test this hypothesis, we sought to disrupt the *ega3* by allele replacement with a drug resistance marker and characterize the phenotype of the resulting *ega3* null mutant. Initial attempts to disrupt *ega3* by our usual approach were unsuccessful but two *ega3* null mutants were finally recovered, one using CRISPR/Cas9 and another using the conventional split marker protocol. Like other mutants in the GAG cluster, these mutants were deficient in biofilm formation and did not produce deacetylated GAG. Surprisingly, complementation with an *ega3* allele failed to restore biofilm formation in both strains, despite restoration of Ega3 protein production as demonstrated by Western blot. These findings were consistent with the presence of a secondary mutation impairing GAG production. Analysis of the expression of the GAG cluster genes revealed that *agd3*, encoding the GAG deacetylase required for the production of mature, cationic GAG, was not expressed in the Δ*ega3*$^{\text{CRISPR}}$ mutant. Genome sequencing revealed that *uge3*, required for GAG production, was mutated in the other *ega3* null mutant. Since we were only able to disrupt *ega3* in the absence of the production of cationic GAG, we hypothesized that *ega3* is conditionally essential in the presence of cationic GAG. To test this hypothesis, *agd3* was expressed in the Δ*ega3*$^{\text{CRISPR}}$ mutant under the control of a tetracycline-inducible promoter (Δ*ega3*$^{\text{CRISPR}}$::*agd3*$^{\text{Tet on}}$). Under *agd3*-expressing conditions, GAG production was restored but fungal growth was inhibited.

Since GAG is a large cationic polymer and Ega3 cleaves cationic GAG, we hypothesized that cationic GAG may be toxic to the cell membrane of *A. fumigatus* and that membrane-bound Ega3 degrades GAG near the membrane. To test whether cationic GAG induces damage to the cell membrane in the absence of Ega3, ATP was measured in fungal culture supernatants as a proxy for cell leakage. Induction of *agd3* expression in the Δ*ega3*$^{\text{CRISPR}}$::*agd3*$^{\text{Tet on}}$ mutant resulted in the release of high levels of ATP suggesting that cationic GAG disrupts the cell membrane of *A. fumigatus*. We therefore hypothesized that secreted GAG may also mediate host cell injury during infection. To test this hypothesis, A549 pulmonary epithelial cells were loaded with radioactive chromium and exposed to culture supernatants from wild-

type *A. fumigatus* +/- Ega3. Exposure to GAG-containing culture supernatants (CS) induced epithelial cell injury, but cells were almost completely protected from damage in the presence of Ega3. Propidium iodide (PI) staining of BMDMs exposed to CS mirrored these results, as did PI/annexin V staining of human NK cells. Using MALDI-TOF MS, wild-type but not deacetylase-deficient (Δ*agd3*) CS were also shown to induce inflammation in mouse lungs. Finally, the Δ*agd3* mutant also exhibited a reduced ability to escape mouse alveolar macrophages as compared to the wild-type fungus. These data suggest that cationic GAG has membrane destabilizing effects in both fungal and host cells and that a major function of Ega3 is to protect fungal cells from the toxic effects of GAG.

## Résumé

*Aspergillus fumigatus* est un champignon omniprésent dans notre environnement. Lorsque des conidies de ce champignon sont inhalés par des individus immunosupprimés, celles-ci germent dans le parenchyme pulmonaire qu'elles envahissent provoquant des pneumonies nécrosantes léthales. L'un des facteurs de virulence principaux d'*A. fumigatus* est la production d'un exopolysaccharide cationique appelé galactosaminogalactan (GAG), un polymère nécessaire à la formation de son biofilm. La synthèse de GAG est prédite par l'activité d'un cluster de cinq gènes, dont l'un, *ega3*, est supposé être responsable de la production d'une glycoside hydrolase ancrée à la membrane plasmique d'*A. fumigatus*.

Des études en spectrométrie de masse ont établi qu'Ega3 dégrade uniquement les sections déacétylées de GAG. Nous avons émis l'hypothèse que tout comme les autres protéines du cluster, Ega3 serait nécessaire à la synthèse de GAG. Afin de vérifier cette hypothèse, nous avons tenté de remplacer *ega3* par un marqueur de résistance antimicrobien, et caractérisé le phénotype du mutant résistant. Les premiers essais visant la délétion d'*ega3* par les approches génétiques conventionnelles ont été infructueuse. Cependant, deux mutants null d'*ega3* ont été obtenu en utilisant pour l'un CRISPR/Cas9 et pour le second l'approche dit de marqueur fractionné. Tout comme pour les autres mutants null du cluster GAG, ces deux mutants sont incapables de former des biofilms, et ne produisent pas de GAG déacétylé. Étonnamment, la complémentation de ces mutants avec un allèle *ega3* n'a pas permis la restauration du biofilm malgré l'expression démontrée d'Ega3 par Western blot. Cette découverte est consistante avec la présence de mutations secondaires impactant la production de GAG. Dans le mutant CRISPR, Δ*ega3*$^{\text{CRISPR}}$, l'analyse de l'expression du cluster de gènes a révélé qu'*agd3*, encodant une déacétylase requise pour la production GAG cationique, n'était pas exprimé. Quant au second mutant, le séquençage du génome a révélé la présence d'une mutation critique d'*uge3*, gène codant pour une épimérase requise pour la production de GAG. Étant donné que la délétion d'*ega3* semble impossible en présence d'un GAG déacétylé, nous avons émis l'hypothèse qu'*ega3* est conditionnellement essentiel en présence de ce polymère. Afin de tester cette hypothèse, *agd3* a été exprimé dans le mutant Δ*ega3*$^{\text{CRISPR}}$ sous contrôle d'un promoteur induit par la tétracycline (Δ*ega3*$^{\text{CRISPR}}$::*agd3*$^{\text{Tet on}}$). Lors de l'expression d'*agd3* chez ce mutant, la production de GAG a été restauré mais la croissance fongique a été inhibé.

Considérant que GAG est un large polymère cationique et qu'Ega3 a été montré capable de dégrader ce polymère, nous avons émis l'hypothèse que GAG puisse perturber l'intégrité de la membrane plasmique d'*A. fumigatus* et qu'Ega3 préviendrait cette toxicité en dégradant GAG près de la membrane. Afin de tester cette hypothèse, l'intégrité cellulaire d'*A. fumigatus* a été évalué via la mesure d'ATP extracellulaire dans les surnageants de culture. En réponse à l'induction de l'expression d'*agd3* dans Δ*ega3*$^{\text{CRISPR}}$::*agd3*$^{\text{Tet on}}$, un fort taux d'ATP a été retrouvé dans le milieu suggérant que le déacétylation de

GAG par Agd3 a compromis l'intégrité des membranes fongiques. Par conséquent, nous avons émis l'hypothèse que GAG puisse endommager les cellules hôtes pendant une infection. La validité de cette hypothèse a été évalué en exposant des cellules épithéliales pulmonaires A549 chargées de chromium radioactif à des surnageants de culture d'*A. fumigatus* sauvages +/- Ega3. Des dommages cellulaires ont pu être ainsi démontré uniquement suite à l'exposition des cellules au surnageant de culture avec GAG en l'absence d'Ega3. Des résultats similaires ont été obtenus en utilisant des cellules BMDMs marqués à l'iodure de propidium, et des cellules NK marquées à l'iodure de propidium et annexine V. De plus, en utilisant l'imagerie par spectrométrie de masse MALDI-TOF MS nous avons démontré que seuls des surnageants de culture de champignon sauvage ont été capable d'induire de l'inflammation. L'injection ex vivo de surnageant de culture contenant uniquement du GAG acétylé provenant de Δ*agd3* n'a pas permis cette observation. Finalement, les hyphes du mutant Δ*agd3* ont aussi démontré une capacité restreinte d'évasion des macrophages alvéolaires comparativement aux hyphes sauvages. Ces données suggèrent que le GAG cationique déstabilise les membranes cellulaires et qu'Ega3 joue en rôle critique dans la protection des cellules fongiques produisant ce GAG toxique.

**Table of Contents**

**Acknowledgements**

First and foremost, I have to thank my supervisor, Dr. Don Sheppard, for all the guidance throughout my project and for making me into the scientist I am today. I'm sure it wasn't easy, but I'm very grateful for the time you put in. Thank you for giving a project that taught me patience, perseverance, and resiliency. I also have to thank the members of the Sheppard lab, particularly Dr. Fabrice Gravelat, for teaching me all you knew about molecular biology and caffeinating with me every morning, and Dr. François Le Mauff for translating my abstract. A special thanks also goes out to my advisory committee members, Dr. Samantha Gruenheid and Dr. Arnold Kristof, for all the valuable advice throughout my project.

My family has also supported me in so many ways during my PhD. I am eternally grateful to my parents, Darryl and Cindy Zacharias, who always knew I could do it. I also have to thank the family I made along the way: my husband David, who never stopped believing in me. Even at my lowest points you helped me dust myself off and get back up. You also gave me the best gift imaginable, our little girl Jacqueline, who always keeps me on my toes and provides some comic relief (and practice with staying awake at all hours, which I needed to write this thesis).

Last but not least are my friends in no particular order: Brittany, Yukiko, Valerie, Marija and Ben (who also proofread this thesis, so double thank you!), who were always there to lend an ear or grab a drink (usually both). You made this long road a hell of a lot more fun to walk and made Montréal feel like home.

## Contributions to Original Knowledge

Chapters 3 and 4 contribute significantly to knowledge on the biology of the important virulence factor galactosaminogalactan (GAG) of *Aspergillus fumigatus.* The following key results are presented in this thesis:

1. Unlike the other 4 genes in the GAG biosynthetic cluster, Ega3 is dispensable for the synthesis of GAG and biofilm formation
    a. Deletion of *ega3* had no effect on the production of fully acetylated GAG, as evidenced in the Δ*ega3*$^{CRISPR}$ strain
    b. Supplementation of the Δ*ega3*$^{CRISPR}$ mutant with recombinant Agd3 results in deacetylation of the GAG produced by this strain and allows it to form an adherent biofilm
2. Ega3 is conditionally essential in the presence of deacetylated GAG
    a. Both *ega3* null mutants produced in this study had secondary mutations in other GAG cluster genes that prevented production of deacetylated GAG
    b. Regenerating protoplasts of the Δ*ega3*$^{CRISPR}$::*agd3*$^{Tet\ on}$ mutant were able to silence *agd3* transcription despite the presence of doxycycline in the medium
3. Ega3 protects *A. fumigatus* from membrane damage by deacetylated GAG
    a. Induction of *agd3* transcription in the Δ*ega3*$^{CRISPR}$::*agd3*$^{Tet\ on}$ mutant results in increased membrane permeability, particularly in the presence of osmotic stress
    b. Conditions where GAG is secreted away from the hyphae of *A. fumigatus* result in less inhibition of growth of the fungus
4. Deacetylated, but not fully acetylated GAG is toxic to mammalian cells and induces expression of inflammation markers in murine lung tissue
    a. Deacetylated GAG induces membrane damage in immortalized human A549 epithelial cells and murine bone marrow derived macrophages
    b. Deacetylated GAG induces apoptosis in primary human natural killer cells
    c. A novel technique, MALDI-MS imaging, was used to detect markers of inflammation in murine lung tissue treated with deacetylated/fully acetylated GAG
5. Deacetylated GAG enhances escape from macrophage phagolysosomes

## Contributions of Authors

This doctoral thesis was prepared in accordance with the guidelines stated in the McGill University "Guidelines for Thesis Preparations". The work of this thesis is presented in the "traditional monograph" format. All the studies have been performed under the co-supervision of Dr. Donald Sheppard. The detailed contributions of each author are listed below in order of mention and designated by their initials:

Caitlin Zacharias, Dr. Donald Sheppard, Dr. Natalie Bamford, Dr. Francois Le Mauff, Ira Lacdao, Dr. Alonso Lira, Laura Montermini, Jeannie Mui, Lorne Taylor, Hong Liu, Dr. Fabrice Gravelat, Dr. Ken Dewar, Matthew D'Iorio, Andreea Gheorghita, Marija Landekic, Linda Heilig, Felix Girolamo-Cousineau, Thi-Thuyet Mai Nguyen and Nidia Lauzon.

**Chapter 1: Literature review:**
CZ wrote and DS edited the literature review.

**Chapter 2: Functional characterization of Ega3.**
CZ and NB (laboratory of Dr. P. Lynne Howell, University of Toronto) performed bioinformatic studies. NB performed protein modeling and crystallization studies. CZ performed biofilm inhibition and disruption assays. FLM performed MALDI-TOF fingerprinting. CZ performed microscopic localization of Ega3 and FLM/IL performed membrane fractionation studies. CZ developed the protocol for EV isolation in collaboration with AL from Dr. Martin Olivier's lab. CZ performed EV isolation and characterization by Nanosight (with the help of LM from Dr. Janusz Rak's lab) and TEM (assisted by JM at FEMR McGill) and protein identification was done at the Proteomics Core of the RI-MUHC. CZ performed the data analysis on the MS-MS data from the EV samples. CZ wrote and DS edited the chapter.

**Chapter 3: Construction and characterization of an *ega3* null mutant strain.**
HL from the lab of Dr. Scott Filler (UCLA) constructed the Δ*ega3*$^{CRISPR}$ strain. FG constructed the Δ*ega3*$^{Ku80}$ and Δ*ega3*::*ega3*$^{CRISPR}$ strains. CZ constructed the Δ*ega3*::*ega3*$^{Ku80}$ and Δ*ega3*$^{Ku80}$::*ega3*$^{Tet\ on}$ strains. CZ performed all qRT-PCRs. CZ performed all biofilm and deacetylated GAG capture assays. CZ performed derivation of culture supernatant monosaccharides under the guidance of FLM for analysis by gas chromatography. FLM ran the gas chromatography. FLM and CZ analyzed gas chromatography data. CZ performed SBA-staining. CZ performed confocal imaging assisted by SF at the Molecular Imaging Platform at the RI-MUHC. CZ performed all image processing. CZ extracted ultra-high molecular weight

DNA for whole genome sequencing of the Δ*ega3*$^{Ku80}$ strain, which was done at Genome Quebec in collaboration with KD and MD, who did the data analysis. CZ did the sample preparation for Sanger Sequencing, also done at Genome Quebec. AG from Dr. P. Lynne Howell's lab performed the protein modeling of Uge3 from the Δ*ega3*$^{Ku80}$ strain. CZ wrote and DS edited the chapter.

**Chapter 4: Galactosaminogalactan is a cytotoxic molecule.**

CZ constructed the Δ*ega3*$^{CRISPR}$::*agd3*$^{Tet\ on}$ strain and performed all of the characterization. (qRT-PCR, biofilm assays, deacetylated GAG capture) . CZ ran growth curve time courses. CZ performed all staining for confocal microscopy as well as imaging at the Molecular Imaging Platform. CZ performed all image processing. CZ performed the protoplast-doxycycline selective pressure assay and high salt tolerance assays. CZ performed ATP release assays.CZ produced the culture supernatants used for all experiments. HL performed chromium release assays. CZ performed isolation, culture and propidium iodide staining of BMDMs under instruction by ML from Dr. Donald Vinh's lab. LH from Dr. Juergen Loeffler's laboratory (University Hospital Wuerzburg) performed NK and T cell assays, staining and flow cytometry. FLM , FGC and CZ performed MALDI-MS imaging sample preparation assisted by TTMN who performed the mouse experiments and NL at the Drug Discovery Platform at the RI-MUHC who cryosectioned the samples. NL performed the MALDI-MS imaging and pixel quantification. TTMN performed the mouse infection and CZ performed the BCA assay for the BAL protein concentration study. CZ wrote and DS edited the chapter.

**Chapter 5: Materials and methods.**

CZ wrote the methods except for the sections done by LT (EV proteomics), HL (making of the Δ*ega3*$^{CRISPR}$ strain), AG (identification of Uge3 mutation in the Δ*ega3*$^{Ku80}$ strain) and LH (NK and T cell isolation and subsequent assays). DS edited the chapter.

**Chapter 6: General discussion**

CZ wrote and DS edited the chapter.

## Academic honesty statement

I, Caitlin Zacharias, affirm that the work in this thesis upholds the ethics standards of McGill University and that any work not done by me has been credited as appropriate.

## List of Abbreviations

| | |
|---|---|
| ABCD | Amphotericin B colloidal dispersion |
| ABPA | Allergic bronchopulmonary aspergillosis |
| ABLC | Amphotericin B lipid complex |
| AGS | α-1,3-glucan synthase |
| AmB | Amphotericin B |
| AMP | Antimicrobial peptide |
| ATP | Adenine triphosphate |
| ATPase | Adenine triphosphatase |
| BCA | Bicinchoninic acid |
| BMDM | Bone marrow derived macrophage |
| CCPA | Chronic cavitary pulmonary aspergillosis |
| CD | Cluster of differentiation |
| CFPA | Chronic fibrosing pulmonary aspergillosis |
| CLR | C-type lectin receptor |
| CPA | Chronic pulmonary aspergillosis |
| CRISPR | Clustered regularly interspaced short palindromic repeats |
| CT | Computed tomography |
| CXCL | Chemokine ligand |
| D-AmB | Amphotericin B deoxycholate |
| DC | Dendritic cell |
| DC-SIGN | DC-specific ICAM 3-grabbing nonintegrin |
| DHN | Dihydroxynaphthalene |
| DNA | Deoxyribonucleic acid |
| Dox | Doxycycline |
| ESCRT | Endosomal sorting complexes required for transport |
| EV | Extracellular vesicle |
| FITC | Fluorescein isothiocyanate |
| GAG | Galactosaminogalactan |
| Gal | Galactose |

| | |
|---|---|
| Gal*f* | Galactofuranose |
| GalN | Galactosamine |
| GalNAC | *N*-acetyl galactosamine |
| GC-MS | Gas chromatography-mass spectrometry |
| G-CSF | Granulocyte-colony stimulating factor |
| GDP | Guanosine diphosphate |
| GEL | Glucanosyltransferase |
| GFP | Green fluorescent protein |
| GH | Glycoside hydrolase |
| GM | Galactomannan |
| GM-CSF | Granulocyte macrophage-colony stimulating factor |
| GXM | Glucuronoxylomannan |
| HRP | Horseradish peroxidase |
| HSP | Heat shock protein |
| IA | Invasive aspergillosis |
| IFN | Interferon |
| IgE | Immunoglobulin E |
| IL | Interleukin |
| IL1-Ra | Interleukin 1 receptor antagonist |
| IPC | Inositolphosphoceramide |
| I-TASSER | Iterative threading assembly refinement |
| L-AMB | Liposomal amphotericin B |
| MALDI-TOF | Matrix assisted laser desorption/ionization-time of flight |
| MASP | MBL-associated serine protease |
| MBL | Mannose binding lectin |
| MDDC | Monocyte-derived dendritic cell |
| MelLec | Melanin-sensing C-type lectin receptor |
| MetAP2 | Methionine aminopeptidase |
| MS | Mass spectrometry |
| MS-MS | Tandem mass spectrometry |
| NADPH | Nicotinamide adenine dinucleotide phophate |
| NETs | Neutrophil extracellular traps |
| NF-KB | Nuclear factor kappa B |
| NLRP3 | NOD-like receptor family, pyrin domain-containing 3 |

| | |
|---|---|
| NK | Natural killer |
| PAMP | Pathogen associated molecular pattern |
| PBS | Phosphate buffered saline |
| PBMC | Peripheral blood mononuclear cell |
| PC | Phosphatidylcholine |
| PCR | Polymerase chain reaction |
| pDC | Plasmacytoid dendritic cell |
| PEI | Polyethanolamine |
| PI | Propidium iodide |
| PI3K | Phosphatidylinositol 3-kinase |
| PKC | Protein kinase C |
| PLL | Poly-L-lysine |
| PMN | Polymorphonuclear cell |
| qRT-PCR | Real-time quantitative reverse transcription PCR |
| rAgd3 | Recombinant Agd3 |
| ROS | Reactive oxygen species |
| SAIA | Subacute pulmonary aspergillosis |
| SBA | Soybean agglutinin |
| SM | Sphingomyelin |
| SMRT | Single molecule real time sequencing |
| SNP | Single nucleotide polymorphism |
| Th | T helper |
| TM | Transmembrane |
| TMHMM | Transmembrane hidden Markov model |
| TNF | Tumor necrosis factor |
| TLR | Toll-like receptor |
| Treg | T regulatory |
| UDP | Uridine diphosphate |

# Chapter 1: General introduction

## 1.1. Introduction to *Aspergillus*

### 1.1.1 *Aspergillus* species

The genus *Aspergillus* (family *Aspergillaceae*, of the phylum *Ascomycota*) encompasses a group of filamentous fungi that reproduce asexually through conidia that are produced in chains from a central structure (1). This genus is comprised of over 250 species of molds, a diverse group including both opportunistic pathogens and economically valuable species that are involved in food production (2, 3). In the environment, Aspergilli play an important role in carbon cycling by decomposing organic material (4). Of the economically important *Aspergillus* species, notable examples include *A. oryzae* and *A. niger*. Soy sauce and sake production depends on metabolites produced by *A. oryzae*, while citric acid is a fermentation product of *A. niger* using molasses or glucose syrup as a carbon source (2, 5). Although these examples highlight the importance of *Aspergillus* species to human food production, a number of *Aspergillus* species pose a growing threat to human health. *A. fumigatus* is the most common cause of invasive mold infection in humans, followed by *A. flavus, A. niger* and *A. terreus* and in rarer cases *A. nidulans* and *A. ustus* (6).

### 1.1.2 Life cycle and morphology

*A. fumigatus* is a saprophytic mold found in soil where it decomposes organic material. It is characterized by its production of abundant grey-green coloured conidia (7). Although a sexual cycle of *A. fumigatus* has been described, this mold mainly reproduces asexually by releasing prodigious amounts conidia into the environment, the efficient dispersal of which is aided by their small size and hydrophobicity (**Figure 1**) (7-9). Conidia of *A. fumigatus* are approximately 2µm in diameter with an echinulate surface that is coated in a rodlet layer composed of immunologically inert rodlet proteins that make conidia hydrophobic (10-12). *A. fumigatus* conidia derive their characteristic colour from 1,8-dihydroxynaphthalene (DHN) melanin, which protects them from UV rays and reactive oxygen species (13, 14). The asexual cycle of *A. fumigatus* begins when dormant conidia land in a favourable environment, which requires the presence of water, oxygen and carbon dioxide where they begin to swell and germinate (**Figure 1**) (15). Under lab conditions at 37$^{o}$C in Roswell Park Memorial Institute (RPMI) medium, isotropic conidia swelling is easily observed after four hours of growth, and is associated with shedding of the rodlet layer, uptake of water and the resumption metabolic activities (15-17).

After the first mitotic division of the conidial nucleus, growth switches from isotropic to polar growth which leads to the formation of a cylindrical germ tube that is detectable after approximately eight hours of growth (18). By nine hours of growth, germlings extend into long, thin young hyphae whose growth proceeds through mitosis and apical extension, (19, 20). The hyphae of *A. fumigatus* are multinucleate and separated into compartments by divisions known as septae which contain a pore to

allow the passage of cytosolic contents throughout the hyphae (21). Shortly after the onset of germination, hyphae begin to branch dichotomously at acute angles to form an expanding network of hyphae (**Figure 1**) (22). After approximately 14-20 hours of growth, depending on conditions, hyphae undergo a dramatic shift in their gene transcription to enter the next phase of development, known as competence (23). Competence is defined by the ability of the fungus to produce asexual reproductive structures or conidiophores. Conidiophores are aerial hyphal structures that extend from a foot cell located proximal to the hyphal tip (**Figure 1**) (9, 24). One of the main triggers of asexual reproduction (conidiation) is exposure to an air-solid/water interphase, based on the observation that cultures grown submerged in liquid will remain in a vegetative state. Other inducers of conidiation are light and stress (9, 25). The process of conidiation requires a number of specialized structures. This process begins with the swelling of the end of the aerial hyphae to form a multinucleate vesicle. Nuclei within the vesicle then undergo mitosis after which each nucleus is walled off by a septum into an elongated structure called a metula. This structure then undergoes mitosis itself to produce flask-shaped cells called phialides. *A. fumigatus* does not form metulae, and nuclei instead proceed directly to phialides (26). The septae of the metulae and phialides contain pores, resulting in sharing of cytoplasm between each nucleate unit. Asexual conidia result from mitosis within the phialides along a single axis, resulting in the formation of unbranched chains of immature conidia. The unit at the end of the phialide becomes walled off to form a dormant conidium ready for dispersal (**Figure 1**) (24, 25).

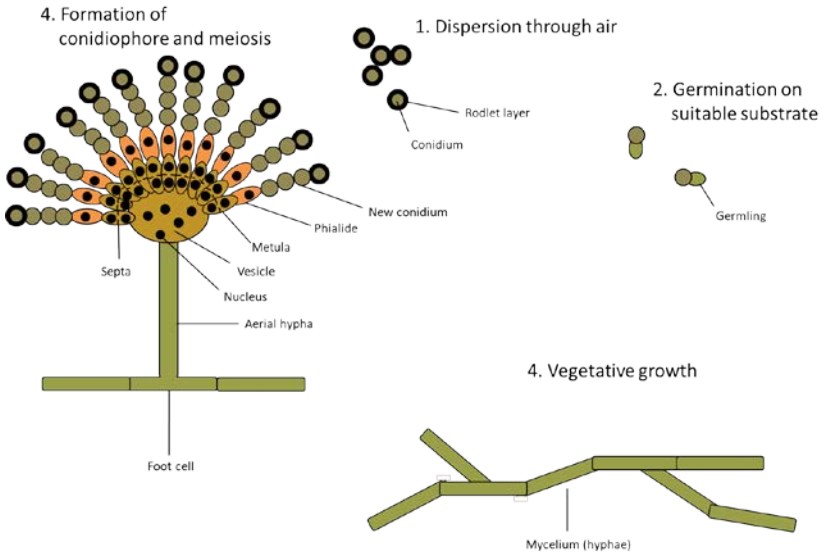


**Figure 1.** Diagram of the morphology and life cycle of *A. fumigatus.*

### 1.1.3 Ecological niche

Aspergilli are prolific decomposers within the environment (27). *A. fumigatus* has the ability to survive in a wide range of habitats due to its comprehensive metabolic repertoire, which includes the production of numerous secreted glycosyl hydrolases, proteinases and lipases necessary for degradation of plant litter that cannot be decomposed by other means (4, 28, 29). The ability of *A. fumigatus* to tolerate a wide range of temperatures and pH also enhances its ability to colonize a wide range of environments. The hyphal form of *A. fumigatus* can grow between temperatures of 12-65$^{o}$C, with optimal growth occurring at 37$^{o}$C, a temperature commonly reached within compost heaps (30, 31). Conidia of *A. fumigatus* can withstand even greater temperatures, and can germinate after treatment at 70$^{o}$C (32). Furthermore, soils with pH between 2 and 8 can support growth of *A. fumigatus* (33).

### 1.2 *Aspergillus* as a cause of human disease

Inhalation of *Aspergillus* conidia is inevitable due to their ubiquity and abundance (30). It is estimated that humans inhale hundreds of conidia daily (7). The conidia of *A. fumigatus* are small enough to reach the terminal airways and if able to evade immune defenses, can germinate into hyphae that invade and degrade host tissue much the same way the fungus would degrade organic matter in nature (7). Although infections of individuals without preexisting conditions have been reported, *Aspergillus* species are largely opportunistic pathogens, causing a range of diseases in individuals with systemic or local immune deficiencies (34, 35). Infections through direct tissue inoculation or other routes can occur, but are far less common than through the respiratory tract (36). Infections in immunocompetent patients, while less common, mainly occur in individuals with impaired lung function (37).

Of the over 200 *Aspergillus* species, only a few are known to cause human disease. The species isolated and the frequency of isolation vary according to geographical location and the site of infection. However, *A. fumigatus* is by far the most commonly isolated *Aspergillus* species in the clinical setting and causes at least 80% of invasive mold infections in humans (38). The next most commonly isolated species is *A. flavus*, followed by less common reports of infections caused by *A. terreus, A. niger* and *A. nidulans* (39-42).

#### 1.2.1 *Aspergillus* exposure in healthy hosts

As noted, disease caused by the inhalation of *Aspergillus* conidia is very rare in those with normal immune and lung function (43). Most inhaled conidia are caught in respiratory mucus and eliminated from respiratory tract by the mucocilioary escalator, where they are swallowed or expectorated (44, 45). Conidia that bypass this defense mechanism to reach the terminal airways are met by the host innate immune system (35). The first line of defense is alveolar macrophages which phagocytose and kill the majority of uneliminated conidia without further activation of the immune responses. Remaining conidia

may begin to germinate and expose a variety of immunogenic pathogen associated molecular patterns (PAMPS) leading to alveolar macrophage activation and recruitment of neutrophils (35). Neutrophils use degranulation and the release of antimicrobial peptides, reactive oxygen species (ROS), and the formation of neutrophil extracellular traps (NETs) to kill *Aspergillus* hyphae (35, 46).

### 1.2.2 *Aspergillus* disease in hosts with impaired immunity

Invasive infections with Aspergillus species occur mainly in hosts that are immunocompromised due to chemotherapy, immunosuppressive therapy like corticosteroids, or following stem cell and solid organ transplantation (7, 47, 48). In the absence of robust innate immune defenses, conidia that bypass the mucociliary elevator and land in the terminal airways can germinate to form filamentous hyphae that can invade the lung parenchyma, resulting in a conidition known as invasive aspergillosis (IA) (49). Tissue invasive hyphae destroy lung tissue through the production of a range of proteases and hydrolases (10, 50). If unchecked, IA can progess to systemic disease when angiotropic *Aspergillus* hyphae invade a blood vessel and break off. These hyphal fragments can disseminate via the blood stream to establish themselves at a new site and continue vegetative growth and tissue destruction (51). The mortality rate of IA is high, ranging from 26-90% depending on the degree of immunosuppression and the type of underlying disease (52). IA is often diagnosed late or misdiagnosed since the filamentous nature of hyphae makes recovery from sputum or other biological specimens challenging and testing methods are poorly sensitive (22, 53). The clinical presentation of IA is non-specific, and includes a fever not responsive to antibiotics, cough, dyspnoea, and hemoptysis in severe cases (54). Once IA is established it becomes very difficult to treat. The firstline treatment for IA is intravenous voriconazole, with alternative therapies of liposomal amphotericin B, other azole drugs or echinocandins also available (55). These treatment options are discussed in greater detail below.

### 1.2.3 *Aspergillus* infection in hosts with chronic lung disease

Patients with pre-existing lung conditions that impair the natural clearance of conidia can become chronically infected with *Aspergillus*, although progressive tissue invasion is a much less prominent feature of disease. Broadly speaking, these infections are divided into true infections, termed chronic chronic pulmonary aspergillosis (CPA), and allergic bronchopulmonary aspergillosis (ABPA), a form of allergic disease in which hyphae colonize the airway and patients become sensitized to *Aspergillus* allergens (56).

### 1.2.4 Chronic pulmonary aspergillosis

CPA is a collective term for several forms of chronic *Aspergillus* infections including aspergilloma (fungal ball), chronic cavitary pulmonary aspergillosis (CCPA), chronic fibrosing pulmonary aspergillosis (CFPA), subacute pulmonary aspergillosis (SAIA), and *Aspergillus* nodule. CCPA is the most common manifestation of CPA, while aspergillomas and *Aspergillus* nodules are more rarely encountered. On the less severe end of the disease spectrum, aspergillomas occur when conidia enter a pre-existing cavity and germinate to form mycelium which along with other debris eventually fills the cavity (7). Simple aspergillomas may be asymptomatic and are usually found while examining the pre-existing disease, however severe bleeding can occur (7). The aspergilloma is contained to the cavity by the immune system, however damage to the lung will eventually occur. Aspergillomas are typically treated by oral antifungals over a long period of time, as treatment progress is usually quite slow. Whenever possible, surgical removal of the aspergilloma is recommended (37).

CCPA is the consequence of slowly progressive (months to years) necrotizing infections leading to cavities that may have thin or thick walls. Balls of hyphae (aspergillomas) may be present within the cavity (57). Symptoms include chest pain, weight loss, chronic productive cough and hemoptysis (56). Left unchecked, CCPA can progress to CFPA where at least two lobes of the lungs exhibit fibrosis as a consequence of destroyed tissue and collapsed cavities. For both CCPA and CFPA oral itraconazole or voriconazole is the first line of treatment, followed by amphotericin B deoxycholate or echinocandin drugs if triazole therapy is contraindicated or poorly tolerated (57, 58). Surgery is also recommended in select patients with limited infection and well preserved lung function (59).

SAIA occurs in patients who are mildly immunocompromised (for example, in those with diabetes mellitus or having advanced age) and has a similar presentation to CCPA but progesses more quickly over weeks rather than months to years (57). SAIA is often associated with the appearance of invasive hyphae in histological samples in addition to a positive serum *Aspergillus* antigen test. It has been suggested that SAIA be managed according to the guidelines set for acute invasive aspergillosis, for which voriconazole treatment is recomended (57, 60).

Finally, *Aspergillus* nodules are small, contained fungal lesions that typically do not lead to cavitation. Their radiographical presentation is similar to other diseases including lung carcinomas and therefore must be diagnosed using histological samples. Progressive tissue invasion does not appear to occur with *Aspergillus* nodules, although they can grow slowly, expanding in size (57). Patients with *Aspergillus* nodules do not typically present with systemic symptoms such as fever and weight loss, but cough and dyspnoea are common (61, 62). Antifungal therapy is not always started if a patient is asymptomatic, and patients are followed with regular CT scans to monitor development of the nodule(s) (61-63).

### 1.2.5 Allergic bronchopulmonary aspergillosis

In some chronic respiratory diseases the clearance of debris from the lungs is impaired and colonization of the airways by *Aspergillus* can result. Patients with *Aspergillus* airway colonization are continuously exposed to *Aspergillus* allergens and may develop hypersensitivity to these antigens. This condition is known as allergic bronchopulmonary aspergillosis (ABPA) and mainly affects cystic fibrosis and asthma patients (64). Both of these subsets of patients have abnormalities in their airway mucus, which allows *Aspergillus* conidia to avoid clearance through the mucociliary escalator and colonize the airways (65-67). A positive *Aspergillus* skin test, eosinophilia and increased immunoglobulin E (IgE) in the blood are hallmarks of ABPA (68). The chronic allergic response can lead to eosinophils egressing into the lumen of the bronchus in numbers high enough to result in bronchial impaction, which can go on to cause bronchiectasis (dilatation of the bronchi due to inflammation-mediated remodelling of the bronchial walls) (67). Treatment of ABPA takes a two-pronged approach: corticosteroid treatment to reduce allergic inflammation in conjunction with antifungals to reduce the burden of allergens (69).

## 1.3 Current treatments for *Aspergillus* infections

When it comes to *Aspergillus* infections, the expression “an ounce of prevention is worth a pound of cure” could not be more true. Once fungal infections are firmly established, they are very difficult to treat. Unfortunately, due to non-specific symptoms and challenges in obtaining viable microbiological samples from patients, fungal pulmonary infections may progress rapidly before the appropriate treatment is started (6). Prevention is especially important in IA patients who have been treated for the disease but must undergo another round of immunosuppression: prophylactic antifungal treatments are necesssary in these cases (6, 70). Other obstacles to effective treatment of IA are the limited number of antifungal agents available to treat this infection, drug interactions, and toxicity of the available drugs as well as the emergence of antifungal resistance. The major antifungal classes used to prevent and treat IA are detailed below.

### 1.3.1 Polyenes

Polyenes, which are produced by *Streptomyces* species, were the first class of antibiotics used in the treatment of fungal infections. Polyenes target ergosterol, a major sterol in the fungal cell membrane that is absent from mammalian cell membranes, to exert their fungicidal effects. It was initially hypothesized that polyenes interact directly with ergosterol in the fungal cell membrane to form pores leading to loss of cellular viability, however other studies indicate that polyenes may actually sponge ergosterol from the cell membrane, making it unstable (71, 72). Polyenes have a narrow therapeutic window as they can bind to the human analogue, cholesterol, leading to cytotoxicity. The most common

manifestation of polyene toxicity is nephrotoxicity, which often limits use of the agent (73). The polyene amphotericin B (AmB) was for many years the treatment of choice for aspergillosis, although this has changed with the advent of safer and more effective antifungals (74). Four forms of amphotericin B exist: AmB deoxycholate (D-AmB), AmB lipid complex (ABLC), AmB colloidal dispersion (ABCD) and liposomal AmB (L-AmB) (6). Prior to the year 2000, D-AmB was the first choice in treatment for IA, until clinical trials comparing D-AmB with other antifungals revealed that it was too poorly tolerated and ineffective in combatting the disease to justify its continued use (75). L-AmB and ABLC exhibit reduced toxicity and better efficacy than D-AmB, with L-AmB currently replacing D-AmB for most uses (6, 76, 77). ABCD is comparable to D-AmB in both tolerability and efficacy (78). Despite the limitations of AmB treatment, there is a low rate of acquired resistance to this drug in *A. fumigatus* which can make it a last line of defense when confronted with azole-resistant *Aspergillus* isolates. This does not apply to all *Aspergillus* species, as *A. terreus* is intrinsically resistant to AmB (72).

### 1.3.2 Azoles

Azoles are synthetic drugs that target the biosynthesis of ergosterol to exert their antifungal effects. Inhibition of ergosterol biosynthesis is achieved by interaction of the drug with C-14 alpha demethylase, which converts lanosterol to ergosterol. The C-14 alpha demethylase is dependent on cytochrome P-450, which is also true of some enzymes that are involved in human steroid production (79, 80). As a result, azoles can have toxic side effects by disrupting these cytochrome P-450-dependent pathways. Use of azole drugs began in the 1980s with the introduction of ketoconazole, followed by multiple generations of subsequent agents. Azoles soon became the drug of choice for treating fungal infections over polyenes with one major advantage being oral delivery (80). Azoles with anti-aspergillus activity include itraconazole, voriconazole, posaconazole and isavuconazole. Clincial trials have demonstrated the safety and efficacy of voriconazole and isavuconzole, which have emerged as the first line of treatment for IA (6, 75, 81). However, in clinical trials directly comparing the efficacies of voriconazole and isavuconazole in relation to the minimum inhibitory concentration of either drug, isavuconazole showed a distinct decrease in all cause mortality after 42 days compared to voriconazole suggesting that isavuconazole is the superior azole (82). Posaconazole has been shown to be a good second option both in safety and efficacy when use of isavuconazole or voriconazole is not well tolerated (70). In neutropenic patients, some success has been seen in clinical trials with prophylactic use of posaconazole to prevent IA and other fungal infections, which performed better than other azoles (83). Serious adverse events are rare with azole use, and side effects are usually minor enough to continue use of the drug. Posaconazole and itraconazole may cause some gastrointestinal disturbances, and voriconazole can cause vision abnormalities at the start of treatment. Fever and headaches are other side

effects of azole drugs. Azole drug use is unfortunately complicated by interactions with a significant amount of other drugs including chemotherapy agents (79). Azole resistance, most often due to mutation in the fungal C-14 alpha demethylase enzyme, has been increasing in both invasive and non-invasive aspergillosis (84). In patients with non-invasive disease such as ABPA, prolonged azole use can give rise to resistance within the patient (85). In invasive disease, patients may be infected with a strain of *A. fumigatus* that is already azole resistant. It has been hypothesized that azole fungicide use is to blame for the emergence of environmental azole-resistant isolates (86).

### 1.3.3 Echinocandins

Echinocandins are lipopeptides that target the synthesis of an important cell wall polysaccharide, β-1,3-glucan, by inhibiting the fungal β-1,3-glucan synthase Fks1 (87). Inhibition of β-1,3-glucan synthesis can result in cell wall disruption, hyphal fragmentation and death. It has been observed, however, that compensatory mechanisms can take place in the *Aspergillus* cell wall, where increased chitin production can offset the inhibition of β-1,3-glucan production (88). Additionally, β-1,3-glucan is also an immunostimulatory pathogen associated microbial pattern molecule that activates the pattern recognition receptor dectin-1 to activate macrophages (89). Treatment of *A. fumigatus* hyphae with echinocandins increases exposure of β-1,3-glucan on the hyphal surface, indicating that echinocandin treatment could have an indirect immunostimulatory effect and increase killing of *A. fumigatus* by PMNs (90). Examples of this class include caspofungin and micafungin, which are both well tolerated are used to treat IA (6). Echinocandins are not favoured as first-line treatments, as clinical trial data indicates they may be inferior to azoles in their activity against *Aspergillus* species (87). However, their importance may increase as azole-resistant *Aspergillus* strains continue to emerge (87). Caspofungin has been used as a salvage therapy alone or alongside L-AmB or voriconazole, with favourable outcomes in about half of the cases (87, 91). Resistance to echinocandins in *Aspergillus* is exceedingly uncommon though it has been observed with other fungi (87, 92).

### 1.3.4 Surgical intervention

In rare cases, surgical intervention may complement treatment with antifungals, usually in patients with an aspergilloma rather than invasive disease as aspergillomas are resistant to drug penetration. Surgery is most beneficial in patients with reasonable lung function and a localized infection (59). In one study, patients with aspergilloma and hemoptysis who received surgery had an improved survival rate over those given traditional therapies alone, with survival rates of 84% and 41% respectively (93). Other indications for surgery include risk of penetration of *Aspergillus* into a major blood vessel causing fatal hemmorhage or failure to respond to to antifungal treatment (94, 95). The choice to proceed

with surgery must be made carefully due to high vascularity of the lungs, the risk of leakage of fungal elements into the pleural cavity, the likelihood of other sites of microscopic infection and the often poor underlying condition of pateints with fungal infection (93).

### 1.4 *Aspergillus fumigatus* virulence factors

The limited number of effective antifungal agents, combined with the rising rate of antifungal resistance in *A. fumigatus* and the ever-increasing amount of patients undergoing immunosuppresive regimens has created an urgent need for the development of novel therapeutics for the treatment IA (96). One approach to the development of new antifungals is to understand the virulence factors of *A. fumigatus*, which may reveal druggable targets that have not yet been exploited. *A. fumigatus* is an opportunistic pathogen which suggests that it is not inherently virulent, however this fungus is the most common cause of invasive mold infections in immunocompromised patients and therefore must possess unique traits that enable it to establish an infection under the right conditions (97, 98). This section discusses the multitude of factors that makes *A. fumigatus* a successful opportunistic pathogen.

#### 1.4.1 Conidial size, hydrophobins and melanin

The conidia of *Aspergillus* are ubiquitous in the environment resulting in humans inhaling tens to hundreds of these organisms daily. Due to their small size (~2µm) and hyrdophobicity, *Aspergillus* conidia readily become airborne and reach the terminal airways (10). The outer rodlet layer is composed of small hydrophobic proteins that are covalently bound to the conidial surface, aiding the spread of conidia on air currents (99, 100). Hydrophobins have a β-sheet core and exposed hydrophobic surfaces that give these proteins their surfactant ability (101). There are seven hydrophobins (*rodA-G*) in the *A. fumigatus* genome that share a conserved set of eight cysteine residues forming four disulfide bonds and are divided into three classes (class 1-3) (12, 102). Class 1 hydrophobins form insoluble monolayers composed of small rods (hence the name “rodlet”), while class 2 hydrophobins can be dissolved in some organic solvents and lack the rodlet shape (103). Class 3 hydrophobins have an intermediate phenotype. RodA-C are class 1 hydrophobins, RodD and RodE belong to class 2, and RodF and RodG belong to class 3. Although RodB is found in conidia, the rodlet layer is composed only of RodA which is geometrically arranged in an amyloid formation on the conidial surface (12, 99). The hydrophobicity of conidia imparted by the rodlet layer also plays a role in their ability to reach the alveoli (12). Another important function of the rodlet layer in the establishment of *A. fumigatus* infection is through the concealment of β-glucan from recognition by phagocytes. Rodlet proteins are immunologically inert (100). Moreover, the rodlet layer enhances conidial resistance to killing by primary murine alveolar

macrophages *in vitro* (100). Additionally, RodA prevents antigen presentation in human dendritic cells that have taken up Δ*rodA* conidia (100).

Beneath the rodlet layer is a coating of DHN melanin, which in addition to protecting the conidial DNA from UV rays, protects the fungus against phagocytic killing and reactive oxygen species produced by cells of the innate immune system (4, 10, 104). There is also evidence that melanin aids the fungus in thermotolerance (105). Melanin-deficient *A. fumigatus* strains are also hypovirulent in animal studies and display increased C3 deposition on the conidial surface in comparison to wild-type *A. fumigatus* (106). In a screen for uncharacterized C-type lectin receptors (CLRs) specific for fungi, a CLR called melanin-sensing C-type lectin receptor (MelLec) recognizing melanin was found. MelLec only bound melanin-producing fungi at stages where melanin was present, which in *A. fumigatus* is only in conidia. Interestingly, when murine tissues were tested for MelLec expression, the highest levels of MelLec transcript were found in lung tissue, suggesting an important role of this CLR in the airways. In immunocompetent MelLec knockout mice intratracheally infected with *A. fumigatus*, a delay in neutrophil recruitment was observed but surprisingly there was no increase is susceptibility compared to wild-type mice (107). However, when immunocompetent MelLec-deficient mice were infected with *A. fumigatus* by tail vein injection, surivival was decreased and fungal burden was increased in comparison to wild-type mice receiving the same infection. In both MelLec-deficient and wild-type mice infected with a melanin-deficient strain of *A. fumigatus*, fungal burden and survival were equivalent. In humans, MelLec is expressed in endothelial (but not lung epithelial) and myeloid cells (108). Moreover, a single nucleotide polymorphism (SNP) in MelLec is associated with increased risk of IA in stem cell transplant patients (107). On the other side of the coin, MelLec deficiency was protective in a mouse model of pulmonary allergy, which may be a result of decreased inflammation in response to fungal exposure that would aggravate the allergic response (109).

### 1.4.2 Thermotolerance

One of the most important decomposers in the environment, *A. fumigatus* is commonly found in compost heaps. The internal temperature of these heaps often exceeds 50°C, and as a result this fungus is adapted to survive at elevated temperatures (16). As a result, *A. fumigatus* grows well at 37°C, allowing it to grow well inside the human body (104). Growth and virulence at 37°C has been shown to be dependent on the nucleolar protein CgrA, the yeast ortholog of which is involved in ribosomal subunit biosynthesis (110). Disruption of this gene in *A. fumigatus* led to an impaired growth rate at 37°C compared to the wild type fungus, as well as loss of virulence in a murine pulmonary infection model (111).

### 1.4.3 Nutrient acquisition

*Aspergillus fumigatus* is a saprophyte with the ability to degrade and utilize many organic substrates. To achieve this feat, the fungus is able to produce a variety of proteases, hydrolases, and phospholipases. Unsurprisingly, these enzymes are also able to degrade tissues in the host, which is an important part of infection and invasion (7, 112). Indeed, an *A. fumigatus* strain deficient in an elastolytic serine protease was found to be hypovirulent in a neutropenic mouse model in comparison to wild-type *A. fumigatus*. Immunogold staining confirmed that the protease was secreted by wild-type *A. fumigatus* during invasion of host tissue (113). A positive correlation between elastase activity and virulence of *A. fumigatus* in humans has been observed with nearly all fungal strains isolated from IA patients exhibiting elastase activity while many environmental isolates do not have enough elastase activity for growth on elastin medium. Elastin is a major component of lung connective tissue (114). It has also been observed that cytoskeletal proteins of alveolar epithelial cells are susceptible to *Aspergillus* alkaline serine proteases (115). Phospholipases likely play a similar role in tissue destruction by hydrolyzing the ester bonds of phosphoglycerides, which could destabilize host cell membranes thereby causing cell lysis and further tissue distruction (112).

Another virulence factor relating to *Aspergillus* nutrient acquisition is the sequestration of iron. Free iron is not widely available within the host, and *A. fumigatus* produces several distinct siderophore molecules in order to trap iron for assimilation and can use them to acquire iron from human transferrin (112, 116). The *sidA* gene of *A. fumigatus* encoding L-ornithine-$N^5$-monooxygenase, the first step of siderophore biosynthesis, has been found to be necessary for virulence in a murine infection model (117).

### 1.4.4 Growth in hypoxic conditions

During infection, damage to tissues and subsequent inflammation disrupts the blood supply and leads to a hypoxic environment (118). *A. fumigatus* is capable of causing a high degree of tissue destruction and inflammation during lung infection, and is able to adapt to hypoxia despite being classically considered to be an obligate aerobe (118, 119). The ability of *A. fumigatus* strains to grow *in vitro* under hypoxia correlates with virulence (118, 120, 121). During the course of one study, the wild-type clinical isolate Af293 was even able to exhibit improved fitness for growth in hypoxia during the course of infection in a mouse (121). Growth under hypoxic condidtions seems to be linked to alterations in sterol biosynthesis and iron uptake in *A. fumigatus*, and the transcription factor SrbA, which is involved in sterol regulation, is necessary for growth in hypoxia (120). Disruption of *srbA* resulted in a strain that was avirulent and displayed increased susceptibility to azole drugs, which target sterol biosynthesis (118). During hypoxia, SrbA also negatively regulates a gene, *srbB*, involved in heme biosynthesis and carbohydrate metabolism, impairing iron uptake (120). Other genes, *rbdA* and *horA* which are involved in the sensing of and response to hypoxia respectively, have also been implicated in virulence (122, 123).

### 1.4.5 Allergens

*Aspergillus* can cause allergic disease, and produces allergens, defined as proteins that bind IgE, that can exacerbate other pulmonary disorders such as asthma (68, 124, 125). There are at least 58 known allergens produced by *A. fumigatus*, the most of any fungus by a wide margin. Among these are secreted proteases and other hydrolytic enzymes (126). *Aspergillus* proteases cause vigorous allergic responses, inducing the release of interleukin (IL)-6, IL-8 and monocyte chemoattractant protein (MCP)-1 by cells of the airway epithelium (125). Secreted proteases and hydrolases also damage the lung tissue, which allows exposure of *Aspergillus* antigens to dendritic cells and subsequent priming of naïve T-helper cells to a Th2 phenotype and eventual secretion of IgE isotype antibodies (125). Unique to *A. fumigatus* is the ribotoxin Asp f1, to which the majority of ABPA patients display IgE reactivity (126, 127). Although not a classic protein allergen, cell wall polysaccharide chitin also has allergenic potential and causes an influx of eosinophils and basophils in the lungs of mice when administered in purified form (125).

### 1.4.6 Mycotoxins

Several putative mycotoxins are produced by *A. fumigatus* with fumagillin and gliotoxin, which are both secreted during infection, being the best studied of these molecules (128-130). Fumagillin acts by binding irreversibly to host methionine aminopeptidase (MetAP)2, inactivating the enzyme and possibly destabilizing cellular maintanence (129). Fumagillin exerts different effects depending on the cell type exposed. Neutrophils exposed to fumagillin are unable to form the nicotinamide adenine dinucleotide phophate (NADPH) complex for respiratory burst, thereby inhibiting their killing capacity (131). Exposure of erythrocytes to fumagillin has been shown to trigger apoptosis (eryptosis) of these cells, and it has been suggested that fumagillin may also play a role in epithelial cell damage during infection (132, 133). Like fumagillin, gliotoxin plays several roles in virulence. Among other things, gliotoxin induces monocyte apoptosis, and inhibits both angiogenesis and proteosome activation (134-136). The much higher frequency of isolation of gliotoxin-producing strains from patients than from the environment also supports a role for gliotoxin in virulence (137)

### 1.4.7 The *Aspergillus* hyphal cell wall: adapted from *The role of* Aspergillus fumigatus *polysaccharides in host–pathogen interactions* (138).

#### *Introduction*

"The *A. fumigatus* cell wall is a key point of contact between *A. fumigatus* and the host (139, 140). The majority of the fungal cell wall is composed of polysaccharides, and, as a result, there has been

great interest in elucidating the role that these macromolecules play in host-fungal interactions. While recent studies with purified polysaccharides and mutant strains with altered polysaccharides have begun to shed light on the role of these molecules during infection, it is important to acknowledge the limitations of both experimental approaches. Purified polysaccharides may vary in size and composition from their native forms, and the immune response to soluble or microparticular polysaccharides may be different from the response to polysaccharides presented in their natural context where they immobilized within the cell wall and linked to other glycans and proteins. These effects have been best illustrated in studies of interactions with the cell wall polysaccharide chitin in which both particle size and the presence of co-stimulatory pattern recognition receptor ligands have a dramatic effect on the type of host response to this glycan (detailed below) (141, 142). The use of synthetic oligosaccharides of defined length and composition may be helpful in this regard, but few studies have used this approach. Studies of mutants lacking specific polysaccharides must also consider the secondary effects that loss of a given polysaccharide may have on cell wall structure and organization. Further, loss of one cell wall polysaccharide can lead to compensatory effects on the production of other polysaccharides. This phenomenon has been well described in *Candida albicans* and other fungi, in which the inhibition of β-glucan synthesis leads to an increase in fungal cell wall chitin content (143, 144).

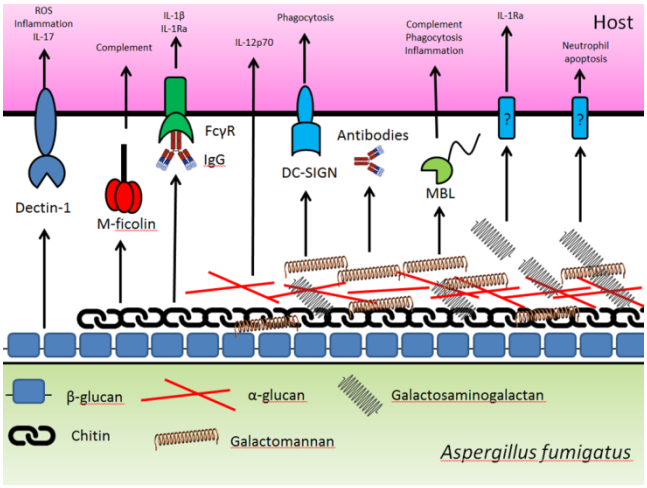


**Figure 1:** Graphical overview of interactions between fungal polysaccharides and host elements.

***β-glucan***

β-glucan is a linear polymer composed of β-(1,3)-linked glucose that is synthesized at the plasma membrane (145). It is a major component of the inner cell wall where it is involved in maintaining cellular structural integrity, and acts as a scaffold for the anchoring of other polymers in the cell wall. *A. fumigatus* strains lacking β-glucan are extremely susceptible to cell wall-destabilizing agents, and exhibit

massive shedding of galactomannan (146). The level of β-glucan exposure on the surface of *A. fumigatus* varies depending on the developmental stage of the organism. In resting conidia, the β-glucan is concealed by the hydrophobic rodlet layer (147). As germinating conidia swell and shed this rodlet layer the underlying β-glucan is transiently exposed, however it is once again masked in hyphae by a layer of the exopolysaccharide galactosaminogalactan (148, 149). Stage-specific β-glucan exposure is thought to be a major signal for the activation of pulmonary leukocyte recruitment in response to early *A. fumigatus* infection. Resting conidia, in which β-glucans remain hidden by the rodlet layer, are phagocytosed by alveolar macrophages or epithelial cells without inducing the production of pro-inflammatory cytokines or chemokines (147). However, if conidia escape this first line of defence, they undergo germination, resulting in exposure of β-glucan, which can be bound by the C-type lectin receptor Dectin-1 on the surface of alveolar macrophages (150). In addition to alveolar macrophages, Dectin-1 is also expressed on an array of immune cells, such as dendritic cells (DCs), neutrophils, monocytes and some T cells (89, 151). In conjunction with toll-like receptor (TLR) 2, Dectin-1 binding to β-glucan leads to Syk recruitment and NF-κB translocation to the nucleus resulting in the expression and release of a multitude of pro-inflammatory cytokines and chemokines including chemokine ligand 1 (CXCL1), interleukin (IL)-1β, tumor necrosis factor (TNF)-α, CXCL2, IL-1α, IL-6, granulocyte-colony stimulating factor (G-CSF), granulocyte macrophage (GM)-CSF, and IFNγ (152). Recognition of β-glucan by DCs exposed to zymosan can also lead to production of the anti-inflammatory cytokine IL-10 through the Syk pathway (153). The net effect of this chemokine and cytokine signalling recruits neutrophils to the site of infection and stimulates a T helper type-1 mediated immune response (148). β-glucan binding to neutrophil Dectin-1 is required for neutrophil production of IL-17 (154) and also leads to activation of protein kinase C (PKC)-δ, which is necessary for ROS generation (152). Dectin-1 mediated activation of the PKC pathway is also found in macrophages, although it is not necessary for fungal killing in this context (152). TLR9 may also participate in the recognition of β-glucan, as it is recruited to phagosomes in macrophages containing β-glucan(155). Consistent with these observations, Dectin-1-deficient mice are more susceptible to *A. fumigatus* challenge in a high-dose infection model of pulmonary invasive aspergillosis (151).

***α-glucan***

The most abundant cell wall polysaccharide in *A. fumigatus* is α-(1,3)-glucan, which comprises approximately 40% of the mycelial cell wall (156). While no host receptor is known for α-(1,3)-glucan is known, purified α-(1,3)-glucan can induce dendritic cell activation, as measured by IL-12 p70 expression (157). Mice vaccinated with purified α-(1,3)-glucan in combination with CpG, or dendritic cells pulsed with α-(1,3)-glucan developed a mixed Th1/Treg response, and exhibited increased survival following

fungal challenge (157). Studies of a mutant lacking α-(1,3)-glucan have revealed that of loss α-(1,3)-glucan synthesis was associated with dramatic alterations in the cell wall of conidia (156). These changes include the exposure of inner cell wall polysaccharides, increased chitin and β-glucan levels within the cell wall and the cloaking of the rodlets in an amorphous layer of pro-inflammatory glycoproteins. These alterations in the conidial cell wall resulted in enhanced phagocytosis and TNF-α production by alveolar macrophages. Mutants deficient in α-(1,3)-glucan have been found to be hypovirulent in both an immunocompetent and immunocompromised mouse model of *A. fumigatus* infection, likely as a consequence of an enhanced early immune response that limits fungal growth (156).

***Chitin***

Chitin is a highly insoluble polymer of β-(1,4)-linked N-acetyl glucosamine that is covalently linked to β-(1,3)-glucan in the inner cell wall (139, 158, 159). Chitin plays an important role in cell wall structure and integrity (139). Experiments using purified polysaccharide have established that chitin activates macrophages, however the size of the chitin particle plays an important role in governing on the type of immune response that is elicited (141). Exposure of macrophages to larger chitin particles (40-70 μm in diameter), more representative of intact fungal hyphae, induces the release of pro-inflammatory TNF-α and IL-17 whereas smaller particles (2-10 μm) induce IL-10 production (141, 160). Stimulation of human peripheral blood mononuclear cells (PBMCs) with small chitin particles (<0.5um) was also reported to induce the secretion of immunosuppressive interleukin-1 receptor antagonist (IL-1Ra) (142). Intriguingly, co-stimulation of PBMCs with the combination of chitin and other non-fungal pattern recognition receptor ligands (lipopolysaccharide, Pam3Cys, or muramyl dipeptide) induced the production of pro-inflammatory produce IL-1β and TNF-α (142). The production of both immunosuppressive and pro-inflammatory cytokines by PBMCs was dependent on immunoglobulin opsonisation of chitin particles followed by Fc-γ-receptor recognition and phagocytosis and was dependent on activation of Syk and phosphatidylinositol 3-kinase (PI3K) (142). Collectively these studies emphasize that the context of glycan presentation (particle size and co-stimulation with other ligands) plays a critical role in determining the character of the host response. Although no chitin-deficient strain of *A. fumigatus* has been constructed, an environmental isolate that exhibits increased chitin exposure at the surface of the cell wall at all stages of growth has been studied in animal models (159, 161). In a model of repeated pulmonary exposure, mice exposed to the environmental isolate exhibited increased eosinophilia of the airways, lower levels of interferon (IFN)-γ producing CD4+ T cells and increased IL-4 and CCL11 (eotaxin) expression as compared with mice exposed to wild-type conidia (159). Consistent with this report, recent studies of acidic mammalian chitinase, a chitinolytic enzyme, suggest that chitin oligosaccharides released by host enzymatic degradation of chitin may

contribute to the activation of the non-protective pulmonary Th2 responses to *A. fumigatus* (162). Chitinase-deficient mice exhibited lower levels of IL-33 production and lower pulmonary fungal burden after *A. fumigatus* challenge, as well as improved lung function following chronic fungal exposure (162).

The cellular receptor(s) that recognizes chitin has yet to be identified; however, interaction of chitin with members of the ficolin family of soluble proteins have been reported (163, 164). The ficolins are a class of innate pattern recognition molecules that belong to the fibrinogen related-domain superfamily (163). M-ficolin is found in the lung, where it is produced by type-II alveolar epithelial cells, monocytes and neutrophils (163). Strong staining of M-ficolin has been observed in human tissue samples proximal to aspergilloma lesions (164). Studies *in vitro* demonstrated that M-ficolin binds purified chitin, and co-localized with chitin-rich parts of the cell wall (164). This binding could be inhibited by soluble N-acetyl glucosamine (164). M-ficolin binding to chitin-poor regions of the cell wall was also noted, however, suggesting that this protein may bind multiple fungal polysaccharides (164). M-ficolin binding of chitin was found to mediate complement activation, and M-ficolin opsonisation of the chitin-containing alkali-insoluble cell fraction of *A. fumigatus* resulted in increased IL-18 secretion by A549 epithelial cells as compared to either component alone (164, 165). The role of M-ficolin binding to *A. fumigatus* chitin has not yet been investigated in animal models of disease.

***Galactomannan***

Galactomannan is composed an α-(1,2)(1,6)-mannopyranose backbone with short branches of β-(1,5)-oligogalactofuranose connected by β-(1,3) and β-(1,6) linkages (166). Galactomannan (GM) is found in both the inner and outer cell wall of *A. fumigatus* hyphae, and is copiously shed by growing hyphae (165, 167). Recently, a second form of galactomannan characterized by longer galactofuranose side chains with 6-*O* substitutions, produced through the action of a unique set of mannosyltransferases, has been identified in the conidial cell wall (168, 169).

Both the galactofuranose and mannan components of GM are recognized by the host immune system. The galactofuranose side chains of GM are antigenic and naturally occurring antibodies in humans recognize these structures (167). The mannan component of *A. fumigatus* GM is an important pathogen-associated molecular pattern molecule that is likely recognized by host mannose receptors including DC-specific ICAM 3-grabbing nonintegrin (DC-SIGN), Dectin-2, and mannose-binding lectin (147).

DC-SIGN is a type II membrane C-type lectin found on the surface of macrophages and dendritic cells(170). Studies of the interaction of conidia and human monocyte-derived dendritic cells (MDDCs) have demonstrated that binding of conidia by MDDCs and IL-10 release is inhibited by both soluble galactomannan and antibodies to DC-SIGN (170). Similar findings were observed with alveolar

macrophage-like bone-marrow derived macrophages (170). In contrast, knockdown of DC-SIGN had no effect on TNF-α and interleukin-12 expression in immature dendritic cells exposed to *A. fumigatus* germ tubes (171). These findings may reflect differences in dendritic cell derivation methods, or alternately indicate that there are important differences between the mechanisms by which innate cells recognize hyphal and conidial GM.

Dectin-2 is a C-type lectin receptor found on the surface of alveolar macrophages which recognizes α-mannans of several fungi (146, 172). Indirect evidence suggests that Dectin-2 likely recognizes the α-mannan backbone of GM (173). Binding of germinating conidia and young hyphae to the THP-1 macrophage cell-line, and subsequent activation of NF-KB was Dectin-2 dependent (174). Similarly, antibodies to Dectin-2 reduced the ability of plasmacytoid dendritic cells (pDCs) to bind Aspergillus hyphae (175). Direct binding or inhibition studies to confirm that the α-mannnan chain is the Dectin-2 ligand responsible for these phenotypes have yet to be performed.

Mannose-binding lectin (MBL) is a soluble circulating collectin-class lectin which binds a variety of fungal mannans (176). Upon binding to these glycans, MBL induces complement activation via complex formation with MBL-associated serine proteases (MASPs) (176). As with Dectin-2, direct evidence for MBL binding of Aspergillus GM is lacking, however MBL binds to the surface of *A. fumigatus* conidia and this binding can be inhibited with soluble mannose (172, 176). Studies in mouse models have yielded somewhat contradictory roles for MBL that may indicate site and disease specific roles for this lectin in the pathogenesis of *Aspergillus* infections and allergy (177-179). MBL treatment enhances phagocytosis of conidia and killing of hyphae by human PMNs and activates the complement cascade (177). Treatment of mice with recombinant human MBL enhances survival in a model of invasive pulmonary aspergillosis in association with increased production of pro-inflammatory cytokines (TNF-α and IL-1β) and reduced production of immunosuppressive IL-10 (177). Conversely, MBL-deficient mice are more resistant to intravenous *A. fumigatus* challenge (178). MBL-deficiency in mice was associated with decreased Th2 cytokine and increased IFN-γ production upon intratracheal challenge with *A. fumigatus* (179). These conflicting results could stem from differences in mouse background, or perhaps indicate that pharmacologic levels of intrapulmonary MBL exert unique effects on pulmonary neutrophils. Finally, in a fungal asthma model MBL-deficient mice were found to produce lower levels of type-2 cytokines and develop less airway hyperreactivity early after *A. fumigatus* challenge (179). Although more work is required to understand these observations, these findings may reflect the relative importance of complement activation versus induction of cytokine production in these different models of disease.

***Galactosaminogalactan***

Galactosaminogalactan (GAG) is an exopolysaccharide found throughout the cell wall and extracellular matrix of *A. fumigatus* (180). The quantity of hyphal-associated GAG produced by other *Aspergillus* species has been correlated with their frequency of isolation from invasive aspergillosis patients, suggesting that this polymer plays an important role in fungal virulence (181). GAG is a heteropolymer of α-(1,4)-linked galactose and partially de-N-acetylated galactosamine that is absent from conidia, but produced at all other stages of growth (180). GAG plays a number of roles in host-fungal interactions. GAG mediates adherence of *A. fumigatus* to host tissues and other substrates (149, 182). Cell wall-associated GAG enhances immune evasion through cloaking immunostimulatory polysaccharides found deeper in the cell wall, such as β-glucan, from detection by pattern recognition receptors (149, 182). Additionally, as GAG is a cationic polysaccharide, cell-associated GAG can act as an electrostatic barrier to intracellular penetration by cationic antimicrobial peptides, such as those found in neutrophil extracellular traps (181)." More recently it was reported that GAG-producing hyphae of *A. fumigatus* activate the inflammasome leading to pyroptosis in bone marrow derived macrophages (BMDMs) as measured by cleavage of caspase 1 and release of IL-1β. The magnitude of this response correlated with GAG production. Mechanistic studies revealed that deacetylated GAG binds to host cell ribosomes in a charge-dependent manner, activating pyroptosis through NOD-like receptor family, pyrin domain-containing 3 (NLRP3) as a result of stress on the endoplasmic reticulum. In contrast to other studies implicating GAG as a virulence factor, mouse experiments suggested that GAG-dependent activation of the inflammasome elicited a protective effect, as caspase 1-deficient mice exhibited higher mortality than wild-type mice when infected with *A. fumigatus* (183).

"Studies of purified fractions of secreted GAG suggest that soluble polysaccharide mediates a variety of direct effects during infection. Soluble GAG induced apoptosis of human neutrophils, via a natural killer cells-dependent mechanism (184, 185). Stimulation of peripheral blood mononuclear cells with soluble GAG induced the release of anti-inflammatory IL-1 receptor antagonist, and suppression of IL-17 and IL-22 production by these cells (186). It has also been reported that GAG stimulates platelet activation, resulting in increased CD62P, CD63, and annexin V exposure on their surface (187). While intravascular thrombosis is a well-described phenomenon in invasive aspergillosis (188), the effects of GAG-mediated platelet activation in thrombosis during pulmonary fungal infection have not yet been studied *in vivo*. Taken as a whole, these studies strongly suggest the presence of a receptor for GAG on host cells, however, attempts to identify a mammalian receptor for GAG have not yet been successful." Since the evidence presented here implicates a key role for GAG in virulence, the rest of this thesis will focus on the GAG biosynthetic pathway and the part in plays in the biology of *A. fumigatus*.

### 1.5 Models of fungal polysaccharide production

Fungi must produce a variety of different exopolysaccharides with overlapping functions in order to produce a protective yet dynamic cell wall capable of responding to the myriad environmental conditions they encounter (189). The biosynthesis of cell wall polysaccharides is orchestrated by the products of many genes within the cell, and upon synthesis must be dispatched to their respective locations in the cell wall. A common theme among exopolysaccharide biosynthetic machinery is their location at cellular membranes, where many polysaccharide synthases are located (190).

### 1.5.1 Synthesis at the plasma membrane

Synthesis of chitin occurs where growth and remodeling are needed by the fungus, such as at the hyphal tips. Chitin is polymerized at the plasma membrane by chitin synthases, which are integral membrane proteins that use cytosolic UDP-GlcNAc as a substrate (139, 189). As chitin is extruded into the extracellular space, linear polymers will hydrogen-bond to form fibrils (191). In *A. fumigatus* there are eight chitin synthase genes, some having either redundant or no apparent function as evidenced by studies of single and combination deletion mutants deficient in these genes (192, 193). For example, ChsC disruption results in a strain that does not differ from wild-type *A. fumigatus* in any detectable way, while disruption of ChsG leads to increased branching and impaired growth and conidiation (192). The most important chitin synthase appears to be ChsE, the disruption of which results in a 30% decrease in chitin content in the cell wall, markedly swollen hyphae and defects in conidiation (190).

Glucans are synthesized in a manner very similar to that of chitin. Glucan synthases are located in the plasma membrane in regions of active hyphal growth, and use UDP-glucose from the cytosol as a substrate (189, 190, 194). Two types of glucans have been observed within the *A. fumigatus* cell wall: β-1,3-glucan and α-1,3-glucan. The synthesis of β-1,3-glucan requires only a single synthase, Fks1, which is essential for normal cell morphology and structural integrity in *A. fumigatus* (189). While deletion of *fks1* is associated with major cell wall fragility and growth impairment, it is not lethal, likely due to compensatory overproduction of chitin (146). Remodeling of β-1,3-glucan takes place within the cell wall and is accomplished by glycosylphosphatidylinositol-anchored glucanosyltransferase (GEL) proteins, which cleave β-1,3-glucan in one strand and join it to another strand. Unlike chitin, β-1,3-glucan is branched, but data on the mechanism behind branching of this polysaccharide is lacking (190). Chitin and β-1,3-glucan are connected by β-1,4 linkages in most fungi including *A. fumigatus* (189). The synthesis of α-1,3-glucan is more complicated, as three α-1,3-glucan synthases (AGS) are found in *A. fumigatus*. Deletion of *ags1* reduces the amount of α-1,3-glucan in the cell wall by half, and double deletion of *ags1* and *ags2* results in altered morphology and conidiation (165). Deletion of all three *ags* genes had little effect on *A. fumigatus* growth. In fact, despite the high α-glucan content of wild-type *A. fumigatus*, in the *ags* triple knockout vegetative growth was normal and although conidiation was minimally reduced,

conidial viability was unaltered. It is therefore unlikely that α-glucans play a significant structural role in the cell wall (195). Complete characterization of α-1,3-glucan synthesis, transport, linkages within the cell wall and remodeling have yet to be completed (165).

### 1.5.2 Intracellular synthesis

Galactomannan (GM) of *A. fumigatus* is among the few fungal polysaccharides that is known to be synthesized intracellularly (196). GM comes in three forms: GM bound to the plasma membrane through an inositolphosphoceramide (IPC) anchor known as lipo-GM, GM covalently bound to β-glucan, or GM secreted into the environment as a free molecule. All three of these are synthesized within the Golgi apparatus. The process begins with polymerization in the lumen of the Golgi by α-mannosyltransferases that use GDP-mannose from the cytosol as a substrate. UDP-galactofuranose (Gal*f*) residues needed to make the side chains of GM are produced from cytosolic UDP-galactopyranose mutase. A transmembrane sugar nucleotide transporter brings UDP-galactofuranose from the cytosol into the lumen of the Golgi, where it is predicted that galactofuranosyl transferases link Gal*f* to the mannan backbone (193, 196). The GM chains then elongate as they transit to the plasma membrane through the trans Golgi (193). The proteins responsible for cross-linking of GM to β-glucan or anchoring to IPC have not been completely characterized (196).

### 1.5.3 Galactosaminogalactan Biosynthesis

The cationic exopolysaccharide GAG is synthesized through the activity of five proteins whose genes are found clustered on chromosome three in *A. fumigatus*. The genes governing GAG synthesis were identified through transcriptomic analysis of non-adherent regulatory mutants (149). The arrangement of the genes in the GAG cluster is similar to that of bacterial operons that encode products for the synthesis of other deacetylated polysaccharides (197) including the bacterial systems for synthesis of polysaccharide intercellular adhesin (*Staphylococcus epidermidis*) and poly-β-1,6-*N*-acetyl-D-glucosamine (*Escherichia coli*) where intracellularly produced monosaccharides are polymerized at the cell membrane and extracellularly deacetylated (197). The function of some of the GAG biosynthetic components are well understood, while others require further study to determine how they are involved in GAG production. The following section details the current model (**Figure 2**) of GAG production in *A. fumigatus*.

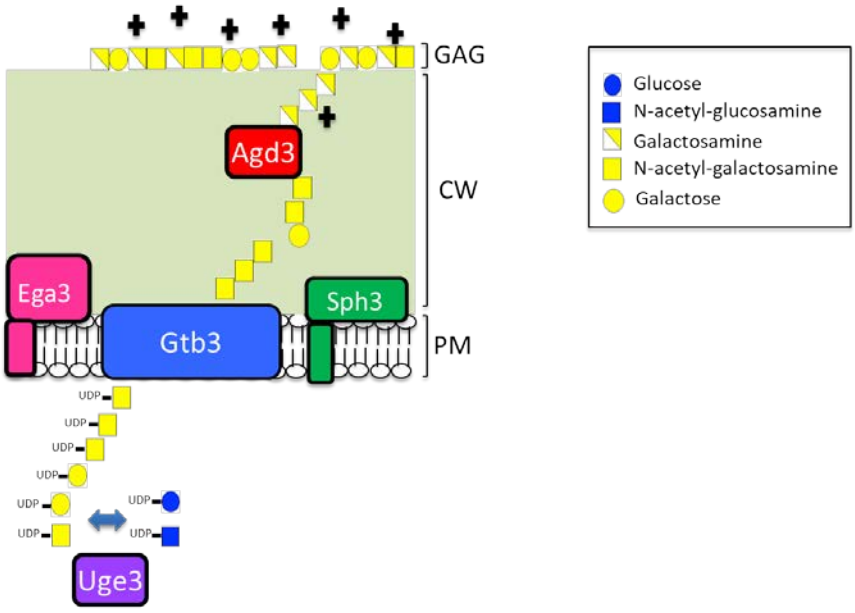


**Figure 2: Diagram of the current model of GAG biosynthesis.**

GAG is a heteropolymer of α-1,4-linked galactose (Gal) and *N*-acetyl galactosamine (GalNAc), that is then partially deacetylated to render the polymer cationic and adhesive (197). Gal and GalNAc pools are produced through the action of the UDP-glucose 4-epimerase Uge3 (Afu3g07910), a group 2 epimerase that can interconvert both UDP-glucose and UDP-*N*-acetylglucosamine into UDP-Gal and UDP-GalNAc, respectively (198). Although other UDP-glucose 4-epimerases are produced by *A. fumigatus*, Uge3 is essential for GAG production as it is the only enzyme that can produce GalNAc, the moiety that will undergo deacetylation and impart GAG with its cationic charge (198, 199). Like other UDP-glucose 4-epimerases, Uge3 contains a conserved SYK (serine, tyrosine, lysine) catalytic triad, as well as a hexagonal arrangement of six amino acids at the active site that perfectly overlapped with a human group 2 UDP-glucose 4-epimerase in homology modelling (198). It is predicted that the UDP-Gal and UDP-GalNAc residues are polymerized by the putative transmembrane glycosyl hydrolase, Gtb3 (Afu3g07860), although this enzymatic activity has yet to be confirmed experimentally (199).

Deacetylation of GalNAc residues to GalN by Agd3 (Afu3g07870) is predicted to occur after polymerization of GAG, and this is supported by evidence that Agd3 is inactive against monosaccharides or short GalNAc oligosaccharides (199). Agd3 is secreted, suggesting that deacetylation is an extracellular process. This hypothesis is supported by the observation that wild-type culture supernatants can complement impaired biofilm formation by deacetylase-deficient *A. fumigatus in vitro* (197). Agd3 is a member of a novel carbohydrate modifying enzyme family, CE18, and functions through the action of a carbohydrate esterase domain, where coordination of a metal ion catalyzes the deacetylation of GalNAc

residues to GalN (199). Deletion of Agd3 does not impair the production of GAG, but results in formation of a fully aceteylated, neutral polymer that is excreted into the environment, and results in a complete loss of adherence of *A. fumigatus* as this GAG no longer adheres to the hyphal cell wall, or to surfaces (197).

The remaining two enzymes in the GAG cluster are the membrane-bound glycoside hydrolases Sph3 (Afu3g07900) and Ega3 (Afu3g07890) (199). Sph3, the founding member of its glycoside hydrolase (GH) family GH135, has been biochemically and structurally characterized (200, 201). The extracellular domain of Sph3 is a barrel composed of eight α-helices and eight β-strands characteristic of GH enzymes. The active site of Sph3 is located on the extracellular face of the plasma membrane to which it is anchored by a transmembrane domain. Enzymatic fingerprinting studies with MALDI-TOF analyses of cleavage products revealed that Sph3 is specific for acetylated GAG (202). Consistent with this finding, co-crystallization studies found that GalNAc binds to the active site of the enzyme, suggesting that Sph3 is an α-1,4-*N*-acetyl galactosaminidase (200, 202). Surprisingly, Sph3 is required for production of GAG, as deletion of *sph3* results in a mutant that does not produce any detectable GAG (200). Three acidic residues in the Sph3 from *A. clavatus*, Asp-166, Glu167 and Glu-222 were found to be necessary not only for optimal hydrolysis of GAG, but also production of GAG, indicating that the enzymatic activity of Sph3 is necessary for synthesis of the polymer (200). It may be counterintuitive that a hydrolytic enzyme would be necessary for production of a polymer, however there are numerous examples of bacterial operons encoding polysaccharide biosynthetic machinery that includes lyases or hydrolases (203). It has been postulated that efficient synthesis and export of GAG may depend on cleavage of the nascent polymer by Sph3 to avoid stalling of the glycosyl transferase (200). Ega3 has been annotated as a potential glycoside hydrolase, and the structural and function confirmation of the role of Ega3 as an endo-α-1,4-polygalactosaminidase is presented in chapter 2 (201).

As hydrolases with the ability to cleave GAG, these proteins have the potential to be used as a therapy to treat IA, either alone or in combination with antifungals. This is particulalry true given the unique nature of GAG and the lack of similar mammalian glycans that could be affected by these enzymes during treatment. Several studies *in vitro* and *in vivo* have explored the antifungal potential of GH therapy, particularly that of Sph3. Recombinant hydrolase domains of Sph3 and Ega3 lacking the transmembrane region were found to both inhibit the formation of *A. fumigatus* biofilms and disrupt pre-formed biofilms *in vitro* (204). Sph3 also potentiates the activity of the azole antifungal posaconazole by hydrolysing GAG and thereby allowing more of the drug to reach its intracellular target (205). Incubation of pulmonary epithelial cells with Sph3 also prevented damage caused by *A. fumigatus* hyphae (205). Intratracheal administration of either Sph3 or Ega3 at the time of infection increased survival in a neutropenic mouse model of *A. fumigatus* pulmonary infection. Interestingly, catalytically active and inactive Sph3 resulted in similar levels of protection, suggesting that the antifungal effects of Sph3 were

not mediated by GAG hydrolysis. Analysis of leukocyte populations in the lungs of these mice indicated that Sph3 itself may have increased neutrophil recruitment to the lungs, and the resulting inflammatory response could have been responsible for the increased survival of the mice (204). However, catalytically inactive Sph3 can bind to GAG and inhibit biofilm formation, therefore it is also possible that the mice were protected from infection through these lectin-like interactions that could have interfered with GAG function (204, 205).

### 1.6 Extracellular vesicles and the transport of polysaccharides and polysaccharide modifying enzymes

Extracellular vesicles (EVs) are small (30 to 200nm in diameter) membrane-bound structures that are secreted from a wide variety of cells. For decades it has been known that *C. neoformans* produces EVs both *in vitro* and *in vivo* as seen in electron micrographs following what was at the time a novel freeze-etching technique (206, 207). Since then, EVs have been described in other yeast, molds, and dimorphic fungi. Fungal EVs are similar to mammalian exosomes in size, protein content, and cellular origin (208, 209). EVs usually bud outward (i.e., away from the cytosol) from endosomal membranes to form multivesicular bodies which then fuse with the plasma membrane to release the vesicles into the environment. The endosomal sorting complexes required for transport (ESCRT) machinery is involved in this process (209, 210). While no specific fungal EV or exosome marker has been discovered, the proteomes of the EVs of these fungi have been compared. EV protein composition was functionally similar across the different species tested but species-specific differences have been observed (211, 212). Common functions of fungal EV proteins include carbohydrate and protein metabolism, stress response and cell wall remodeling (211, 213). These vesicles normally contain a distinct set of nucleic acids, lipids and proteins depending on their function, but mammalian exosomes always contain membrane tetraspanins and Rab GTPases. The exact mechanism of EV release has yet to be elucidated, but EVs in *C. neoformans* tend to be released in damaged areas of the cell wall. Fungal EVs can contain both polysaccharides and glycosyl hydrolases, providing a possible explanation for how large macromolecules can traverse the network of the rigid inner cell wall to reach the outer cell wall or capsule (214, 215). The importance of EVs in the transport of polysaccharides to the outer cell wall has been best demonstrated in the synthesis of the *Cryptococcus neoformans* capsular polysaccharide glucuronoxylomannan (GXM). GXM is a linear polysaccharide composed of an α-1,3-mannose backbone with β-1,2-linked glucuronic acid at the first mannose of every repeating unit. Different serotypes of *C. neoformans* have either β-1,2- or β-1,4-linked xylose residues in different ratios to the other monosaccharide units (216, 217). The building blocks for GXM are GDP-mannose, UDP-glucuronic acid and UDP-xylose. GDP-mannose and UDP-glucuronic acid are produced in the cytosol. UDP-xylose is made from UDP-glucuronic acid via the

UDP-glucuronic acid decarboxylase, the subcellular location of which is unknown (217). Synthesis of GXM takes place in the Golgi apparatus following transport of UDP-mannose from the cytosol (218). The mannan chain is synthesized first, followed by addition of the glucuronic acid and then xylose residues. Once the chain is ready for export, it is hypothesized that vesicles bud from the trans Golgi and become incorporated into a multivesicular body which will then fuse with the plasma membrane, releasing the GXM-containing vesicles for their transit through the cell wall (217, 219). The mechanisms underlying the release of GXM from these EVs and subsequent incorporation into the capsule is not well characterized, but there is evidence to suggest that α-1,3-glucans and chitin play a role in anchoring the capsule to the cell and that incorporation of new capsule polysaccharides occurs near the cell wall (217, 220). *Paracoccidioides brasiliensis* also exports a GXM-like molecule to the outer cell wall in EVs, as determined by recognition with a GXM-EV monoclonal antibody (221).

In addition to their role in polysaccharide transport, EVs of *Candida, Cryptococcus, Fusarium oxysporum* and others can produce EVs containing cell wall remodeling proteins including glycoside hydrolases (212). In *C. albicans,* a strain deficient in EV production exhibited impaired biofilm formation and a reduced polysaccharide content within the extracellular matrix, indicating a role for EVs in polysaccharide-dependent biofilm formation (222). In *S. cerevisiae,* EVs are enriched in β-glucan and chitin synthases and appear to play an important role in maintenance of the cell wall, as mutants with cell wall defects could be protected from cell wall stressors in the presence of *S. cerevisiae* EVs. EVs depleted in chitin synthase did not afford as much protection, further supporting a role for EVs in cell wall repair in this organism (213).

More recently, fungal EVs have been implicated in the modulation of host immune responses. *C. neoformans* EVs can release GXM extracellularly to induce apoptosis of T cells (208, 223). *C. neoformans* EVs may also have an effect on the innate immune system, and can induce the release of TNF-α, IL-10 and TGF-β by RAW264.7 macrophages *in vitro* which enhanced killing of the fungus (224). Conversely, it has been shown that *C. neoformans* EVs cause increased fungal burden *in vivo* in a murine brain infection model (225). Proteins associated with virulence such as laccase (involved in melanin biosynthesis) and urease (which hydrolyses urea to ammonia) have also been found in *C. neoformans* EVs (208). EVs produced by this yeast are easily disrupted by serum albumin, which raises the question of the role of EVs *in vivo*, however they have been found in the bloodstream of patients and in mice after infection (215, 226). EVs containing allergens from the fungus *Malassezia sympodialis* elicited release of IL-4 and TNF-α from PBMCs (227). EVs from several fungal pathogens including *Aspergillus* sp. can elicit a proinflammatory response from macrophages (228, 229). Fungal EVs appear to be phagocytosed, although it remains to be proven whether they fuse with host cell membranes to directly release their contents into the cytoplasm (215).

### 1.6.1 *Aspergillus fumigatus* extracellular vesicles

The EVs produced by *A. fumigatus* are between 100-200nm in size and are constantly released during active growth (229). Proteomics studies have identified the presence of proteins involved in carbohydrate metabolism, cell wall stress response, and pathogenesis in *A. fumigatus* EVs. *A. fumigatus* EVs can stimulate macrophages and neutrophils, and increase their capacity to produce pro-inflammatory cytokines and kill fungi (229). Studies on the biogenesis of *A. fumigatus* EVs were done using protoplasts, which are generated by enzymatic digestion of the *A. fumigatus* cell wall in osmotically stable medium, in order to better visualize the release of the EVs. A network of "fibril-like" material was observed in areas where EVs were located around the surface of the protoplasts, suggesting that EVs assist in cell wall regeneration. Additionally, the amount of EVs released increased during cell wall regeneration in comparison with freshly generated protoplasts, supporting a role in cell wall biogenesis for *A. fumigatus* EVs. Glucose and GAG were found in these EVs, but no evidence of chitin was found (230). There may also be a role for EVs intercellular communication in *A. fumigatus*, as EVs released from the fungus under UV stress were able to be taken up by unstressed fungus, and induced transcription of the *mapk* ortholog *mpkc* as well as *akuA*, which is involved in DNA double stranded break repair (231). Taken together, it is becoming clearer that EVs play an important role not only in pathogenesis, but in maintenance of the fungal cell wall and extracellular matrix.

## 1.7 Hypothesis and research objectives

Given the multiple roles of GAG in mediating *A. fumigatus* virulence, it is a promising target for the development of novel antifungal therapies. Defining the biosynthetic pathways governing GAG production is a key step in the development of novel anti-GAG therapies, which are sorely needed in the face of the high mortality rate of IA (232-234). While significant progress has been made in elucidating the mechanisms underlying GAG biosynthesis, many unanswered questions remain. Chief among these is the function of Ega3 and its role in GAG biosynthesis (149, 197-201). As the other four members of the cluster have been found to be necessary for GAG synthesis, we hypothesized that *ega3* would also be required for GAG production. The contribution of Ega3 to the biosynthesis of GAG is currently not understood and it is difficult to discern what role it would have due to the locations of enzyme and substrate. Ega3 is predicted to be membrane-bound and is annotated as an endo-α-1,4-polygalactosaminidase, which is a family of proteins that hydrolyze polymers of polygalactosamine (200, 235). Galactosamine chains are present within GAG, and are a product of deacetylation by secreted Agd3 and are thus found in the outer cell wall (197, 199). We therefore hypothesize that Ega3 is transported to the outer cell wall in EVs to carry out its role in GAG biosynthesis.

The first objective of this work was to characterize *A. fumigatus* EVs and determine whether they contain Ega3. Next, we sought to disrupt *ega3* and characterize the resulting mutant, which we hypothesized would be deficient in GAG. However, as discussed in chapter 2, Ega3 was not detected in EVs, and we unable to disrupt *ega3* without the occurrence of secondary mutations in GAG synthesis. Further work demonstrated that Ega3 is not required for GAG synthesis or biofilm formation as we had initially hypothesized.

Given these unexpected findings, we hypothesized that *ega3* was a conditionally essential gene in the presence of deacetylated GAG. In chapter 3, we confirmed this hypothesis and discovered a role of Ega3 in protecting the fungal cell membrane from the toxic effects of polycationic GAG. With evidence to suggest that deacetylated GAG is toxic to fungal cell membranes, we also explored the toxicity of GAG to host cell membranes and to determine the direct effects of GAG in the setting of a pulmonary infection. Deacetylated GAG was found to damage and kill human pulmonary epithelial and natural killer cells. A role for GAG in the escape from macrophage phagolysomes was also identified. This work reveals a novel role for GAG as a polysaccharide secreted microbial toxin, and for Ega3 as an antitoxin that protects *A. fumigatus* from the toxic effects of this polymer. These findings underline the importance of GAG as a therapeutic target, and may open avenues for new treatments to combat invasive aspergillosis.

# Chapter 2: Functional characterization of Ega3

## Preface

While much work has been done in characterizing the function of the enzymes responsible for synthesis of GAG in *A. fumigatus*, the function of one of these enzymes, Ega3, had yet to be described. Though previous work from our group described the biochemical functions of Ega3, i.e. which regions of GAG it hydrolyzes and the amino acids involved in hydrolysis of the polysaccharide, the role of Ega3 in biosynthesis of GAG was unknown. Since Ega3 is specific for hydrolysis of deacetylated GAG, which is found in the fungal outer cell wall, and Ega3 was predicted to be a membrane-bound protein, we explored the possibility that Ega3 is carried to the outer cell wall by extracellular vesicles. In this chapter we show the localization and specificity of Ega3, outline the protocol we developed for EV isolation in *A. fumigatus*, and the protein content of the isolated EVs.

## Results

### Ega3 is an endo-α-1,4-polygalactosaminidase containing a transmembrane domain.

A cluster of 5 genes coding for the proteins involved in GAG synthesis was previously discovered through comparative transcriptomic studies of regulatory mutants deficient in biofilm formation (23, 26, 200). Among these 5 genes is *ega3*, annotated as an endo-α-1,4-polygalactosaminidase. When using the predicted amino acid sequence for *A. fumigatus* gene Afu3g07890 (fungidb.org) as an input, the glycoside hydrolase (GH) domain of Ega3 was predicted to belong to GH family GH114, which is comprised of mainly bacterial endo-α-1,4-polygalactosaminidase proteins (http://www.cazy.org, June 22, 2022) (236). Using the same amino acid sequence for *A. fumigatus* Ega3 as above, the TMHMM server predicted that Ega3 contains a transmembrane (TM) domain near the N terminus and a GH domain in the extracellular space near the C terminus of the protein with a linker region joining the two domains (237). This prediction was consistent with protein modeling using the Phyre2 server, which predicts protein folding through alignment with homologous protein sequences. This model was visualized using PyMol software (Schrödinger LLC) (**Figure 1A**) (201, 238) and also revealed a deep electronegative groove (**Figure 1B**). In collaboration with the lab of Dr. P. Lynne Howell at the University of Toronto, purified recombinant Ega3 (residues 46-318, referred to as $Ega3^{46-318}$) was produced in *Pichia pastoris* and co-crystallized with GalN or GalNAc using the hanging drop vapour diffusion method, which allows supersaturation of the protein when liquid evaporates from the hanging drop, leading to crystallization of the protein. The product of this crystallization process was then used for X-ray diffraction at the Canadian Light Source (201, 239). Successful co-crystallization only occurred with GalN, confirming specificity for this monosaccharide at the molecular level and confirming that Ega3 is a member of the GH114 family of hydrolases. Only a slight conformational change was observed upon binding of GalN to the active site of Ega3, with a tunnel containing a tryptophan that is involved in substrate binding forming over the GalN (**Figure 1C**).

Through matrix assisted laser desorption ionization-time of flight mass spectrometry (MALDI-TOF MS) studies of oligosaccharides released after digestion of pre-formed *A. fumigatus* biofilms with $Ega3^{46-318}$, it was found that $Ega3^{46-318}$ hydrolyzes deacetylated regions of GAG, specifically the α-1,4 linkages between two GalN residues (**Figure 1D**). Mutagenesis experiments confirmed that the hydrolytic activity of Ega3 was dependent on acidic Asp and Glu residues in the active site of the protein. Treatment with $Ega3^{46-318}$ was also found to both inhibit and disrupt biofilm formation of *A. fumigatus*, due to hydrolysis of GAG, the essential polysaccharide for biofilm formation in this fungus. Pel-dependent *P. aeruginosa* biofilms are also susceptible to disruption by $Ega3^{46-318}$, which is not unexpected given that Pel and GAG both contain partially deacetylated α-1,4-linked GalNAc, and the similarities between the

structure of Ega3 and PelA hydrolase (201, 236). Taken together, these data demonstrate that Ega3 has specificity for hydrolysis of deacetylated GAG (201).

**Ega3 is localized to the plasma membrane of *A. fumigatus* hyphae.**

The presence of a transmembrane domain within Ega3 suggests that the protein may be located at the plasma membrane. To test this hypothesis, immunofluorescence microscopy was employed to localize Ega3. An anti-GFP polyclonal antibody conjugaged to FITC was used to stain *A. fumigatus* germlings that had been transformed with an Ega3-GFP fusion protein and visualize the compartment in which Ega3 is located. Distinct staining of the perimeter of germlings was observed, indicating that Ega3-GFP is present either in the cytoplasmic membrane or the cell wall of *A. fumigatus* (**Figure 2A**). In order to confirm that Ega3 is present in the plasma membrane and not the cell wall, membrane fractions were isolated from *A. fumigatus* hyphae grown in liquid culture. The fungal biomass was separated from the supernatant and homogenized, and the membrane fraction was isolated through differential centrifugation. This membrane fraction was then trypsinized and underwent protein identification through MS-MS. To identify the peptides present in the sample, the raw data was converted into a format that could be loaded into a search engine, which was used to compare the peptides found in the sample with predicted sequences for *A. fumigatus* Af293. Peptides corresponding to Ega3 were found among the proteins identified (**Figure 2B**). Other proteins known to be present in the membrane fraction of *A. fumigatus,* including α-1,3-glucan synthase, and classic membrane proteins such as plasma membrane ATPase among a host of other predicted membrane proteins were also found, confirming the quality and specificity of the membrane preparation and detection methodology. Collectively, the findings of our microscopy and proteomic studies provide strong evidence that Ega3 is found within the membrane fraction of *A. fumigatus.*

**Ega3 is not transported in EVs.**

Our biochemical studies characterizing the enzymatic activity demonstrated that Ega3 activity is specific to deacetylated GAG and that it is unable to cleave fully acetylated polymer. Previous work from our group has demonstrated that GAG is synthesized at the plasma membrane as a fully acetylated precursor polymer and is only deacetylated upon reaching the outer cell wall by the secreted, extracellular polysaccharide deacetylase Agd3 (197). The presence of Ega3 in the plasma membrane at a distance from its substrate was therefore somewhat surprising.

It is well established in other fungi, particularly the yeasts *C. neoformans* and *S. cerevisiae,* that EVs play an important role in cell wall biogenesis (213, 214). In *C. neoformans,* EVs transport GXM, the main polysaccharide forming the capsule, through the cell wall to be incorporated in the capsule (214). In

*S. cerevisiae*, EVs transport cell wall remodeling enzymes including β-glucan synthase Fks1 and chitin synthase Chs3, and were found to protect Chs3-deficient *S. cerevisiae* from antifungals targeting β-glucan synthesis (213). In *C. albicans*, approximately 40% of EV proteins are cell wall-related (240). In *A. fumigatus* the increased release of EVs when the fungus is in a protoplast state suggests a possible role for vesicles in the regeneration of the cell wall (230).

We therefore hypothesized that Ega3 could be transported to the outer cell wall via EVs where it could then act on its substrate, deacetylated GAG. At the time of these experiments, no studies had been reported describing the isolation or characterization of *A. fumigatus* EVs, therefore we adapted a *Leishmania* exosome isolation protocol for use with *A. fumigatus* (241). Briefly, culture supernatants (CS) were separated from the fungal biomass by filtration and then ultracentrifuged to pellet the EVs. We were able to isolate a relatively pure population of EVs approximately 100nm in diameter without need for separation on a sucrose gradient (**Figure 3A**). We also used this sample for negative staining for TEM, which revealed that the morphology of our EVs was consistent with that of exosomes from *L. major* (**Figure 3B)** (241). However, when EV samples were trypsinized and analyzed using MS-MS, Ega3 was not among the proteins found (**Figure 3C**). Proteins that have been associated with EVs from *C. neoformans* and *C. albicans*, such as actin, tubulin, plasma membrane ATPase, glyceraldehyde phosphate dehydrogenase and various aminopeptidases were present in the sample, helping to validate our EV preparation (**Table 1**) (208, 242). Other cell wall modifying proteins such as the 1,3-β-glucanosyl transferase proteins (also known as the Gel proteins) were found in this EV preparation, highlighting a potential role for polysaccharide modification for *A. fumigatus* EVs as has been reported in other fungi (213, 214, 243). However, while the vesicles we isolated were clearly EVs that contained cell wall proteins like other fungal EVs, Ega3 was not among the proteins found (213, 214). Therefore, while our data supports a role of *A. fumigatus* EVs in cell wall production/maintenance, they are unlikely used to transport Ega3 to the outer cell wall to hydrolyze GAG.

***Conclusion***

Ega3 is a member of the GAG biosynthetic cluster and is specific for hydrolysis of α-1,4-linked GalN, which is found in the outer cell wall as a product of GalNAc deacetylation by secreted Agd3. However, Ega3 also has a TM domain, anchoring it to the membrane and is found in the membrane fraction of *A. fumigatus*. We therefore hypothesized a model where Ega3 would be transported from the plasma membrane to the outer cell wall by way of EVs. Surprisingly, while we were able to document that *A. fumigatus* produces EVs that contain cell wall remodeling enzymes, Ega3 was not among them. This observation suggested the need to re-examine the role of Ega3 in GAG biosynthesis. The role of

Ega3 in the synthesis of GAG is further elucidated in Chapter 3, through the construction and characterization of an *ega3*-null mutant strain of *A. fumigatus*.

**Tables and Figures**

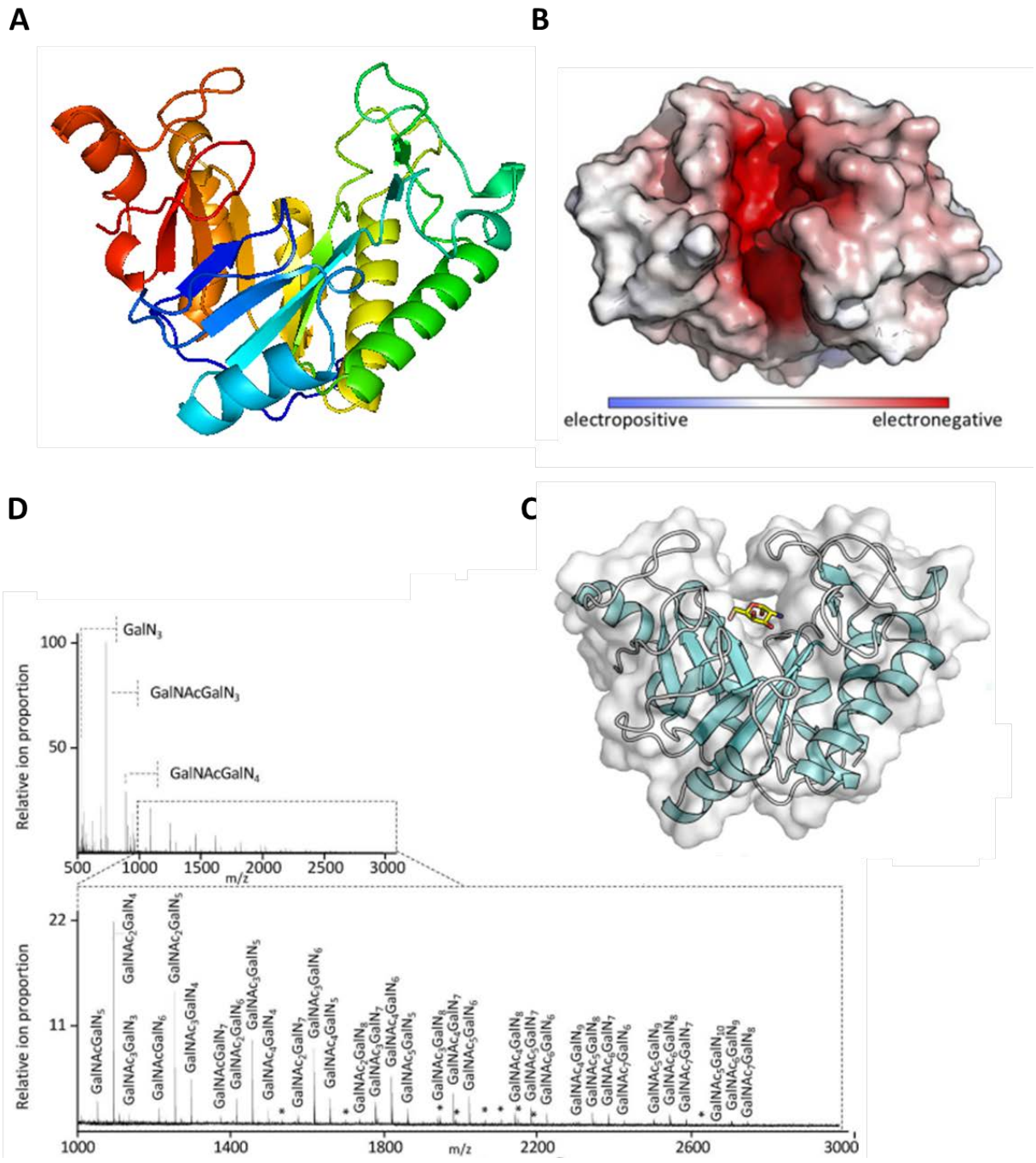


**Figure 1: Ega3 is a glycoside hydrolase specific for deacetylated regions of GAG. A)** The predicted structure of the GH domain of Ega3 (N-terminus in red, C-terminus in blue). **B)** Map of predicted electronegative regions of the GH domain of Ega3. **C)** Structure of Ega3 bound to GalN with transparent overlay of surface in space-filling representation. **D)** Oligosaccharide spectra generated by MALDI-TOF MS analysis of Ega3-digested biofilms showing that Ega3 hydroyzes GalN-GalN bonds. # represents oligosaccharide reducing ends.

**A**

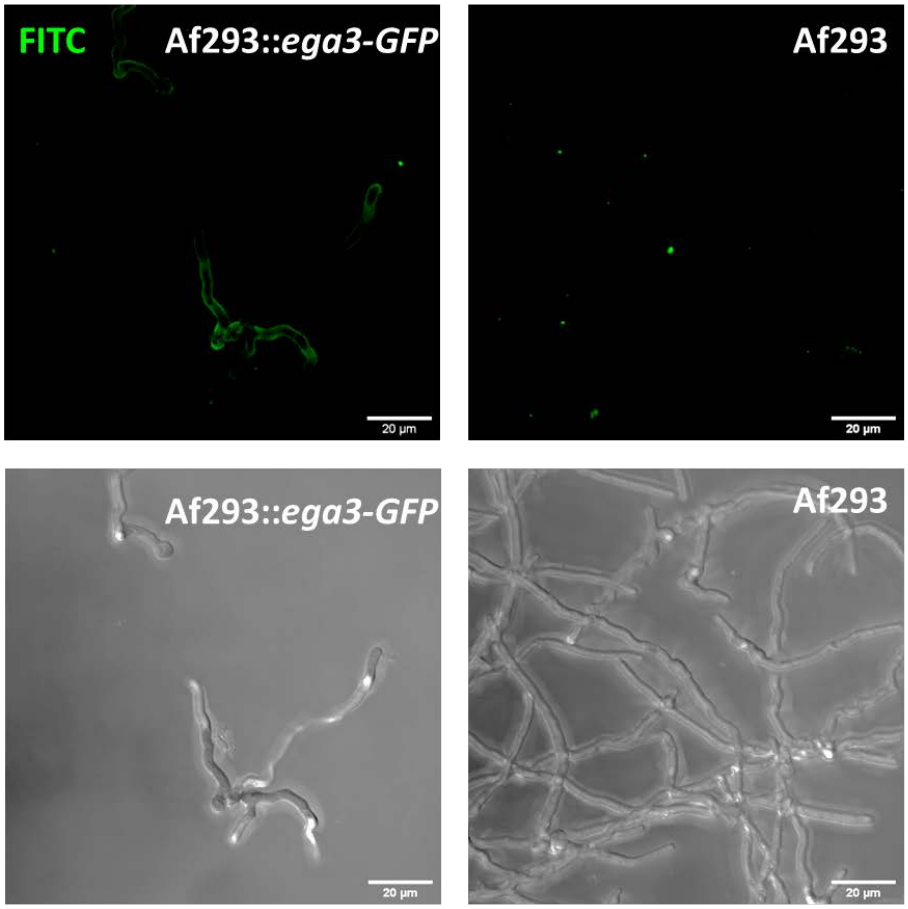


**B**

Display Options: Total Unique Peptide Count | Req Mods: No Filter | Search: endo

Probability Legend: over 95% | 80% to 94% | 50% to 79% | 20% to 49% | 0% to 19%

Bio View: 1156 Proteins in 973 Clusters With 1145 Filtered Out

| # | Visible? | Starred? | | Accession Number | Alternate ID | Molecular Weight | Protein Grouping Ambiguity | Af293 |
|---|---|---|---|---|---|---|---|---|
| 1 | ☑ | ☆ | Endo-chitosanase OS=Aspergillus fumigatus Z5 OX=1437362 GN=Y699_03669 PE=... | A0A0J5PSJ4 (+2) | Y699_03669 | 25 kDa | | 4 |
| 2 | ☑ | ☆ | Endo alpha-1,4 polygalactosaminidase OS=Aspergillus fumigatus Z5 OX=1437362 ... | A0A0J5PZB5 (+3) | Y699_01765 | 42 kDa | | 4 |
| 3 | ☑ | | Cluster of Proteasome endopeptidase complex OS=Aspergillus fumigatus Z5 OX=1... | A0A0J5Q690 [4] | Y699_03794 | 30 kDa | ★ | 6 |
| 4 | ☑ | ☆ | Glucan endo-1,3-beta-glucosidase eglC OS=Aspergillus fumigatus Z5 OX=1437362 ... | A0A0J5PSU6 (+3) | Y699_07606 | 45 kDa | | 4 |
| 5 | ☑ | ☆ | Aspartic endopeptidase Pep2 OS=Aspergillus fumigatus Z5 OX=1437362 GN=Y699... | A0A0J5PY94 (+3) | Y699_01415 | 43 kDa | | 3 |
| 6 | ☑ | ☆ | L-PSP endoribonuclease family protein (Hmf1) OS=Aspergillus fumigatus Z5 OX=14... | A0A0J5PHV4 (+4) | Y699_08932 | 13 kDa | | 2 |
| 7 | ☑ | ☆ | Aspartic-type endopeptidase, putative OS=Neosartorya fumigata (strain ATCC MY... | Q4WPI7 | AFUA_4G09400 | 68 kDa | | 1 |
| 8 | ☑ | ☆ | Endosomal cargo receptor (Erp5), putative OS=Neosartorya fumigata (strain ATCC ... | Q4WNY5 | AFUA_4G07390 | 26 kDa | | 1 |
| 9 | ☑ | ☆ | Endosomal cargo receptor (Erv25), putative OS=Aspergillus fumigatus Z5 OX=143... | A0A0J5Q3K3 (+3) | Y699_04833 | 25 kDa | | |
| 10 | ☑ | ☆ | Endosomal cargo receptor (P24), putative OS=Aspergillus fumigatus Z5 OX=14373... | A0A0J5PWK4 (+5) | Y699_08128 | 24 kDa | | |

**Figure 2: Ega3 is found at the plasma membrane of *A. fumigatus.* A)** Confocal images of germlings of *A. fumigatus* expressing an Ega3-GFP fusion protein (left) and the Af293 strain (right) stained with an anti-GFP antibody conjugated to FITC. The phase-contrast image channel is shown below for each sample. **B)** Search results for peptides detected by tandem mass spectrometry from a membrane fraction isolated from *A. fumigatus* hyphae indicating the presence of Ega3.

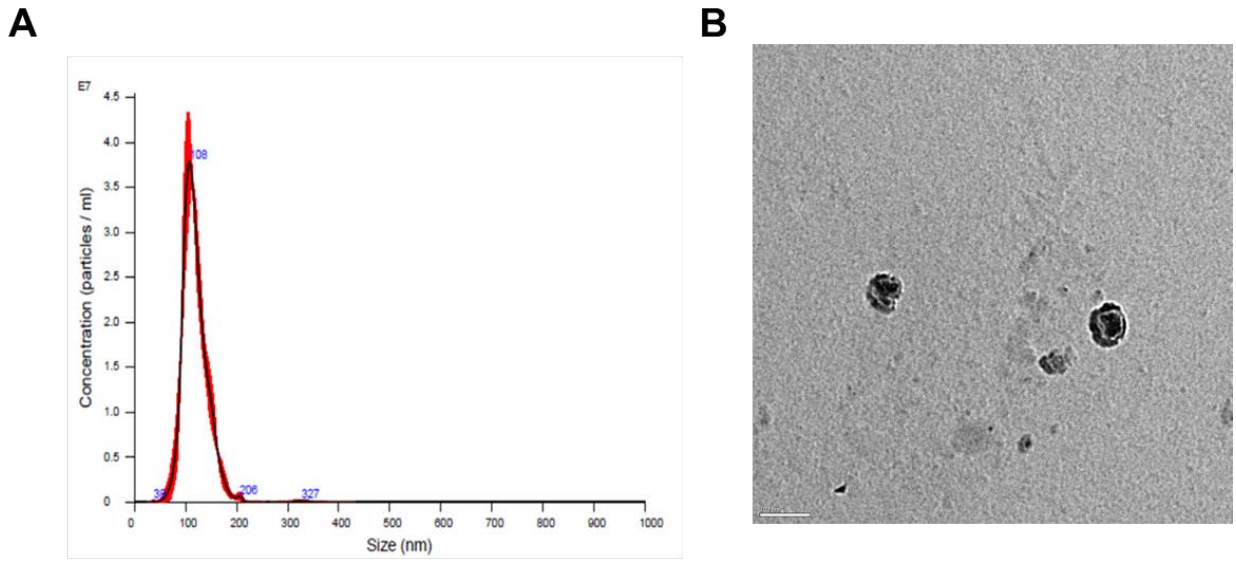


**Figure 3: Isolation of relatively pure EVs from three-day *A. fumigatus* liquid shaking cultures. A)** Nanoparticle tracking analysis reveals a nearly pure population of vesicles measuring approximately 100nm in diameter after filtration of liquid cultures to remove biomass and two subsequent centrifugations at 100,000x*g*. **B)** Negative staining of vesicles isolated from *A. fumigatus* with uranyl acetate viewed using transmission electron microscopy. Scale bar is equal to 100 nm.

**Table 1.** Proteins identified from pooled *A. fumigatus* EV samples listed in order of peptide abundance. Whether they have been found in the list of published peptides from *A. fumigatus* EVs is indicated.

| Accession number | Gene product/predicted function | Previously found in A. fumigatus EVs? |
|---|---|---|
| Afu5g02330 | AspF1 | Yes |
| Afu1g11460 | Bgt1 | Yes |
| Afu5g10490 | Putative amidase | Yes |
| Afu4g01290 | Endo-chitosanase, pseudogene | No |
| Afu2g01170 | Gel1 | Yes |
| Afu3g00840 | FAD-dependent oxygenase, putative | No |
| Afu4g09030 | Aminopeptidase | No |
| Afu3g00270 | Bgt2 | No |
| Afu4g06820 | Ecm33 | Yes |
| Afu1g14560 | MsdS | No |
| Afu5g01200 | Cp6 | No |
| Afu7g00940 | Isoamyl oxidase, putative | No |
| Afu1g16190 | AspF9 | Yes |
| Afu1g17590 | Phosphoesterase superfamily protein | No |
| Afu2g05340 | Gel4 | Yes |
| Afu2g03730 | Ctr copper transporter family protein | Yes |
| Afu6g04570 | translation elongation factor eEF-1 subunit gamma, putative | Yes |
| Afu3g07640 | Pma1 | Yes |
| Afu4g03660 | Acid phosphatase, putative | No |
| Afu3g03060 | AspF34 | No |
| Afu3g00880 | GPI-anchored membrane protein | Yes |
| Afu2g03120 | Utr2 | Yes |
| Afu1g04130 | FG-GAP repeat protein, putative | No |
| Afu6g11390 | Gel2 | No |
| Afu2g09030 | DppV | Yes |
| Afu5g13300 | Pep1 | No |
| Afu4g03490 | Tripeptidyl peptidase Sed2 | No |
| Afu6g08510 | Crh1 | No |
| Afu6g03620 | MreA | Yes |
| Afu4g13770 | Glycosyl hydrolase, putative | No |
| Afu6g00310 | CpdS | No |

| | | |
|---|---|---|
| Afu1g01180 | Not found | No |
| Afu3g14980 | CsnC | No |
| Afu6g00430 | IgE-binding protein | Yes |
| Afu3g14680 | Plb3 | Yes |
| Afu3g12690 | GlfA | Yes |
| Afu4g14640 | FetD | No |
| Afu5g03540 | Thioredoxin reductase, putative | No |
| Afu2g00690 | Glucan 1,4-alpha –glucosidase, putative | No |
| Afu4g06670 | AspF7 | No |
| Afu7g02340 | L-PSP endoribonuclease family protein (Hmf1), putative | Yes |
| Afu3g03610 | Conserved hypothetical protein | Yes |
| Afu5g01990 | BYS1 domain protein, putative | Yes |
| Afu4g13990 | Not found | No |
| Afu4g12450 | conserved lysine-rich protein, putative | Yes |
| Afu2g14480 | oxidoreductase, FAD-binding, putative | No |
| Afu5g10520 | alpha-1,2-mannosidase family protein | No |
| Afu1g16600 | ribonuclease T2, putative | Yes |
| Afu6g04690 | Conserved hypothetical protein | No |
| Afu3g00550 | Hypothetical protein | No |
| Afu4g09890 | Conserved hypothetical protein | No |
| Afu2g05240 | Conserved hypothetical protein | N0 |
| Afu5g01970 | GpdA | Yes |
| Afu5g14740 | FleA | No |
| Afu2g07500 | PepP | Yes |
| Afu1g03570 | PhoA | Yes |
| Afu6g02800 | Uncharacterized protein | Yes |
| Afu5g02820 | Conserved hypothetical protein | No |
| Afu5g08030 | extracellular cellulase CelA/allergen Asp F7-like, putative | No |
| Afu5g13730 | NlpC/P60-like cell-wall peptidase, putative | No |
| Afu5g03760 | ChiA1 | Yes |
| Afu2g12630 | AspF13 | No |
| Afu3g02253 | Not found | Yes |
| Afu2g12850 | Gel3 | No |

| | | |
|---|---|---|
| Afu4g08960 | GPI anchored cell wall protein, putative | Yes |
| Afu1g17400 | peptidase S41 family protein | No |
| Afu5g14510 | beta-lactamase, putative | No |
| Afu3g00310 | extracellular phytase, putative | No |
| Afu4g00280 | conserved hypothetical protein | No |
| Afu8g01970 | Probable endopolygalacturonase B | No |
| Afu1g04040 | UbiA | Yes |
| Afu6g10610 | ribose 5-phosphate isomerase A | Yes |
| Afu1g11400 | alpha/beta fold family hydrolase, putative | No |
| Afu7g03970 | conserved hypothetical protein | Yes |
| Afu8g04890 | conserved hypothetical protein | Yes |
| Afu5g09230 | transaldolase | Yes |
| Afu3g14940 | AeiA | No |
| Afu2g00220 | Aminopeptidase, putative | Yes |
| Afu5g09210 | Alp2 | Yes |
| Afu8g01710 | antigenic thaumatin domain protein, putative | Yes |
| Afu1g02550 | tubulin alpha-1 subunit | Yes |
| Afu3g01360 | siderochrome-iron transporter, putative | Yes |
| Afu5g10380 | Probable pectin lyase A | No |
| Afu3g00320 | XynF11A | No |
| Afu3g14910 | FacC-like extracellular signaling protein, putative | No |
| Afu5g00600 | NPP1 domain protein, putative | No |
| Afu5g08700 | myosin type II heavy chain, putative | Yes |
| Afu6g00770 | extracellular arabinanase, putative | No |
| Afu1g14810 | serine/threonine protein kinase (Kin4), putative | Yes |
| Afu1g17050 | Hypothetical protein | No |
| Afu2g00760 | Probable pectate lyase A | No |
| Afu3g00590 | AspHS | No |
| Afu5g00800 | Conserved hypothetical protein | No |
| Afu6g09740 | GliT | No |
| Afu8g00930 | Endo-chitinase | No |
| Afu2g00800 | PelA | No |
| Afu2g03030 | Prp8 | Yes |

| | | |
|---|---|---|
| Afu4g06700 | GPI anchored cell wall protein, putative | No |
| Afu3g09250 | Crh3 | Yes |
| Afu3g00420 | acetyl xylan esterase (Axe1), putative | No |
| Afu7g04910 | phosphatidylglycerol specific phospholipase C, putative | No |
| Afu5g10930 | Conserved hypothetical protein | No |
| Afu1g10590 | GPI anchored protein, putative | Yes |
| Afu3g00340 | Glycosyl hydrolase, putative | Yes |
| Afu1g06910 | arabinogalactan endo-1,4-beta-galactosidase GalA | No |
| Afu6g10300 | AspF28 | Yes |
| Afu4g04318 | Not found | Yes |
| Afu7g06750 | phosphoglycerate mutase family protein, putative | No |
| Afu2g05000 | Proline iminopeptidase | Yes |
| Afu5g02130 | Probable alpha-galactosidase B | No |
| Afu3g09690 | extracellular thaumatin domain protein, putative | No |

# Chapter 3: Construction and characterization of an *ega3* null mutant strain

**Preface**

In the previous chapter we showed that Ega3 is not transported by EVs to the outer cell wall, however this did not bring us closer to answering the question of how Ega3 is involved in the synthesis of GAG. Previous studies have demonstrated that four of the five proteins encoded within the GAG biosynthetic clusters (Uge3, Agd3, Sph3, and Gtb3) are all necessary for the production of adhesive GAG. We therefore hypothesized that Ega3 would also be required for GAG synthesis and subsequent biofilm formation. In this chapter, we investigated this hypothesis by disrupting *ega3*, characterizing the mutant and then complementing the *ega3* null mutant with a wild-type *ega3* allele. Disruption of *ega3* was not successful using our traditional methods, but we were able to utilize CRISPR/Cas9 and a modified version of our classic split marker method in order to disrupt *ega3* in two different strain backgrounds of *A. fumigatus*. In doing so, we showed that Ega3 does not play a role in synthesis of GAG and is dispensable for biofilm formation.

## Results

### Disruption of *ega3* in two *A. fumigatus* strain backgrounds.

To date, all mutant strains of *A. fumigatus* in which GAG biosynthetic cluster genes have been deleted have been found to be deficient in the production of deacetylated GAG and biofilm formation. We therefore hypothesized that Ega3 would be also be required for GAG biosynthesis and biofilm formation (197, 198, 200, 201). To test this hypothesis, we set out to disrupt *ega3* in *A. fumigatus*. Initial attempts at gene disruption were carried out in the wild-type *A. fumigatus* isolate Af293 which had been used successfully to construct disruption mutants for the 4 other genes within the GAG biosynthetic gene cluster. Surprisingly, repeated attempts to delete *ega3* in this strain resulted in a lack of viable transformants, transformants in which the resistance marker was inserted ectopically, or transformants in which successful integration of the disruption cassette was accompanied by a duplication of the wild-type *ega3* gene at its native locus. These gene duplications were detected by PCR analysis of the *ega3* locus in which primers flanking the deletion locus yielded products consistent with both wild-type ega3 and successful integration of the disruption cassette. We therefore switched to the Δ*akuB*$^{Ku80}$ strain (henceforth referred to as "Ku80") which is often used for its improved transformation efficiency. The Ku80 strain is a mutant of the *A. fumigatus* clinical isolate CEA10 that is deficient in the homolog of the human Ku80 protein (coded by the *akuB* gene in *A. fumigatus*) and as a result has a decreased ability to undergo nonhomologous end joining, reducing the likelihood of genetic constructs being integrated at off-target sites. The transformations done to disrupt *ega3* in the Ku80 strain were as unsuccessful in generating an *ega3* deletion strain as the transformations done in Af293 (**Table 1**) (244). In light of these repeated failed transformations we hypothesized that *ega3* could be an essential gene. However, to ensure the failure to generate deletion mutants was not a consequence of our disruption strategy or methodology, we tested two alternative strategies for *ega3* deletion: disruption using CRISPR/Cas9 in strain Af293, and transformation of the Ku80 strain with different flanking sequences that excluded *ega3* terminator which was predicted to have a complex secondary structure (**Table 1**). Surprisingly, both of these strategies yielded single Δ*ega3* clones as verified by genomic PCR and qRT-PCR gene expression analysis (**Figure 1A**).

Since Ega3 is a member of the GAG cluster, and GAG is the principal determinant of biofilm formation, we next studied whether the two Δ*ega3* clones were able to produce GAG and, as a consequence, form an adherent biofilm. To test biofilm formation, the Δ*ega3* mutants and their respective parent strains were grown in 96 well plates for 20 hours and then vigorously washed. The remaining biomass was stained with crystal violet. Neither of the Δ*ega3* clones remained adherent to the plate after washing (**Figure 1B**), as has been observed with other GAG-deficient mutants. To confirm that the biofilm defect of these two strains was due to a lack of production of adhesive, deacetylated GAG, we

performed a plastic-capture GAG detection assay where high-binding plates were incubated with CS of the strains of interest to capture soluble deacetylated GAG, which was then detected using a combination of biotinylated GAG-specific lectin (soybean agglutinin, SBA) and avidin-HRP. Consistent with their lack of adherent biofilm, deacetylated GAG was not detected in culture supernatants from either the Δ*ega3*$^{CRISPR}$ or Δ*ega3*$^{Ku80}$ strain (**Figure 2A**). This deficiency in adhesive GAG production was confirmed by confocal imaging of germlings stained with SBA-FITC, once again revealing that there was no GAG detected on the hyphal surface (**Figure 2B**). Collectively, these findings strongly suggest that the loss of Ega3 leads to a failure to produce GAG, and as a consequence, impaired biofilm formation.

To confirm that the phenotype of the two Δ*ega3* clones was a consequence of *ega3* deletion, we reintroduced a wild-type allele of *ega3* allele into each strain. Different strategies were used for the Δ*ega3*$^{CRISPR}$ and Δ*ega3*$^{Ku80}$ strains. For the Δ*ega3*$^{CRISPR}$ strain, the *ega3* allele was reintroduced at the native locus using a CRISPR/Cas9 repair strategy. Briefly, an *ega3* allele with a synonymous single nucleotide polymorphism (SNP) was used as a repair template with guide RNAs targeted to make cuts at two sites, one on either side of the hygromycin cassette that had been used to disrupt *ega3*. The SNP-containing template was employed to distinguish between true repair of the locus and not simply recovery of contaminating wild-type *A. fumigatus*. For the Δ*ega3*$^{Ku80}$ strain, the entire *ega3* locus was cloned with flanking sequences homologous to the upstream and downstream regions of the *akuB* gene to use as a construct for gene complementation. This approach was required since ectopic insertion of the wild-type allele, the standard approach for complementation, is nearly impossible in Ku80 due to this strain's deficiency in non-homologous recombination. The *akuB* locus was chosen as a "safe" site for insertion as it had been previously disrupted to generate the Ku80 parent strain.

Genetic and protein complementation of both Δ*ega3* clones was successful as determined by qRT-PCR and Western blotting, respectively (**Figure 3A, 3C**). Surprisingly however, despite restoration of *ega3* expression, biofilm formation was not restored in either clone as determined by crystal violet assay (**Figure 3B, 3D**). Although gene expression and protein production of Ega3 exceeded wild-type levels in the Δ*ega3*$^{CRISPR}$ strain, this was not the case in Δ*ega3*$^{Ku80}$ where expression of *ega3* was at about 25% of parent strain levels in all 3 isolated clones (**Figure 3E**). We therefore hypothesized that at least in the Δ*ega3*$^{Ku80}$ strain, failure to complement biofilm formation could be due to the relatively low levels of *ega3* expression. To address this issue, a tetracycline-inducible *ega3* allele was introduced into the Δ*ega3*$^{Ku80}$ strain, again at the *akuB* locus. Despite expression of *ega3* at levels that greatly exceeded Ku80 *ega3* expression (**Figure 3F**), biofilm formation was not restored (**Figure 3G**) in this strain. Taken as a whole, these findings suggested that the deficiency in biofilm adherence and GAG production in the Δ*ega3*$^{Ku80}$ and *ega3*$^{CRISPR}$ mutant strains was not a consequence of the loss of *ega3*.

**The impaired biofilm formation of the Δ*ega3*$^{CRISPR}$ and Δ*ega3*$^{Ku80}$ strains are due to secondary mutations in genes required for GAG biosynthesis.**

The failure to complement the biofilm formation defect in either Δ*ega3* strain with reinsertion of a wild-type *ega3* allele suggested the presence of a secondary mutation impairing biofilm formation in these strains. Since *A. fumigatus* biofilm formation requires the production of deacetylated GAG, we hypothesized that these secondary mutations may lie within genes in the GAG biosynthetic pathway (197, 198, 200). To test this hypothesis, we first measured expression of the GAG biosynthetic cluster genes in both the Δ*ega3*$^{CRISPR}$ strain and Δ*ega3*$^{Ku80}$ mutants by qRT-PCR. Expression of *agd3, gtb3, sph3* and *uge3* were normal in the Δ*ega3*$^{Ku80}$ mutant (**Figure 4C**), however expression of *agd3* was found to be undetectable in both the Δ*ega3*$^{CRISPR}$ mutant and complemented strain (**Figure 4A**). Previous work from our group has demonstrated that a deficiency of Agd3 results in the production of fully acetylated GAG that is non-adhesive, and cannot support biofilm formation. The absence of Agd3 therefore may underlie the impaired biofilm formation by the Δ*ega3*$^{CRISPR}$ strain and explain the failure of complementation of Δ*ega3*$^{CRISPR}$ strain with a wild-type allele *ega3* allele to restore biofilm formation in this strain (197). To confirm a potential *agd3* mutation in the Δ*ega3*$^{CRISPR}$ strain we performed a PCR analysis of the *agd3* locus to assess for potential deletions or insertions. These studies revealed that a portion of the 3' end of *agd3* was deleted in the Δ*ega3*$^{CRISPR}$ strain (**Figure 4B**). The deleted segment of *agd3* was located in the region where the primers used for quantification of *agd3* expression by qRT-PCR would normally bind, suggesting that, consistent with our expression data, while a mutated Agd3 transcript may be produced in the Δ*ega3*$^{CRISPR}$ mutant, it would not be detectable using qRT-PCR.

Strains deficient in Agd3 produce fully acetylated GAG that is non-adhesive and cannot support biofilm formation. To determine if the mutation in *agd3* detected in the Δ*ega3*$^{CRISPR}$ strain led to an Agd3-deficient phenotype, we sought to confirm the production of acetylated GAG by this strain. GC-MS analysis of dialyzed culture supernatants from this Δ*ega3*$^{CRISPR}$ and complemented strain revealed the presence of GalNAc in the secreted polysaccharide fraction of both strains (**Figure 5A**). Since in *A. fumigatus* GalNAc is uniquely found in GAG, this finding is consistent with the production of GAG by this mutant (149, 198). To confirm that the Δ*ega3*$^{CRISPR}$ strain produced fully acetylated GAG we sought to determine the effects of complementing with exogenous recombinant Agd3 (rAgd3). To this end, CS produced by the Δ*ega3*$^{CRISPR}$ mutant were combined with rAgd3 and tested for the presence of deacetylated GAG using the GAG plastic capture assay described previously. Of note, in this assay only deacetylated, but not acetylated, GAG binds to anionic plastic within a microtiter plate. Deacetylated GAG was detected in culture supernatants of the Δ*ega3*$^{CRISPR}$ strain only upon addition of rAgd3, suggesting production of fully acetylated GAG by this strain despite the absence of *ega3* (**Figure 5B**). This was further confirmed by staining of germlings with SBA-FITC for visualization with confocal

microscopy. GAG adherent to the surface of the hyphae was observed only when the Δ*ega3*$^{CRISPR}$ strain was incubated with rAgd3. Although the conidia of the untreated Δ*ega3*$^{CRISPR}$ strain were also stained by SBA, this observation has been previously noted in other GAG-deficient strains and is not representative of GAG on the conidia (**Figure 5D**). To test if failure to produce deacetylated GAG was responsible for the biofilm defect of the Δ*ega3*$^{CRISPR}$ strain, the ability of the Δ*ega3*$^{CRISPR}$ strain to form a biofilm in the presence of rAgd3 was evaluated. Addition of rAgd3 to Δ*ega3*$^{CRISPR}$ resulted in the formation of adherent biofilms, suggesting that the defect in biofilm formation exhibited by this strain is indeed a consequence of a secondary deficiency of Agd3. By extension, these findings also suggest that Ega3 is dispensable for biofilm formation (**Figure 5C**).

To determine if the biofilm-deficiency of the Δ*ega3*$^{Ku80}$ strain was also a consequence of a secondary mutation affecting GAG biosynthesis, a similar approach was taken. As noted, and in contrast to the findings in the Δ*ega3*$^{CRISPR}$ strain, the genes within the GAG biosynthesis cluster were expressed at wild-type levels in the Δ*ega3*$^{Ku80}$ mutant (**Figure 4C**). This observation however, did not exclude the possibility of a mutation that could affect GAG production without altering GAG biosynthetic gene expression. We therefore analyzed the monosaccharide content of CS isolated from the Δ*ega3*$^{Ku80}$ to determine if GAG was produced by this strain. GC-MS analysis of the monosaccharide content of secreted glycans from the Δ*ega3*$^{Ku80}$ mutant and complemented strains revealed a complete absence of GalNAc, suggesting that no GAG polymer is produced by these strains, and that there is likely a mutation within one or more of the GAG biosynthetic genes that prevents polymer synthesis (**Figure 6**).

To identify potential mutations in genes required for GAG biosynthesis, whole genome sequencing of the Ku80 parent and Δ*ega3*$^{Ku80}$ was performed using the ultra-long read single molecule real time (SMRT) sequencing platform from PacBio. The Ku80 genome was first reconstructed using the closely related *A. fumigatus* A1163 genome as a reference, since there is no published genomic sequence for Ku80 (245). Upon comparison of the reconstructed genomes of Ku80 and Δ*ega3*$^{Ku80}$, a small inversion in the *uge3* sequence from Δ*ega3*$^{Ku80}$ was detected (**Figure 7A**). The mutation was confirmed by Sanger sequencing (data not shown). As *uge3* is required for GAG synthesis, a mutation in this gene is consistent with the lack of GAG production observed in the Δ*ega3*$^{Ku80}$ mutant.

To explore the consequences of this sequence inversion, *in silico* modelling of the wild-type and mutant Uge3 proteins was performed. An overlay of the two models revealed that they were nearly identical except for a single loop region (**Figure 7B**). Within this region I-TASSER modelling identified an R384P mutation in a region that was predicted to be important for UDP-sugar binding, suggesting that this mutation likely impairs the enzymatic activity of the protein. Taken as a whole, our findings suggest that, in contrast to what has been observed with the other four genes within the GAG biosynthesis cluster, *ega3* is not essential for GAG production and biofilm formation.

***Conclusion***

Two *ega3*-deficient mutants were generated using two strategies in two different strain backgrounds. Both lacked the ability to produce deacetylated GAG, suggesting that *ega3* may be conditionally essential in the presence of this cationic molecule. The Δ*ega3*$^{CRISPR}$ strain was able to produce fully acetylated GAG, and form biofilms when complemented with rAgd3, therefore suggesting that Ega3 is not required for GAG biosynthesis and biofilm formation as was previously hypothesized.

**Tables and Figures**

**Table 1. Strategies used to disrupt *ega3*.** Unless otherwise stated, disruption was attempted using the split marker technique (246).

| Strain transformed (n) | Outcome |
|---|---|
| **Af293 (9)** | Gene duplication/ectopic insertion of marker |
| **Δ*uge3* (8)** | Gene duplication/ectopic insertion of marker |
| **Δ*agd3* (6)** | Gene duplication/ectopic insertion of marker |
| **Ku80 (3)** | No viable clones/ectopic insertion of marker/unknown secondary mutation |
| **Δ*uge3*$^{Ku80}$ (1)** | Gene duplication |
| **Af293*** | Successful deletion of *ega3* |
| **Ku80**** | Successful deletion of *ega3* |

*CRISPR/Cas9
**Classic split marker approach using different 3' homology sequence

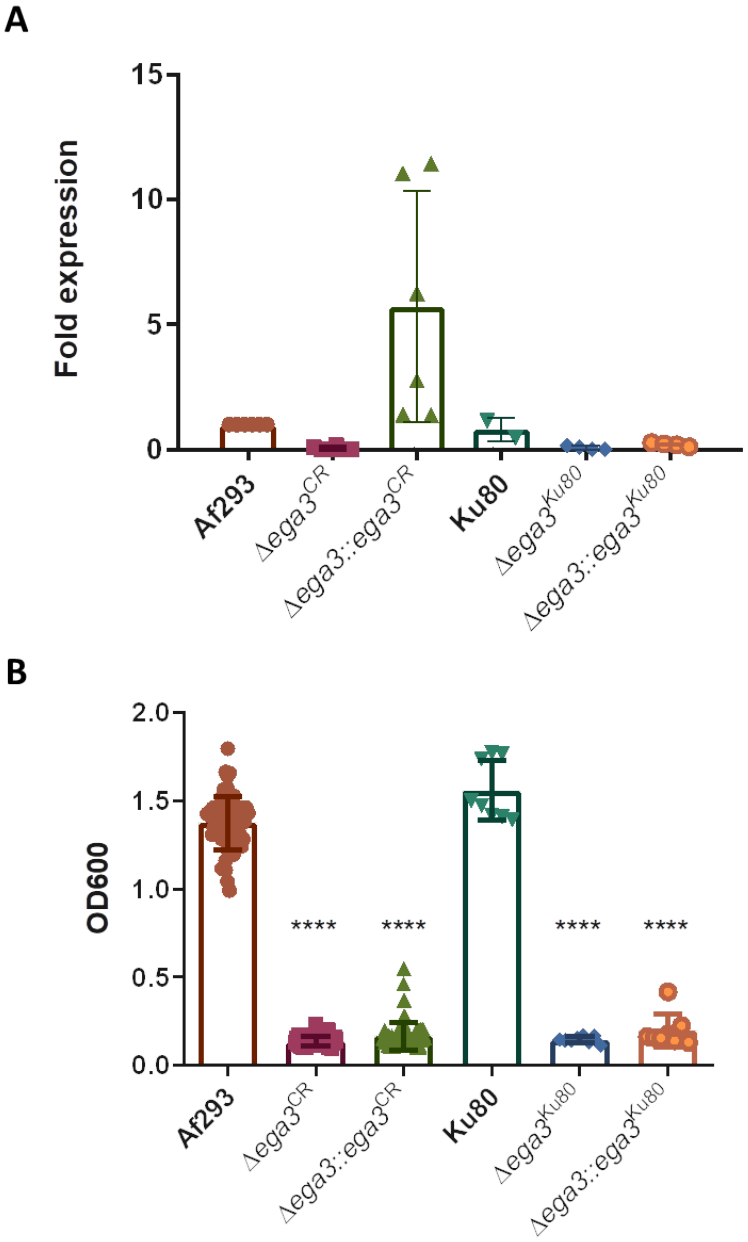


**Figure 1: Disruption of *ega3* in *A. fumigatus* abrogates *ega3* expression and results in impaired biofilm formation. A)** Expression of *ega3* in *ega3* null mutants grown for 18 hours in YPD medium as measured by qRT-PCR and normalized to the expression of *ega3* in the wild-type Af293 strain (fold expression over Af293). Bars indicate combined means of 4 (Δ*ega3*$^{Ku80}$ strain) and 6 (Δ*ega3*$^{CRISPR}$ strain) experiments with 2-3 technical replicates for each condition and error bars represent standard deviation. **B)** Crystal violet staining of residual adherent biofilm formed by the indicated strains following washing. Bars represent mean +/- standard deviation. **** indicates P<0.0001 as determined by one-way ANOVA with Dunnett's multiple comparison test. n=2 biological replicates for the CRISPR strain set, n=1 biological replicate for the Ku80 strain set with three technical replicates for each experimental condition.

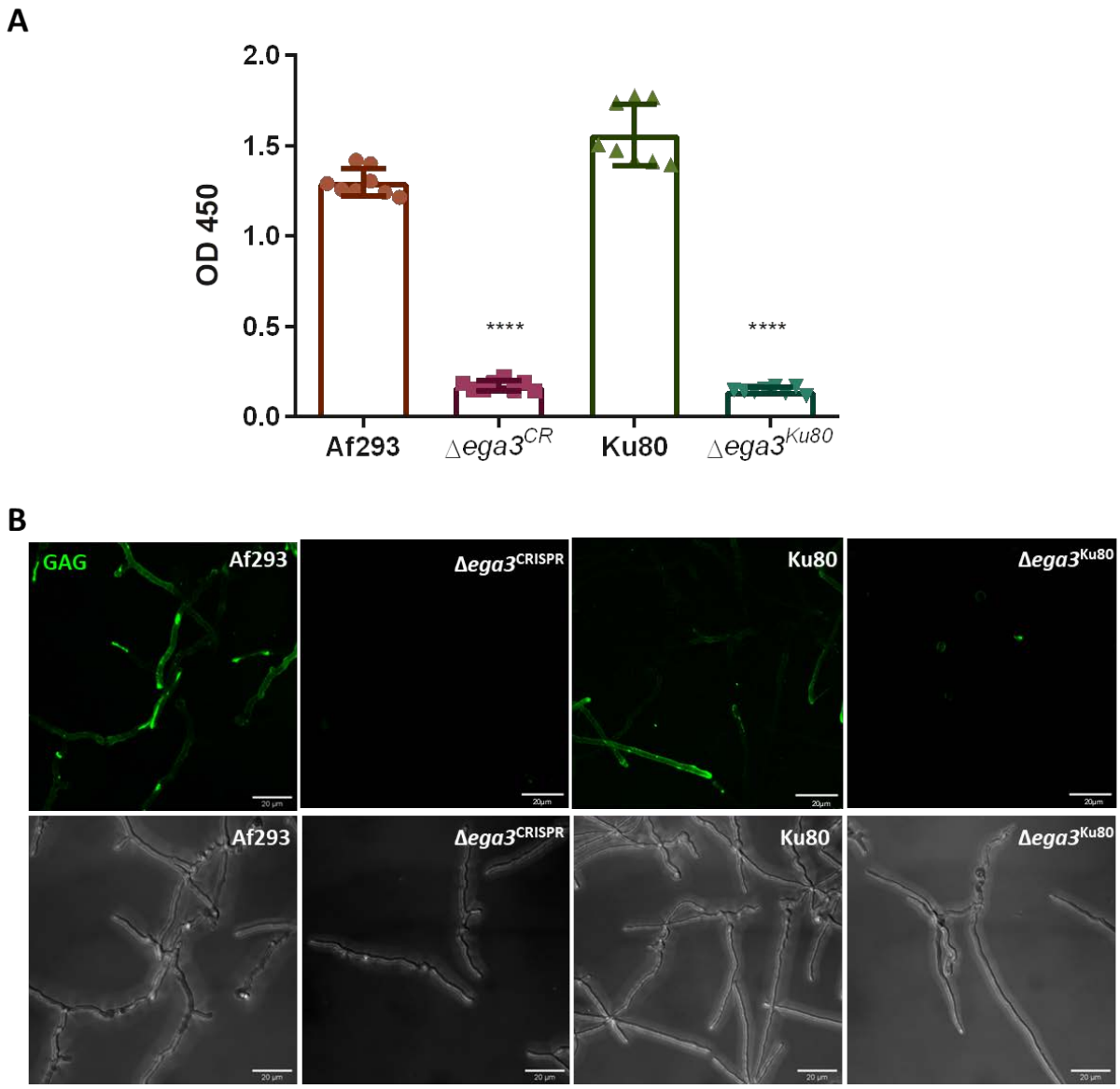


**Figure 2: The Δ*ega3*$^{CRISPR}$ and Δ*ega3*$^{Ku80}$ strains do not produce detectable deacetylated GAG. A)** Detection of deacetylated GAG by enzyme-linked lectin assay using biotinylated SBA and avidin-HRP culture supernatants produced by the indicated strains after 3 days of growth. Bars represent mean, error bars represent standard deviation. **** indicates P<0.0001 as determined by one-way ANOVA with Dunnett's multiple comparison test. n=1 biological replicate with 8 technical replicates per experimental condition. **B)** Confocal imaging of germlings of the indicated strains grown for 12 h in RPMI media and then stained with SBA-FITC to visualize hyphal-associated GAG. Phase-contrast channel is shown below each respective sample.

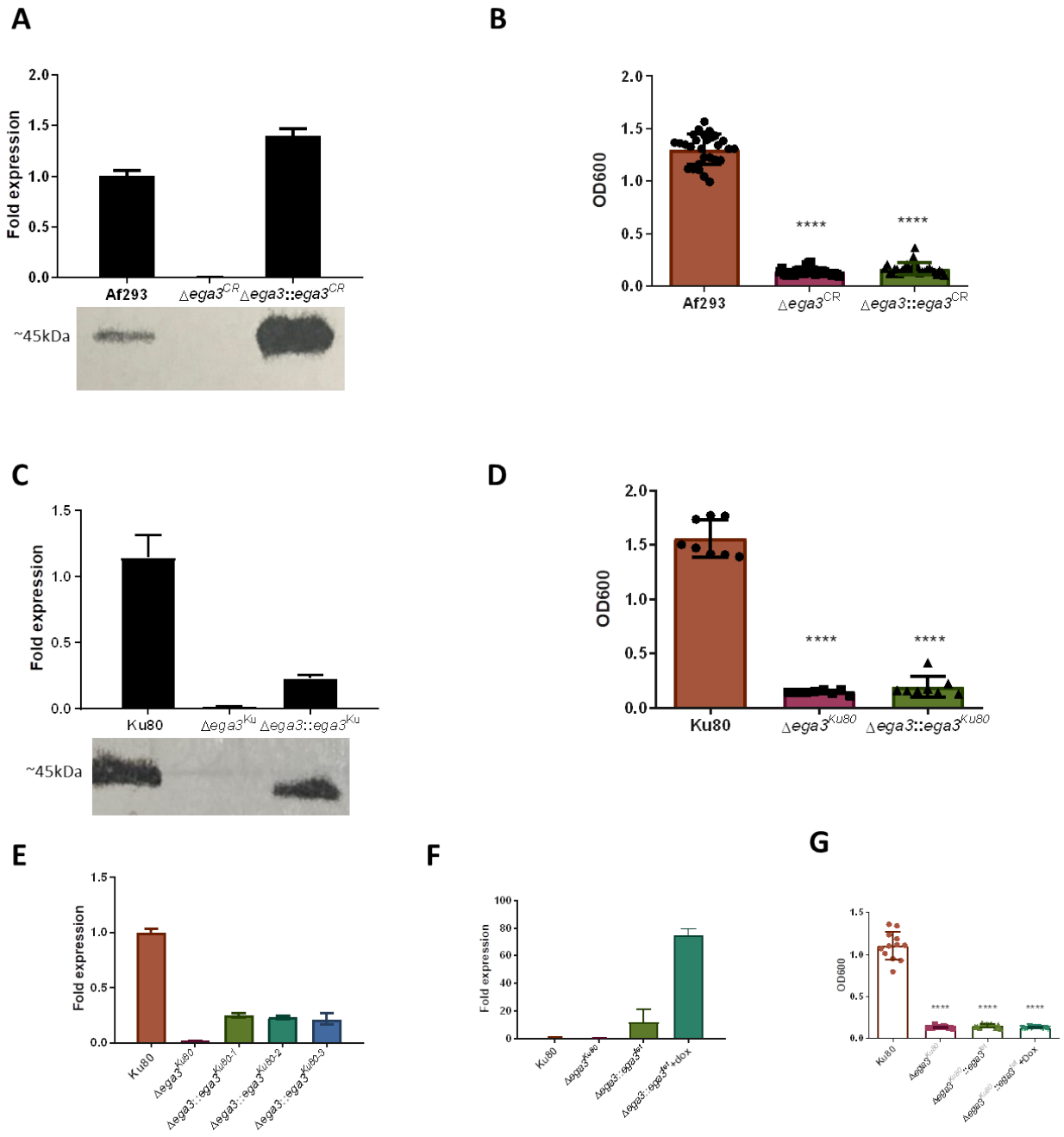


**Figure 3: Complementation of the Δ*ega3* munt strains with a wild-type allele of *ega3* fails to restore biofilm formation.** **A, C)** Expression of *ega3* as determined by qRT-PCR in the indicated strains normalized to the expression of the parent strain of each mutant strain set (top) and Ega3 protein production measured by Western blot (bottom) in biomass of the indicated strains grown for 18 hours (for gene expression) or 48 hours (for protein expression) in YPD medium. Bars represent mean, error bars represent highest value replicate. n=1 biological replicate with 3 technical replicates. **B, D, G)** Crystal violet quantification of adherent biofilm formation by the indicated strains after washing. Bars represent mean, error bars represent standard deviation. **** indicates P<0.0001 as determined by one-way ANOVA with Dunnett's multiple comparison test. n=1biological replicate with at least 8 technical replicates per experimental condition. **E, F)** Expression of *ega3* as determined by qRT-PCR for the indicated strains grown for 18 hours in YPD medium and normalized to expression by the parent strain. Bars represent mean, error bars represent highest and lowest experimental value. n=1biological replicate with 3 technical replicates per experimental condition.

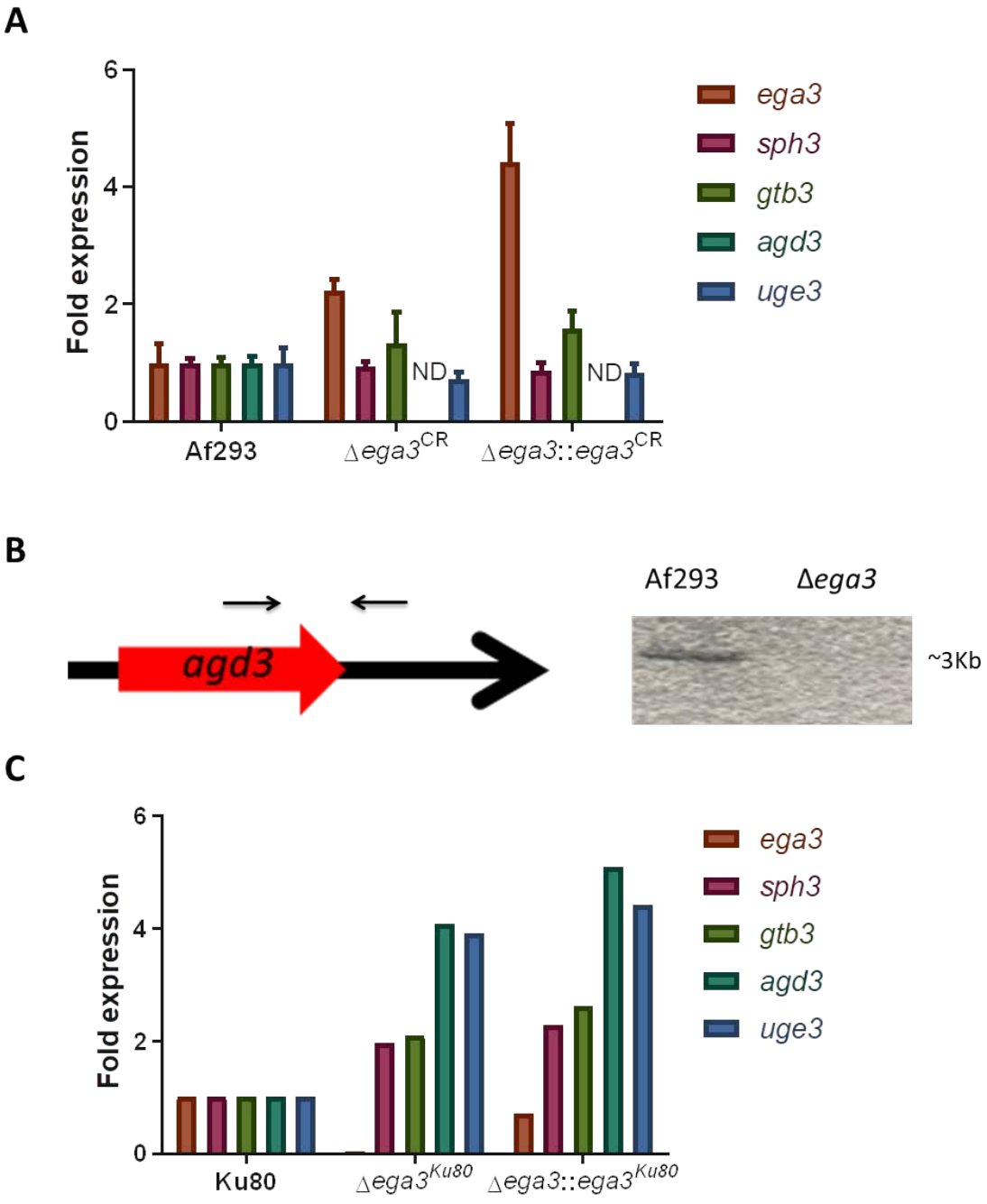


**Figure 4: The Δ*ega3*$^{CRISPR}$ strain has a secondary mutation at the *agd3* locus. A)** Expression of GAG biosynthetic genes in the Δ*ega3*$^{CRISPR}$ strain as compared to the gene expression in Af293 measured by qRT-PCR after growth for 18 hours in YPD medium. ND= not detected. Bars represent mean, error bars represent highest value replicate. n=2 biological replicates with 3 technical replicates per condition. **B)** Schematic (left) of the deletion at the 3' end of *agd3* as detected by PCR products in an agarose gel (right). **C)** Expression of GAG biosynthetic genes in the Δ*ega3*$^{Ku80}$ strain compared to the gene expression in Ku80 as measured by qRT-PCR after growth for 18 hours in YPD medium. Bars represent mean. n=1biological replicate with 2 technical replicates per experimental condition.

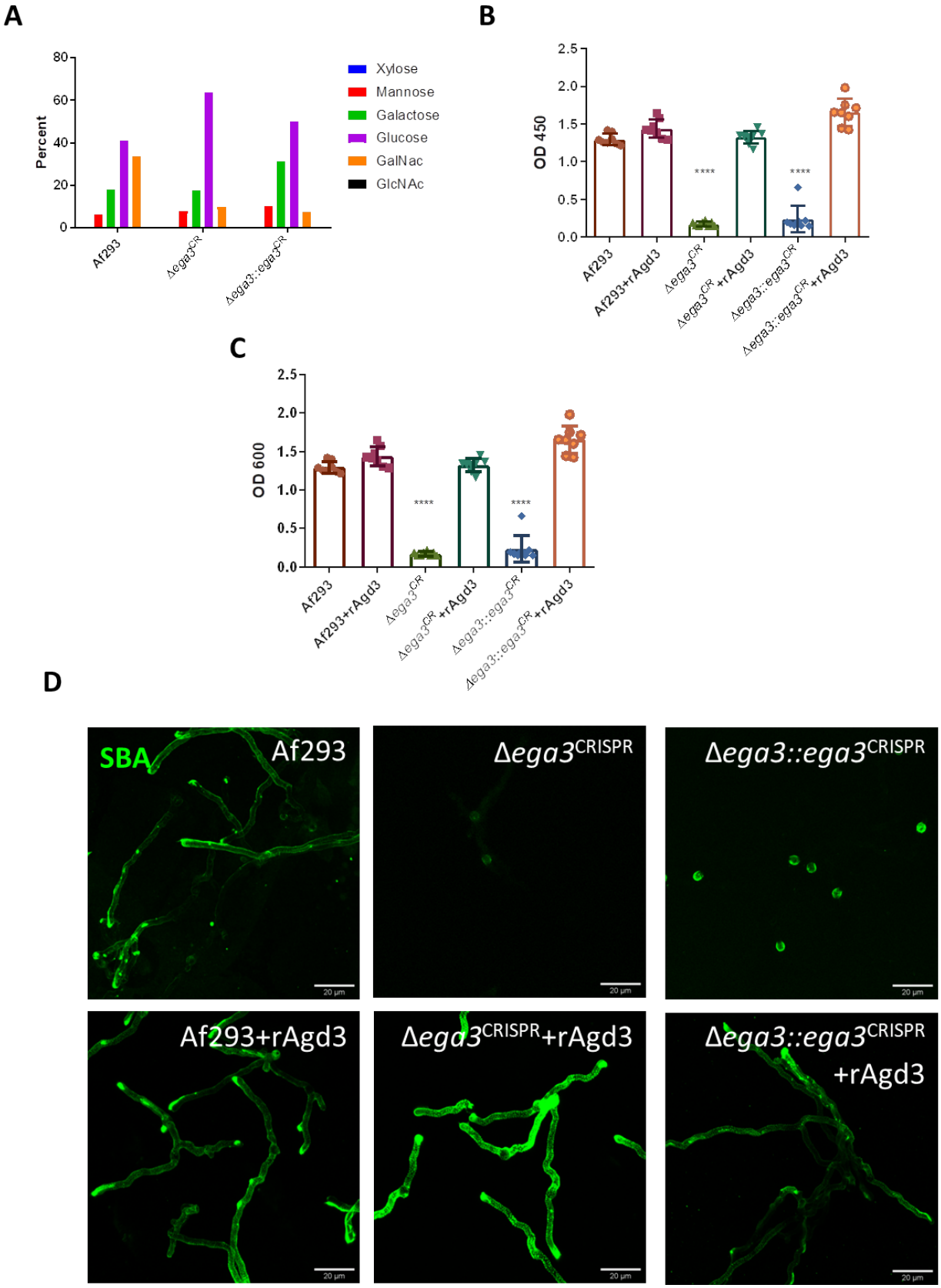
A
Percent
80
60
40
20
0
Xylose
Mannose
Galactose
Glucose
GalNac
GlcNAc
Af293
Δega3CR
Δega3::ega3CR
B
OD 450
2.5
2.0
1.5
1.0
0.5
0.0
****
****
Af293
Af293+rAgd3
Δega3CR
Δega3CR +rAgd3
Δega3::ega3CR
Δega3::ega3CR +rAgd3
C
OD 600
2.5
2.0
1.5
1.0
0.5
0.0
****
****
Af293
Af293+rAgd3
Δega3CR
Δega3CR +rAgd3
Δega3::ega3CR
Δega3::ega3CR +rAgd3
D
SBA
Af293
ΔegA3CRISPR
Δega3::ega3CRISPR
Af293+rAgd3
ΔegA3CRISPR+rAgd3
Δega3::ega3CRISPR
+rAgd3
20 µm

**E**

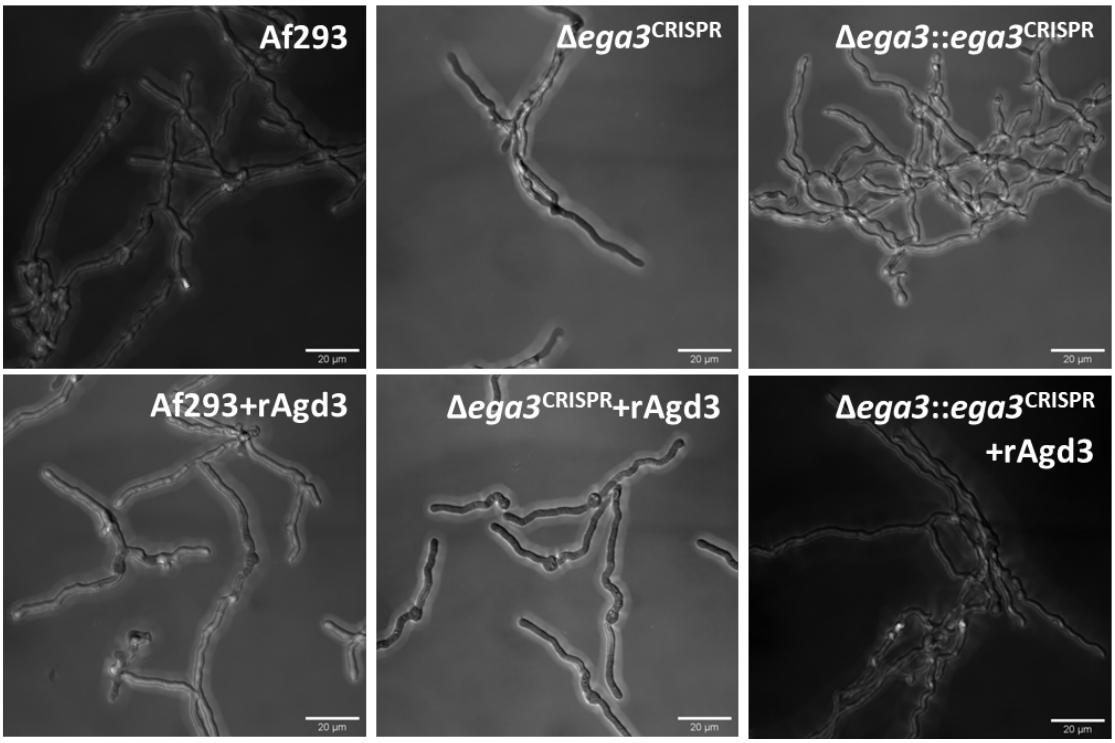


**Figure 5: The Δ*ega3*$^{CRISPR}$ strain produces fully acetylated GAG. A)** Monosaccharide composition of 3-day culture supernatants produced by the indicated strains that were lyophilized and then hydrolyzed with 2N HCl at 110°C and chemically derivatized for identification with gas chromatography. N-acetyl galactosamine was detected in all strains indicating the production of acetylated GAG. **B)** Detection of deacetylated GAG by enzyme-linked lectin assay using biotinylated SBA and avidin-HRP culture supernatants produced by the indicated strains after 3 days of growth. Bars represent mean, error bars represent standard deviation. **** indicates P<0.0001 as determined by one-way ANOVA with Dunnett's multiple comparison test. n=1biological replicate with 8 technical replicates per experimental condition. **C)** Crystal violet quantification of adherent biofilm formation by the indicated strains after washing. Bars represent mean, error bars represent standard deviation. **** indicates P<0.0001 as determined by one-way ANOVA with Dunnett's multiple comparison test. n=1 biological replicate with 8 technical replicates per experimental condition. **D)** Confocal imaging of germlings of the indicated strains grown for 12 h in RPMI media +/- rAgd3 and then stained with SBA-FITC to visualize hyphal-associated GAG. **E)** Differential interference contrast channel of the images in 5D.

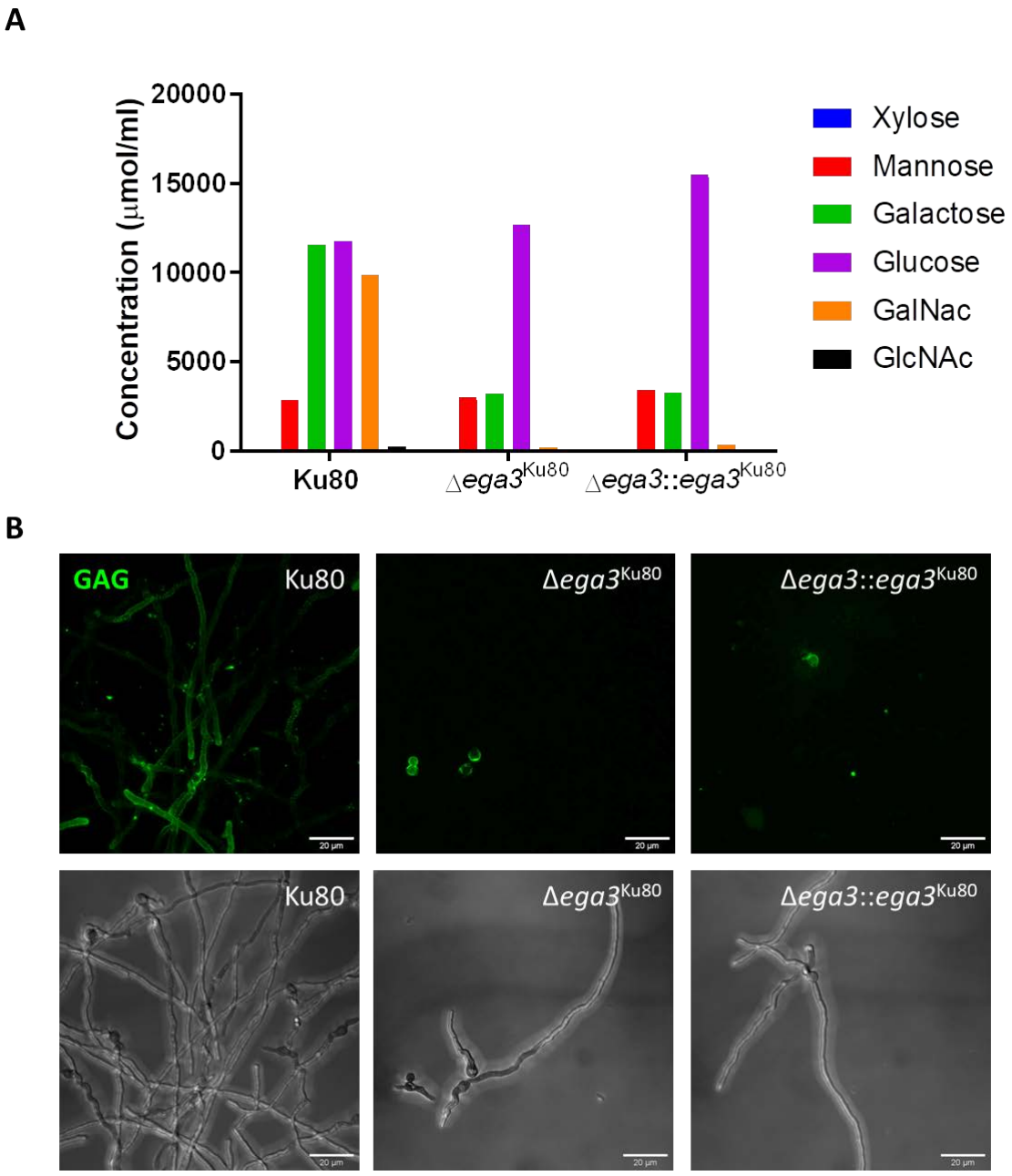


**Figure 6: GAG is not produced by the Δega3$^{Ku80}$ strain despite normal expression of GAG cluster genes. A)** Monosaccharide composition of 3-day culture supernatants produced by the indicated strains that were subsequently lyophilized and then hydrolyzed with 2N HCl at 110°C and chemically derivatized for identification with gas chromatography showing that GalNAc is not produced by the Δ*ega3*$^{Ku80}$ strain**. B)** Confocal imaging of germlings of the indicated strains grown for 12 h in RPMI media and then stained with SBA-FITC to visualize hyphal-associated GAG. Phase-contrast channel is shown below each respective sample.

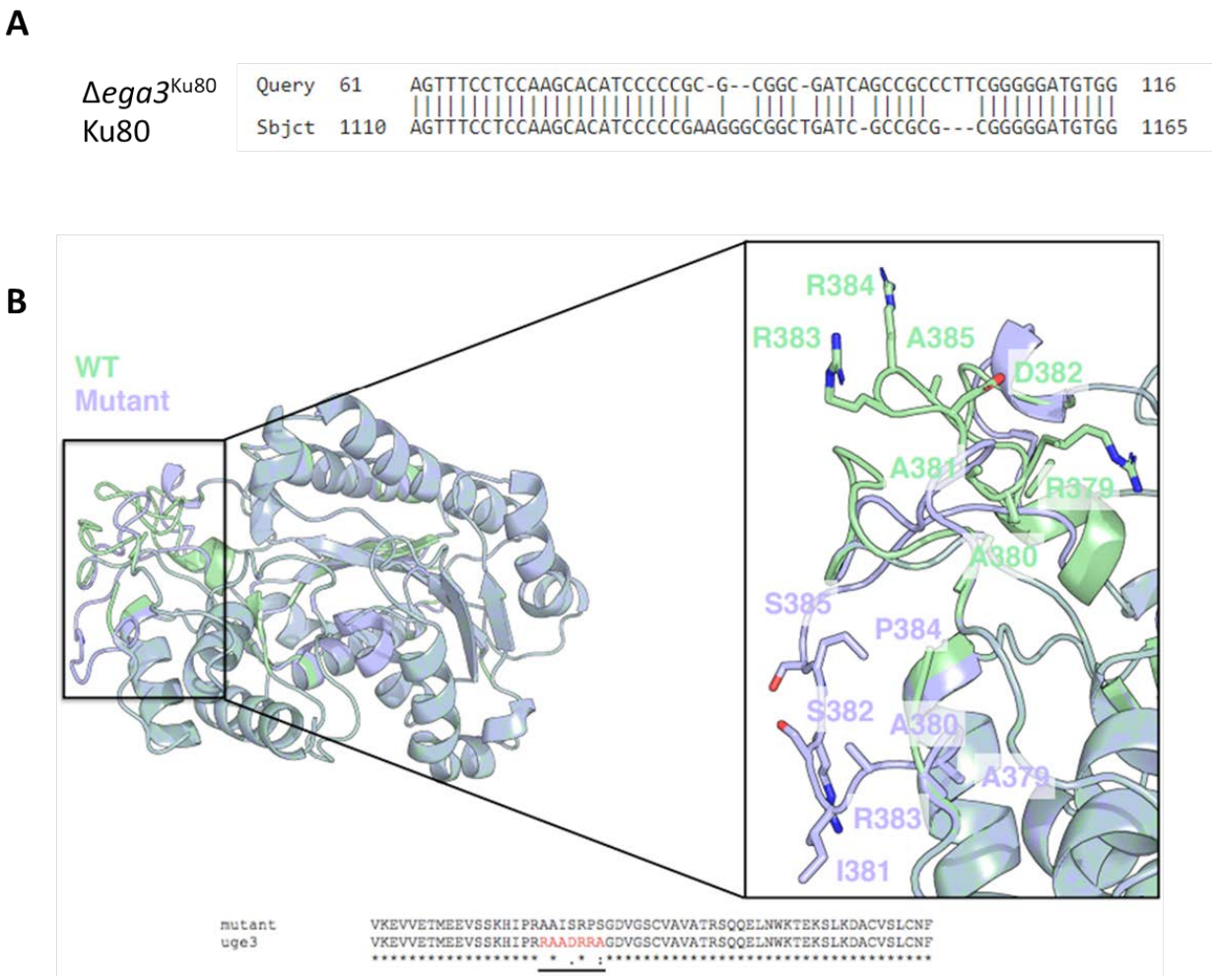


**Figure 7: A secondary mutation in the *uge3* gene of the Δ*ega3*$^{Ku80}$ strain is predicted to affect substrate binding. A)** Identification of a mutation in *uge3* by ultra-long read sequencing using the Pacbio SMRT system. **B)** The predicted model generated by the I-TASSER and Phyre[2] servers of Uge3 from the Δ*ega3*$^{Ku80}$ strain (purple) overlaid with wild-type Uge3 (green) showing a conformational change in a loop structure predicted to be important for binding either UDP-glucose or UDP-glucosamine when compared with a model of a human galactose epimerase (238, 247, 248).

# Chapter 4: Galactosaminogalactan is a cytotoxic molecule

**Preface**

The inability to disrupt *ega3* except in the presence of a secondary mutation that abrogates GAG production suggests the possibility that Ega3 may be conditionally essential, and is required in the presence of deacetylated GAG. By extension, this observation suggests that GAG may exert a toxic effect on fungal cells in the absence of Ega3. Deacetylated GAG is a long polycationic polymer, and polycationic molecules have been well-established as toxic to membranes of host and microbial cells.

**Antimicrobial peptides**

A well-known example of positively charged molecules inducing cell damage and death are cationic antimicrobial peptides (AMPs). AMPs are an important component of the innate immune system of many animals and plants that exhibit direct and indirect antimicrobial activity (249, 250). In humans, cathelicidin AMPs are stored in neutrophil granules in an inactive form that must undergo proteolytic cleavage to become active (250). Most antibacterial AMPs are positively charged amphipathic molecules that interact with, and cause damage to both Gram positive and Gram negative cell membranes. Parasitic, enveloped viral and fungal cell membranes are also susceptible to specific AMPs (251, 252).

There is a paucity of data on the charge of fungal cell membranes, however it has been suggested that the fungal cell wall may also be a target of these AMPs. Yeast cell walls have a net anionic charge due to their mannoprotein content, and the pathogenic yeast *C. albicans* is susceptible to various AMPs *in vitro* (253, 254). *A. fumigatus* is encased in positively charged extracellular matrix composed mainly of cationic GAG, and there is some controversy on whether certain AMPs are effective against this fungus, highlighted in more detail below (197).

Insects share an ecological niche with fungi and are as a consequence vulnerable to fungal infection. A type of insect AMP called the cecropins have been observed to induce the activation of the apoptosis pathways in *C. albicans* by inducing a buildup of reactive oxygen species (ROS) in the yeast, although the mechanism underlying this observation is not known (255, 256). Interestingly, use of a synthetic N terminal peptide of human lactoferrin demonstrated *in vitro* synergistic activity with fluconzaole against the fungal pathogen *Candida albicans*. It is hypothesized that the lactoferrin peptide caused a mitochondrial abnormality that increased the sensitivity of the fungus to fluconazole (257). Other mechanisms for killing of *C. albicans* by lactoferrin are the ability of lactoferrin to sequester iron, and the iron-free (apo)-lactoferrin can induce membrane permeability and consequently leakage of cytoplasmic proteins (258, 259). A lactoferrin derivative also had antifungal activity against *A. fumigatus* hyphae through an unspecified mechanism while lactoferrin itself inhibits conidial growth through iron sequestration (260, 261). Another class of AMPs produced by humans, the histatins, have also been found to be active against both yeasts and molds. (262). Histatin 5 in particular is fungicidal against both *C.*

*albicans* and conidia of *A. fumigatus*. The mechanism of action of histatin 5 against *C. albicans* is not completely understood, but it is effective in killing protoplasts of this fungus, indicating that the cell wall is probably not the target. Dye-loaded *C. albicans* did not lyse upon treatment with histatin 5 either, suggesting that cell membrane permeability is not induced by this AMP (262). Instead, histatin 5 was found to bind to heat shock protein (HSP) 70, which is found in the membrane and whose absence reduces the susceptibility of the fungus to histatin 5. There is also evidence to suggest that histatin 5 targets the mitochondria of *C. albicans*, and causes a efflux of ATP into the cytoplasm and from the cells, and is not effective against "petite" mutants (those that do not undergo respiration) (262, 263). It has also been observed that the ATP released into the cytoplasm leads to ROS generation and eventual cell death. The model that has been proposed is that histatin 5 binds to HSP70, translocates across the membrane and exerts its effects on the mitochondria which as a result release ATP, triggering ROS generation leading to death (264). There is little data on how histatin 5 acts against *A. fumigatus*, however a synthetic version of the peptide has antifungal activity against AmB resistant strains, suggesting that the mechanism of killing by these two molecules is not the same (265, 266).

There are conflicting studies on whether the human cathelicidin LL37 has antifungal activity against *A. fumigatus*. In one study LL37 bound *A. fumigatus* hyphae and prevented growth and adhesion while damaging the cell wall (267). Another study showed that LL37 exposure promoted growth and virulence of the fungus (268), while no significant effect on growth was observed in *A. fumigatus* exposed to LL37 in a third study (269). Different *A. fumigatus* strains were used in these studies, and perhaps this contributes to the differences in growth as a result of treatment with LL37. It is surprising that either of these effects are observed, considering that *A. fumigatus* hyphae are embedded in a matrix of positively charged GAG which would be expected to repulse positively charged molecules such as LL37 (270).

***Cationic polymers: their use and effects on cellular membranes***

Polycations have been studied extensively in the context of transfection. Their role as vehicles for DNA delivery into cells made them an attractive option since they are less immunogenic than virues and easier to use than lipids. However cytotoxicity of many cationic polymers can complicate their usage, especially for gene therapy. The toxicity of cationic polymers used in transfection is not well understood, but increased transfection efficiency and size of the polycation correlates with increased toxicity (271, 272).

The study of polycations in transfection has revealed some potential effects of polycations on mammalian cells. First, when they are endocytosed, polycations may become protonated in the low pH that occurs upon fusion of the endosome with the lysosome, resulting in an influx of chloride ions and osmotic rupture of the endolysosome (271). Second, it was found that two commonly used polycations used in transfection, poly-L-lysine (PLL) and polyethylenimine (PEI), can induce apoptosis in several

different cell lines. In these studies it was hypothesized that cell death was through activation of protein kinases or through mitochondrial signalling respectively (273). Finally, another study on a variety of cationic polymers including PEI and PLL on mouse L929 fibroblasts observed membrane damage as a consequence of electrostatic intereractions. The mechanism of cell death was caspase-independent and was therefore characterized as necrosis rather than apoptosis. (272).

Anionic charges in cell membranes have an important role in architecture and functions of the cell. It is therefore possible that electrostatic adsorption of cationic polymers to the cell surface may thus disrupt the basic cellular structure, cellular adhesion, cation transport membrane integrity and/or osmotic balance (274). However, the exact mechanism behind cell damage induced by electrostatic interactions between polycations and cellular membranes is not well-defined. Two mechanisms that have been posited are intercalation of the polymer with the membrane or donation of a proton by the polymer to hydrolyse phospholipids of the cell membrane, leading to membrane distortion. (275). The molecular mechanism of this observation was previously shown in reactions between phospholipid membranes and cationic drugs, where it was determined that the ester linkages of the phospholipids were acidically hydrolyzed by protonated moieties of the drugs. This resulted in membrane fragments diffusing away from the model membrane (276).

Cationic polymers of biological origin have also been found to exhibit toxic effects against microorganisms. Chitosan derived from the reduction of amines in the chitin of crustaceans and insects, (chitosan is also a natural component of the fungal cell wall, however it is deacetylated by chitin deacetylases rather than chemically reduced) has bacteriostatic activity (277, 278). The proposed mechanisms for the bacteriostatic activity of chemically reduced chitosan are i) electrostatic interaction with the bacterial surface resulting in hydrolysis of peptidoglycan or pore formation in the plasma membrane; ii) complexing with bacterial DNA; or iii) chelation of metal ions and thereby interefering with cellular metabolism (278). However, chitosan is poorly soluble, which complicates its use as an antimicrobial (277). Addition of nitrogen-containing rings or other cationic residues to chitosan can improve solubility as well as antimicrobial activity, which is mediated through membrane disruption (277, 279). For example, addition of arylfuran groups to chitosan improved its activity against *P. aeruginosa*, with electrostatic interactions playing a significant role (280).

The best evidence for the toxicity of cationic polymers secreted by fungi comes from studies of a GalN-containing polymer produced by the ascomycete *Neurospora crassa*. As with *A. fumigatus* GAG, this cationic polymer is composed of partially acetylated galactosamine, though it lacks the galactose component found in GAG. Surprisingly, this molecule exhibited autotoxicity towards the parent *Neurospora* strain. When *N. crassa* conidia were exposed to polygalactosamine, polymer adsorption to the conida surface led to an efflux of radiolabeled intracellular metabolites. Other polycationic polymers

such as chitosan and PLL exhibited similar effects. The calcium channel blocker lanthanum inhibited adsorption of polygalactosamine to the conidial surface, suggesting polymer binding to sites of calcium uptake or interference with calcium-dependent ligands (281). Similar observations were reported in a second study in which polygalactosamine exposure resulted in reduced uptake of radiolabeled metabolites and decreased viability of *Neurospora* conidia. Binding of the polymer to conidia was hypothesized to be mediated, at least in part, by electrostatic interactions. It was also hypothesized that conidial viability was impacted by disturbances to the cell membrane, however this was not tested further. It is also unclear how the uptake of metabolites was inhibited, since the molecules tested were uncharged and therefore unlikely to be electrostatically repelled by cationic polygalactosamine (282). In both studies, adsorption of the polymer to conidia was inhibited in the presence of increased salt concentration, supporting the role of electrostatic interactions between polymer and conidia (281, 282).

Taking into account the large body of evidence implicating polycations as cyotoxic molecules, it seems likely that deacetylated GAG could also be toxic to fungal cell membranes. Ega3 is conditionally essential in the presence of deacetylated GAG, and work in chapter 2 revealed that Ega3 is anchored in the fungal plasma membrane, with an extracellular hydrolase domain that cleaves deacetylated GAG. We therefore hypothesized that Ega3-mediated GAG hydrolysis serves to protect the fungal plasma membrane from damage induced by polycationic GAG. We further extended this hypothesis to include the ability of GAG to cause damage to other host cell membranes, which in turn could be protected in the presence of Ega3. In light of these new hypotheses, our updated experimental objectives were to 1) characterize the effects of GAG on the cell membranes of *A. fumigatus* in the absence of Ega3 by inducing production of deacetylated GAG in the Δ*ega3*$^{CRISPR}$ strain; 2) expose host cells to deacetylated GAG and probe for cellular injury; and 3) determine if Ega3 can prevent cellular injury to host cells in the presence of deacetylated GAG.

## Results

### Complementation of the Δ*ega3*$^{CRISPR}$ strain with a tetracycline-inducible *ega3* allele results in a significant growth defect that is media-dependent.

Given that the two independently made Δ*ega3* strains also exhibited defects in the ability to produce deacetylated GAG, we hypothesized that *ega3* is conditionally essential when cationic, deacetylated GAG is produced. To test this hypothesis, we sought to express *agd3* under the control of a tetracycline-inducible promoter in the Δ*ega3*$^{CRISPR}$ strain. A representation of this inducible *agd3* overexpression construct is shown in **Figure 1A**. The resulting strain was designated Δ*ega3*$^{CRISPR}$::*agd3*$^{Tet\ on}$. Following PCR confirmation of successful transformation, we confirmed the effects of exposure to doxycycline (Dox), an analog of tetracycline, on expression of *agd3*. The Δ*ega3*$^{CRISPR}$::*agd3*$^{Tet\ on}$ strain was grown in the presence of increasing concentrations of Dox and *agd3* expression quantified by qRT-PCR. Dose-dependent increase in *agd3* expression that exceeded levels of *agd3* expression in the Af293 wild-type parent strain was observed in response to Dox exposure, confirming that the construct was functioning as expected (**Figure 1B**). Detectable expression of *agd3* was observed in the Dox-untreated Δ*ega3*$^{CRISPR}$::*agd3*$^{Tet\ on}$ strain suggested that the tetracycline-inducible system is somewhat "leaky" (i.e., the reverse transactivator can still bind to the $TetO_7$ operator in the absence of Dox, allowing some expression of the *agd3* gene), an occurrence frequently observed with this system (283).

When testing the effects of Dox on *agd3* expression, it was noted that there was a marked decrease in biomass when the Δ*ega3*$^{CRISPR}$::*agd3*$^{Tet\ on}$ strain was grown in the presence of 20 μg/ml Dox from the time of inoculation in YPD as compared to growth in YPD media only. To confirm that the effects of *agd3* overexpression on inhibition of growth of Ega3-deficient *A. fumigatus* were not non-specific effects mediated by the Agd3 overproduction, the tetracycline-inducible *agd3* construct was also introduced into wild-type *A. fumigatus*. A positive clone was isolated in which the construct had been successfully introduced, named Af293::*agd3*$^{Tet\ on}$. The Af293::*agd3*$^{Tet\ on}$ strain exhibited no growth inhibition in Dox, and was found to express *agd3* under these conditions. This finding suggests that when *agd3* overexpression is induced in Af293 growth of the strain is normal, thanks to the presence of Ega3.

In order to better quantify the effects of Agd3 expression in Ega3-deficient hyphae, time course growth studies were performed. The Δ*ega3*$^{CRISPR}$::*agd3*$^{Tet\ on}$ strain was grown in microtiter plates in the presence and absence of Dox, and optical density measurements were taken every hour for 48 hours at 37$^{o}$C using a protocol adapted from a previous study on *Aspergillus* growth rates (284). Beginning at 30 hours of growth, the Dox-treated Δ*ega3*$^{CRISPR}$::*agd3*$^{Tet\ on}$ strain exhibited a significant growth defect as compared to wild-type *A. fumigatus* grown in the presence of the highest concentration of Dox used (**Figure 2A**). A lesser degree of growth impairment was observed in the Δ*ega3*$^{CRISPR}$::*agd3*$^{Tet\ on}$ strain grown in the absence of Dox. This observation is consistent with the background level of *agd3*

transcription that occurs in the absence of Dox in this strain (**Figure 1B, 1C**), and may indicate a dose-dependent inhibitory effect of Agd3 in the absence of Ega3 (283). In the Af293::*agd3*$^{\text{Tet on}}$ clones, no growth defect was observed. Based on these observations, it appears as though absence of Ega3 is not lethal to *A. fumigatus*, but it is crucial for normal growth of the fungus in the presence of deacetylated GAG.

Since there is growth of the Δ*ega3*$^{\text{CRISPR}}$::*agd3*$^{\text{Tet on}}$ strain in the presence of Dox, albeit decreased in comparison with Δ*ega3*$^{\text{CRISPR}}$::*agd3*$^{\text{Tet on}}$ in the absence of Dox treatment, we were able to characterize the formation of an adhesive biofilm by the Δ*ega3*$^{\text{CRISPR}}$::*agd3*$^{\text{Tet on}}$ strain in the presence of Dox to confirm the activity of Agd3. As predicted, biomass of the Dox-treated Δ*ega3*$^{\text{CRISPR}}$::*agd3*$^{\text{Tet on}}$ strain remained adhered to the plate after washing due to the presence of deacetylated GAG (**Figure 2B**). Taken together, this data suggests that while the Dox-treated Δ*ega3*$^{\text{CRISPR}}$::*agd3*$^{\text{Tet on}}$ strain has a significant growth defect, the surviving mycelium is viable despite the fact that it is producing deacetylated GAG. At this time, the mechanism for the GAG-resistance of these mycelia remains unclear.

In previous studies, we have demonstrated that growth in Brian media increases the levels of secreted GAG and results in reduced amounts of hyphal-associated GAG (149). We hypothesized that increased secretion of GAG away from the hyphae of the Δ*ega3*$^{\text{CRISPR}}$::*agd3*$^{\text{Tet on}}$ strain during *agd3* expression might be protective to this strain. Consistent with our hypothesis, when Brian media was used instead of YPD, growth of the Dox-treated and untreated Δ*ega3*$^{\text{CRISPR}}$::*agd3*$^{\text{Tet on}}$ strains was similar (**Figure 2C**). This finding suggests that environmental factors may play a role in toxicity of GAG to *A. fumigatus*, even in the absence of Ega3.

**The *ega3*$^{\text{CRISPR}}$::*agd3*$^{\text{Tet on}}$ strain can downregulate *agd3* expression through an unknown mechanism.**

Residual growth was observed in hyphae of the Dox-treated Δ*ega3*$^{\text{CRISPR}}$::*agd3*$^{\text{Tet on}}$ strain, leading us to question of the health status of these hyphae. To probe this question, we stained Dox-treated Δ*ega3*$^{\text{CRISPR}}$::*agd3*$^{\text{Tet on}}$ with the fungal viability dye FUN 1, where dead cells stain bright green throughout and living cells stain less brightly and have red-stained vacuolar structures within them when viewed on a confocal microscope. The FUN 1-stained, Dox-treated Δ*ega3*$^{\text{CRISPR}}$::*agd3*$^{\text{Tet on}}$ strain contained red vacuoles as did the untreated Δ*ega3*$^{\text{CRISPR}}$::*agd3*$^{\text{Tet on}}$, while ethanol-killed Af293 stained bright green with no vacuoles (**Figure 3A**), indicating that the residual hyphae in Dox-treated Δ*ega3*$^{\text{CRISPR}}$::*agd3*$^{\text{Tet on}}$ are indeed viable.

Based on the above findings, we questioned whether or not resistance to Agd3 in the Δ*ega3*$^{\text{CRISPR}}$::*agd3*$^{\text{Tet on}}$ strain could be occur. Of note, although upregulation of endogenous Agd3 inhibited growth of the the Δ*ega3*$^{\text{CRISPR}}$ strain, the exogenous addition of soluble rAgd3 had no effect on

fungal growth. Even endogenous production of Agd3 is not entirely lethal under many circumstances. We therefore hypothesized that the intact cell wall may play an important role in separating deacetylated GAG and the plasma membrane, and that Ega3 plays a role in clearing GAG that is deacetylated during to secretion. To test this hypothesis, we chemically protoplasted the Δ*ega3*$^{\text{CRISPR}}$::*agd3*$^{\text{Tet on}}$ strain in the presence of Dox to determine if protoplasts would exhibit increased sensitivity to deacetylated GAG. An equal number of protoplasts was plated on minimal media ± Dox and left to regenerate, and the number of colonies was counted after 24 hours of growth at 37°C. Surprisingly, the number of colonies of the Δ*ega3*$^{\text{CRISPR}}$::*agd3*$^{\text{Tet on}}$ mutant did not vary significantly between the media with or without Dox, however the colonies were much smaller on the Dox plates than on the Dox-free plates (**Figure 3B**). In order to characterize them in more detail, colonies of the Δ*ega3*$^{\text{CRISPR}}$::*agd3*$^{\text{Tet on}}$ mutant were isolated and regrown in the presence or absence of Dox. The resulting biomass was assayed for *agd3* gene expression by qRT-PCR. Surprisingly, in these clones, the addition of Dox did not increase *agd3* transcription dramatically (**Figure 3C**). It is unknown whether the selection pressure exerted by Dox caused ejection of the plasmid. These data are consistent with the development of a mechanism to suppress Agd3 expression in the presence of deacetylated GAG exposure. Further testing, possibly including RNA sequencing, would need to be done in order to fully characterize this finding and elucidate the mechanism whereby these breakthrough colonies have lost the ability to express Agd3.

**Expression of *agd3* in the Δ*ega3*$^{\text{CRISPR}}$ strain results in leakage of cytoplasmic contents.**

We next sought to probe the mechanisms of the growth defect of the Δ*ega3*$^{\text{CRISPR}}$::*agd3*$^{\text{Tet on}}$ strain in the presence of Dox. In light of the published data implicating polycationic molecules as harmful to cellular plasma membranes (250, 252, 267, 269, 272, 273, 276, 285) we hypothesized that in the absence of Ega3, deacetylated GAG causes damage to cell membrane of *A. fumigatus.* We would therefore predict that the Δ*ega3*$^{\text{CRISPR}}$::*agd3*$^{\text{Tet on}}$ mutant would exhibit increased sensitivity to growth inhibition by highly osmotic media in the presence of doxycycline due to membrane fragility. To test this hypothesis, the Δ*ega3*$^{\text{CRISPR}}$::*agd3*$^{\text{Tet on}}$ strain was grown in either YPD±0.6M KCl with or without Dox. As previously observed, reduced growth of the Δ*ega3*$^{\text{CRISPR}}$::*agd3*$^{\text{Tet on}}$ strain was observed when grown in YPD+Dox, as compared with YPD alone (**Figure 4A**). No significant difference in the growth of the Af293 strain was observed between regular and high-salt media, however when the Δ*ega3*$^{\text{CRISPR}}$::*agd3*$^{\text{Tet on}}$ strain was grown in YPD+0.6M KCl, a minimal addition of Dox resulted in a near absence of growth, a much greater level of growth inhibition than was seen with KCl supplementation, or Dox treatment alone (**Figure 4A**). The increased sensitivity of theΔ*ega3*$^{\text{CRISPR}}$::*agd3*$^{\text{Tet on}}$ strain to high salt concentration under conditions of *agd3* expression is consistent with membrane damage due to increased membrane permeability induced by deacetylated GAG.

To probe the hypothesis that deacetylated GAG induces membrane injury in the absence of Ega3, we sought to determine the effects of deacetylated GAG production on leakage of intracellular contents of the Δ*ega3*$^{CRISPR}$::*agd3*$^{Tet\ on}$ strain. The Δ*ega3*$^{CRISPR}$::*agd3*$^{Tet\ on}$ strain was grown with and without Dox and measured the release of intracellular ATP. As predicted, ATP release was highest in the Δ*ega3*$^{CRISPR}$::*agd3*$^{Tet\ on}$ strain grown in Dox-containing media and near background levels in both wild-type and the Δ*ega3*$^{CRISPR}$ strain (**Figure 4B**). This finding strongly suggests that the loss of cellular viability in the Δ*ega3*$^{CRISPR}$::*agd3*$^{Tet\ on}$ strain in *agd3*-inducing conditions is due to loss of cytosolic contents through increased membrane permeability.

**Deacetylated GAG is harmful to host cells.**

Our findings to date support the hypothesis that deacetylated GAG is toxic to fungal cell membranes. Given that deacetylated GAG is secreted during infection, we hypothesized that it could also injure host cell membranes (197, 286). We tested this hypothesis by testing the cytotoxicity of GAG in a modified version of our chromium-release epithelial cell damage assay (205). Briefly, radioactive chromium [$^{51}$Cr]-loaded A549 pulmonary epithelial cells were exposed to fungal culture supernatants containing either deacetylated or fully acetylated GAG (purified from the Agd3-deficient mutant of *A. fumigatus*) and cell damage was measured by quantification of the amount of [$^{51}$Cr] released. Exposure of A549 cells to 40% vol/vol fungal culture supernatants containing deacetylated GAG but not those containing fully acetylated GAG resulted in significant release of [$^{51}$Cr], suggesting that deacetylated GAG is toxic to human cell membranes. Pre-treatment of culture supernatants containing deacetylated GAG with recombinant Ega3 completely prevented this cell damage (**Figure 5A**). Collectively these findings are consistent with the hypothesis that cationic deacetylated GAG is cytotoxic.

Next, we sought to confirm that GAG-induced cellular injury could lead to cell death. As A549 epithelial cells are an immortalized cell line, we turned to murine bone-marrow derived macrophages (BMDMs) for these experiments. To test for GAG-induced cell death, BMDMs were incubated with the same set of GAG-containing culture supernatants ± recombinant Ega3 that were used for the chromium release assay, and cell death as a function of membrane permeability was then measured using propidium iodide (PI) staining (287). As with the chromium release assay, co-culture of cells with deacetylated GAG was the only condition found to cause cell death above background levels. Pre-treatment with with Ega3 prevented death in cells exposed to deacetylated GAG, confirming that polycationic GAG is cytotoxic (**Figure 5B**).

As detailed above, cationic polymers have been reported to induce cell death both by apoptosis that is mediated by the toxic efffect of the polymer on mitochondria, and/or through necrosis due to direct damage to the cell membrane as a consequence of the charge-charge interactions (273, 288). In order to

explore down the mechanism of cell death and to further broaden the number of cell types tested, we exposed primary human natural killer (NK) and T cells to the same set of conditions as the previous two assays. Cells were then stained with PI and annexin V, which binds phosphatidylserine that has been flipped to the outer plasma membrane leaflet during apoptosis. The populations of annexin V positive/PI negative cells, representing cells undergoing early apoptosis, was measured using flow cytometry. Once again, toxicity was greatest with the wild-type (deacetylated GAG-containing) CS. The effect was most pronounced in the NK cells, with the T cells following the same trend but to a lesser magnitude (**Figure 5C**). Taken together, deacetylated GAG is toxic to an array of different cell types, and likely induces mammalian cell death through apoptosis, however the mechanism may be more complex than charge interactions between deacetylated GAG and the plasma membrane.

**Deacetylated GAG induces exposure of inflammatory markers in murine lung tissue.**

Given the ability of deacetylated GAG to induce injury and death in mammalian cells *in vitro,* we sought to determine if a similar phenomenon might occur during infection. To assess the effects of deacetylated GAG on lung tissue injury we turned to the novel approach of MALDI imaging mass spectrometry. MALDI imaging can be used to measure presence of biomolecules without the need for an antibody or other label and measure their distribution *in situ* (289). For these experiments, lungs from healthy wild-type mice were harvested and inflated *ex vivo* with 1 ml CS from the wild-type or deacetylase-deficient *A. fumigatus* strains before flash freezing. Lung tissue 20µm cross sections were obtained through cryosectioning and used for MALDI imaging. While MALDI markers of tissue damage have not been validated, tissue damage is tightly linked to inflammation, and we therefore used markers of inflammation as a surrogate measure of tissue injury (290). Sphingomyelin (SM) in the plasma membrane is a precursor for sphingolipid production, and has been validated as a MALDI measure of inflammation (291). We therefore used detection of SM ions to measure tissue damage. Measurement of the membrane phospholipid phospatidylcholine (PC) was used as a marker for normal tissue. Higher levels of sphingomyelin were observed in the images obtained from lungs exposed to deacetylated GAG than those exposed to fully acetylated GAG (**Figure 6A**). Pixel quantification confirmed that higher levels of SM were detected in lung tissue exposed to deacetylated GAG as compared with fully acetylated GAG (**Figure 6B**), confirming a role for deacetylated GAG in inducing tissue injury and subsequent inflammation in intact lungs.

With evidence to suggest that deacetylated GAG induces cellular inflammation in lung tissue *ex vivo*¸we next looked to confirm these findings *in vivo* using an immunosuppressed mouse infection model, where neutrophils of Balb/C mice are depleted with an anti-Ly6G antibody prior to infection. Previous work in similar animal models has suggested that loss of GAG deacetylation is associated with

reduced virulence (197). We therefore hypothesized that deacetylated GAG may injure the cells of the lungs, releasing protein into the airways and contributing to virulence. To test the effects of deacetylated GAG on lung tissue of these mice, they were infected with the wild-type and deacetylase-deficient strains of *A. fumigatus*. After 24 hours, the lungs of the mice were removed and the airways were lavaged with PBS to collect proteins. We then measured the protein concentration of each group using a BCA assay. Surprisingly, there was no significant difference in the protein concentration between groups (**Figure 6C**), suggesting that infection of mice producing deactylated or fully acetylated GAG-producing strains cause similar amounts of cellular damage at this point in infection. These findings suggest that in the context of infection with whole organisms, factors other than GAG play a role in mediating tissue injury early post infection.

**Deacetylated GAG may aid escape from macrophage phagolysosomes.**

Our experiments exposing host cells to deacetylated GAG focussed on the interactions of this secreted polymer with the plasma membrane of mammalian cells, however in an animal model, tissue damage was not different between strains that produce deacetylated and non-deacetylated GAG. During infection, conidia of *A. fumigatus* are phagocytosed by alveolar macrophages, and then escape from the phagolysosome by germination and extension. The mechanisms by which germinating hyphae escape the phagolysome include inhibition of pagolysosome acidification which involves DHN melanin in the conidial cell wall, but are otherwise poorly understood (292, 293). The mechanism for penetration of the hyphae through the phagolysosomal membrane has also not been characterized. Given that deacetylated GAG is produced at the time of conidial germination, and is able to damage lipid membranes, we hypothesized that deacetylated GAG might also play a role in phagolysosomal escape by facilitating damage and ultimately disruption of the phagolysosomal membrane. To test this hypothesis, MH-S immortalized mouse alveolar macrophages were infected with conidia of wild-type or Δ*agd3* strains of *A. fumigatus* and confocal microscopy was performed to visualize germination and cellular escape by growing hyphae. Interestingly, while wild-type *A. fumigatus* was able to rapidly escape from macrophages and form long extracellular hyphae, the Δ*agd3* mutant remained largely contained within macrophages and exhibited reduced hyphal growth. This observation, although preliminary, suggests that deacetylated GAG may play a role in phagolysosomal escape and subsequent fungal growth (**Figure 7**).

**Figures**

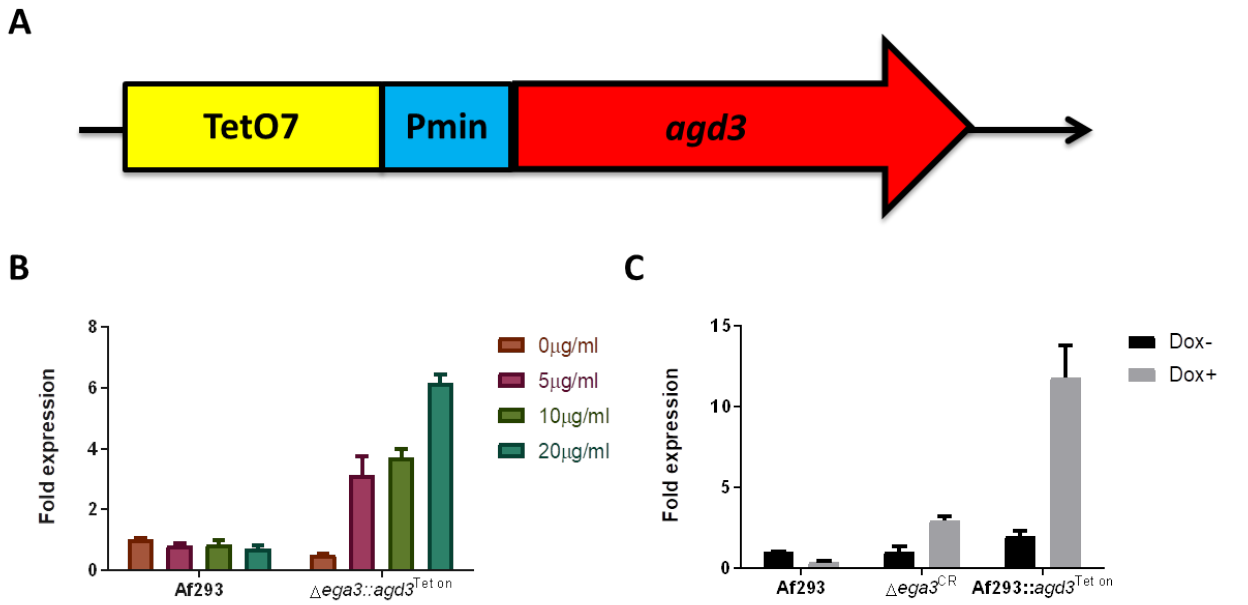


**Figure 1: Construction of tetracycline-inducible *agd3* allele for expression in the Δ*ega3*$^{CRISPR}$ strain. A)** Schematic of the construct used to transform Δ*ega3*$^{CRISPR}$. **B)** Fold-expression of *agd3* in the Δ*ega3*$^{CRISPR}$ ::*agd3*$^{Tet\ on}$ strain in comparison to untreated wild-type in response to the indicated doses of Dox added at the time of inoculation. Strains were grown for 18 hours in YPD medium. Bars represent mean, error bars represent highest value replicate. n=1biological replicate with 3 technical replicates per experimental condition. **C)** Expression of *agd3* in the Δ*ega3*$^{CRISPR}$::*agd3*$^{Tet\ on}$ and Af293::*agd3*$^{Tet\ on}$ strains in response to growth in YPD medium + 40 µg/ml Dox for 18 hours. Bars represent mean and error bars represent highest value replicate. n=1biological replicate with 3 technical replicates per experimental condition.

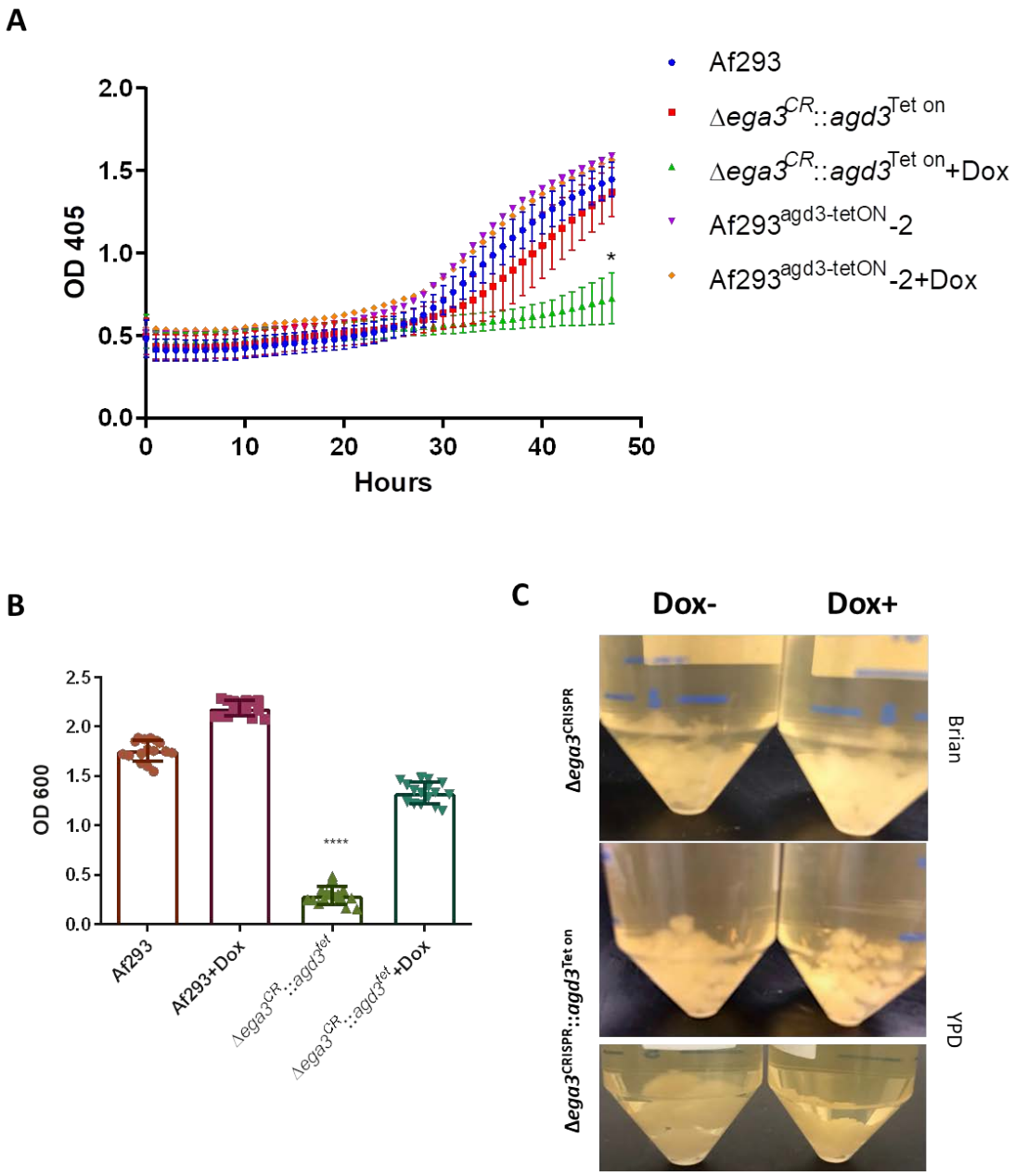


**Figure 2: Expression of *agd3* in the Δ*ega3*$^{\text{CRISPR}}$::*agd3*$^{\text{Tet on}}$ strain results in a growth defect. A)** Growth of the indicated strains in YPD media+0.1% Tween 80 v/v with or without 20 µg/ml Dox as measured by optical density over a 48 hour period in a 96 well plate. * indicates $P \leq 0.05$ determined by one way ANOVA with Dunnett's multiple comparisons test. n=3 biological replicates with 3 technical replicates per experimental condition, the combined means of which are represented on the graph as a mean (point) ± standard deviation (bars). **B)** Crystal violet staining of adherent biofilm formed by the indicated strains when grown in Brian medium with or without Dox for 21 hours. **** indicates . **** indicates P<0.0001 as determined by one-way ANOVA with Dunnett's multiple comparison test. n=1 biological replicate with 16 technical replicates per experimental condition. **C)** Growth of the Δ*ega3*$^{\text{CRISPR}}$::*agd3*$^{\text{Tet on}}$ mutant (middle) and its parent strain (top) grown in synthetic Brian medium with and without Dox. Growth of the Δ*ega3*$^{\text{CRISPR}}$::*agd3*$^{\text{Tet on}}$ mutant in YPD is included for comparison (bottom two panels).

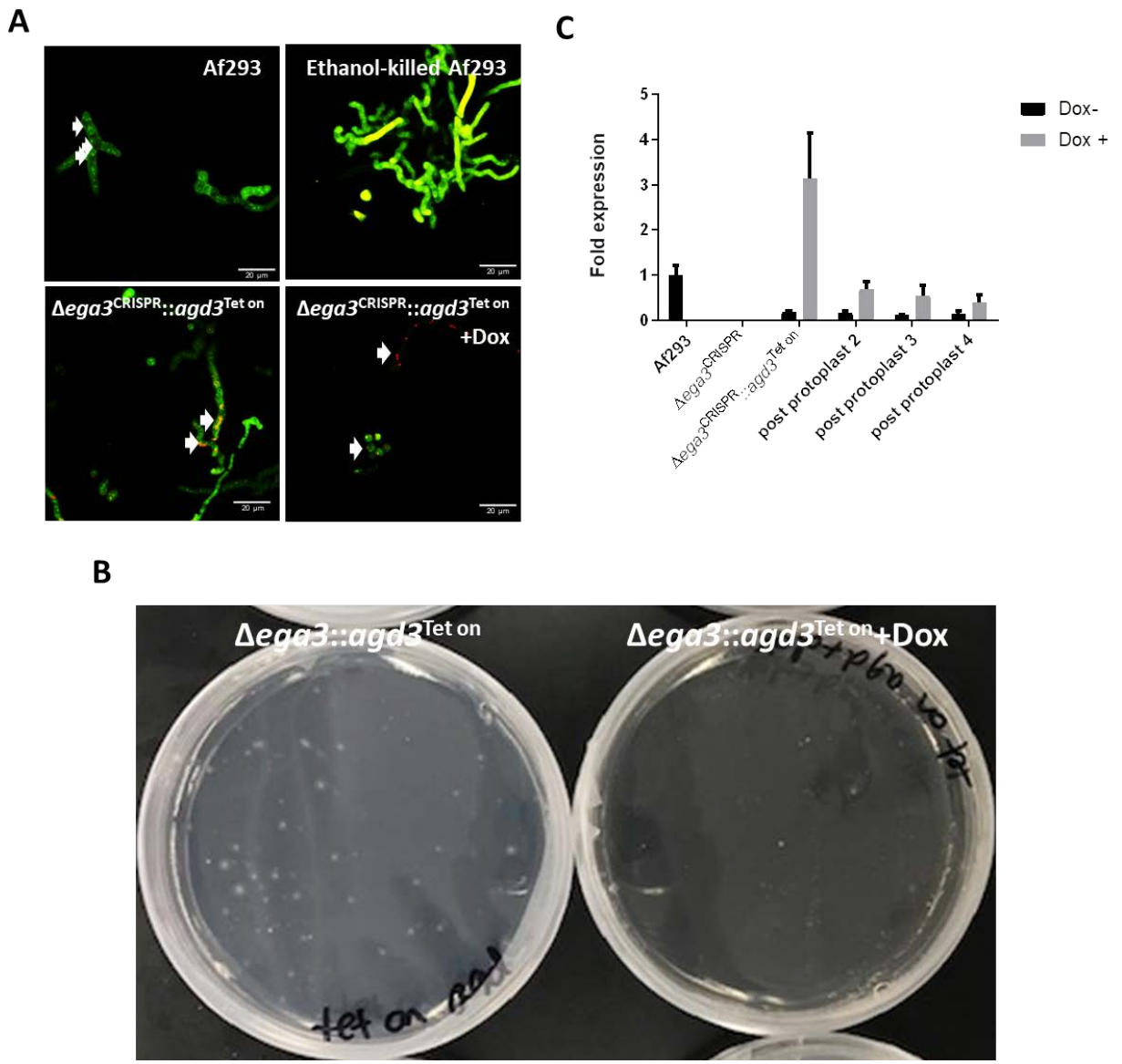


**Figure 3: Expression of *agd3* in the Δ*ega3*$^{\text{CRISPR}}$*::agd3*$^{\text{Tet on}}$ strain isn't lethal but can be downregulated by *A. fumigatus.* A)** Confocal microscopy of FUN1 stained 18 hour hyphae of the Δ*ega3*$^{\text{CRISPR}}$::*agd3*$^{\text{Tet on}}$ strain. Red vacuoles (white arrows) indicate viable hyphae. **B)** Gene expression of hyphae from conidia harvested from regenerated protoplasts of Δ*ega3*$^{\text{CRISPR}}$::*agd3*$^{\text{Tet on}}$ measured by RT-qPCR. After 18 hours of growth in YPD medium. Bars represent mean, error bars represent highest value replicate. n=1 biological replicate with 3 technical replicates per experimental condition. **C)** Regenerated protoplasts of Δ*ega3*$^{\text{CRISPR}}$::*agd3*$^{\text{Tet on}}$ (top) and Δ*ega3*$^{\text{CR}}$::*agd3*$^{\text{Tet on}}$ + Dox (bottom).

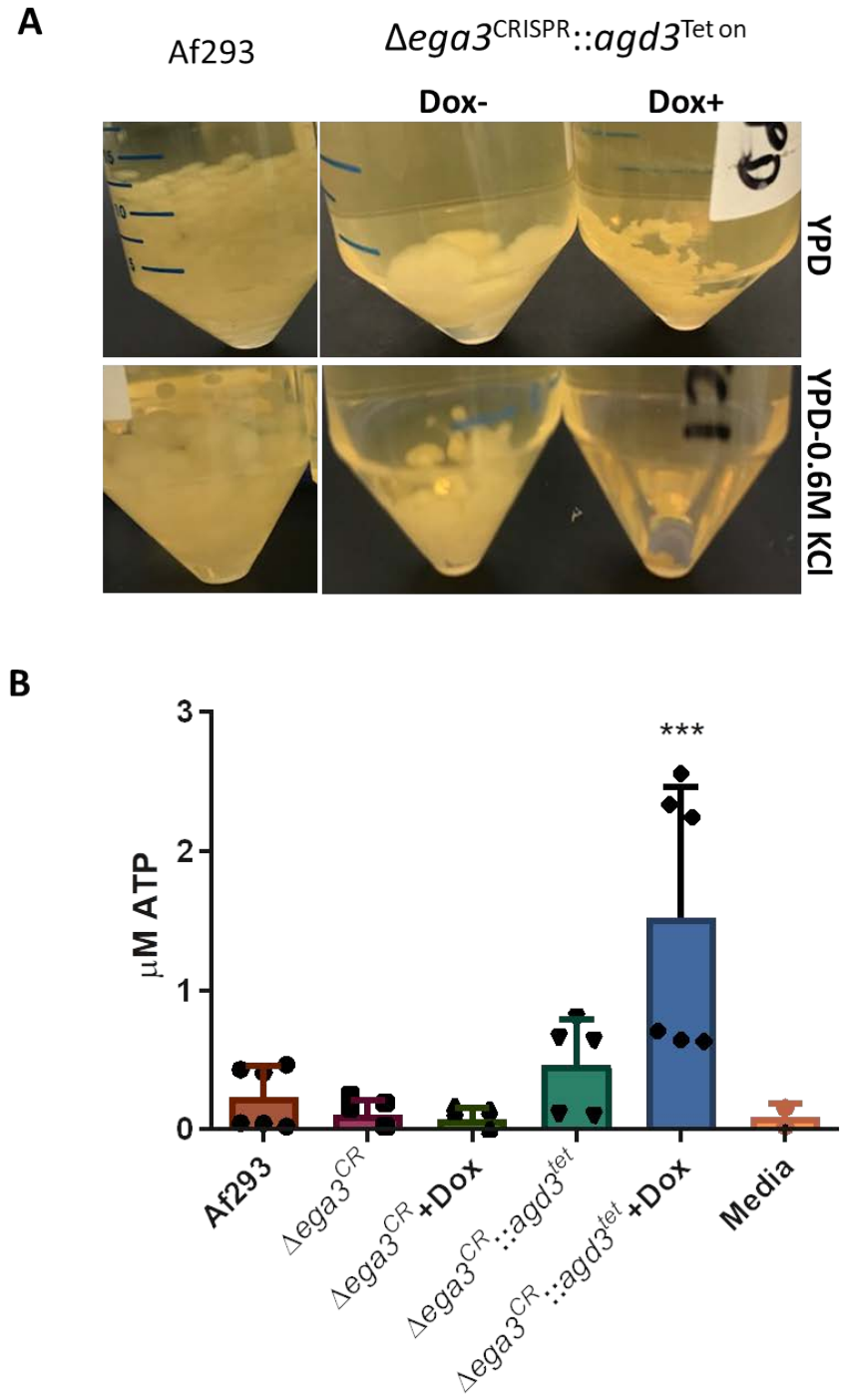


**Figure 4: Expression of *agd3* in the Δ*ega3*$^{\text{CRISPR}}$::*agd3*$^{\text{Tet on}}$ strain results in membrane instability under osmotic stress and leakage of the cytosol. A)** Growth of the Δ*ega3*$^{\text{CRISPR}}$::*agd3*$^{\text{Tet on}}$ mutant and its parent strain (Δ*ega3*$^{\text{CRISPR}}$) in YPD +/-0.6M KCl in the presence of absence of Dox after 18 hours. **B)** Quantification of luminescence produced by firefly luciferase consumption of ATP released into the CS of the indicated strains grown for 18 hours in YPD medium in the presence or absence of Dox. *** indicates P<0.001 as calculated by one-way ANOVA with Dunnett's multiple comparisons test. n=2 biological replicates with 3 technical replicates per experimental condition.

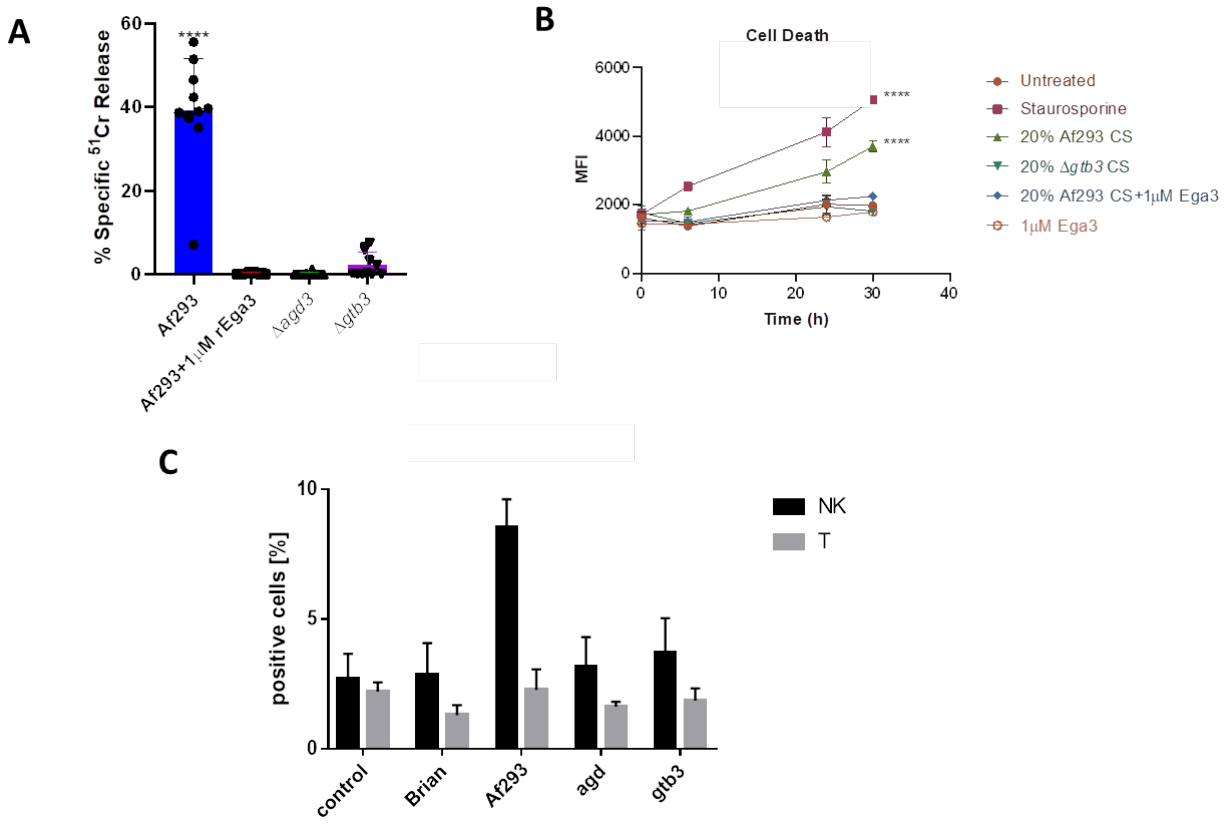


**Figure 5: Exposure to deacetylated GAG results in cytosolic efflux, membrane damage and death in mammalian cells.** **A)** Epithelial cell injury following exposure to deacetylated GAG. $^{51}$Cr loaded A549 pulmonary epithelial cells were co-cultured with fungal CS from the indicated strains +/- recombinant Ega3 hydrolase for 24 hours. Cellular damage was measured by quantification of the fraction of $^{51}$Cr release. Each bar represents the mean of three independent experiments performed in triplicate with error bars indicating SEM. **** indicates $p<0.0001$ as determined by one-way ANOVA with Dunnett's multiple comparisons test. n=3 biological replicates with 3 technical replicates per experimental condition. **B)** Decreased cellular viability after exposure to deacetylated GAG. Bone marrow derived macrophages from mice were incubated in CS from the indicated fungal strains +/- recombinant Ega3 hydrolase in the presence of propidium iodide (PI). **** indicates $P<0.0001$ as determined by two-way ANOVA with Tukey's multiple comparison test. Points represent mean, error bars represent standard deviation. n=3 biological replicates with 3 techical replicates per experimental condition. **C)** Death of primary human NK and T cells following exposure to deacetylated GAG-containing CS. After 20h co-culture with CS of the indicated strains, cells were stained with PI and annexin V to gate for cells undergoing apoptosis. Bars represent the mean number of cells undergoing apoptosis and error bars represent standard deviation. n=3 biological replicates.

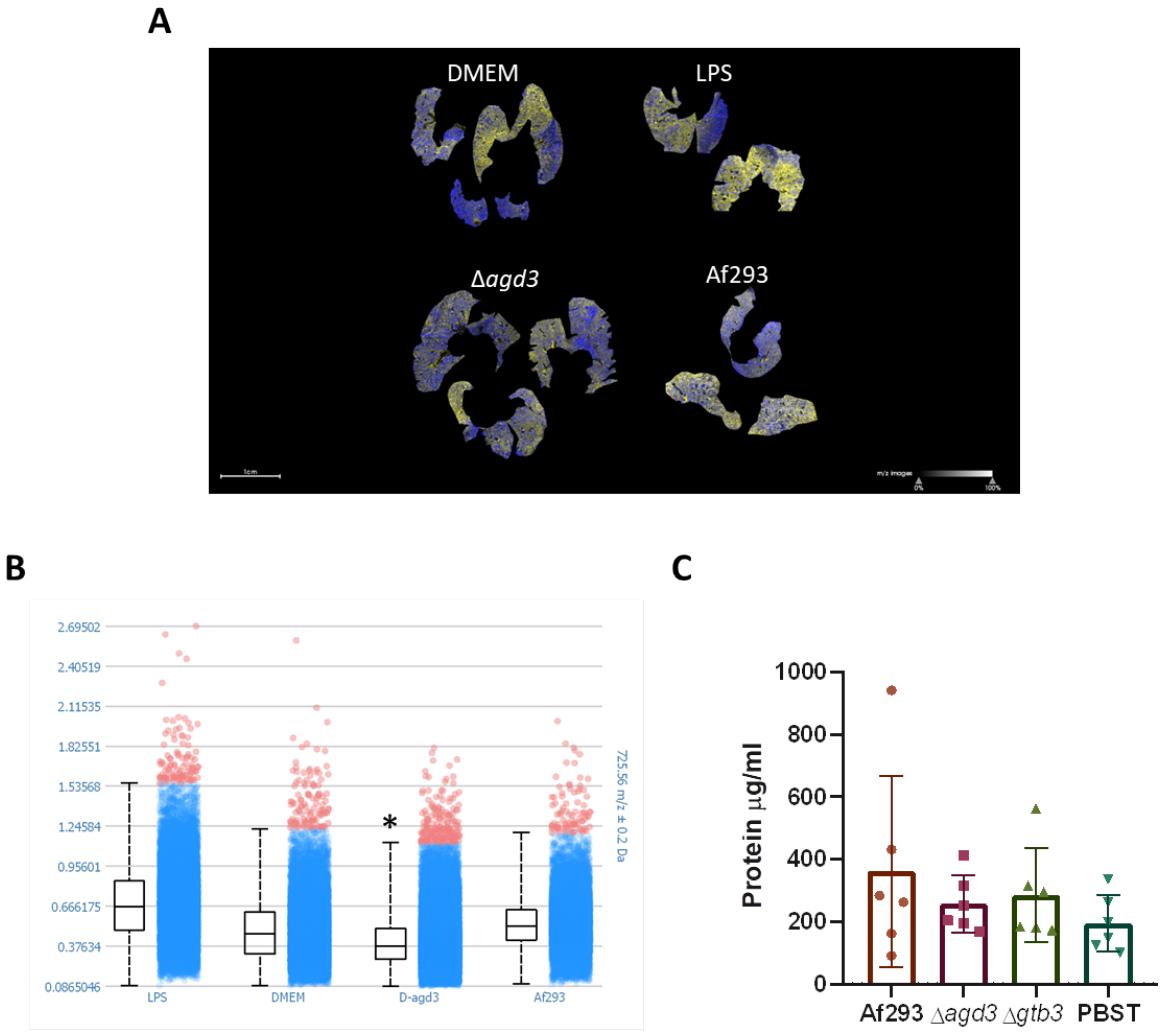


**Figure 6: Deacetylated GAG induces expression of inflammatory lipids. A)** MALDI-TOF imaging on mouse lung sections shows an increase in inflammatory sphingomyelin exposure in lungs inflated with wild-type *A. fumigatus* culture supernatants. **B)** Plot of intensity of sphingomyelin mass/charge (*m/z*) peak from every pixel of MALDI-TOF images. Box plots represent median intensity and interquartile range. * indicates $P<0.05$ as determined by Student's t test. n=2 biological replicates with 1 mouse per group. **C)** 6-8 week old Balb/c mice infected with $5x10^6$ conidia per mouse were sacrificed 24 hours after infection. Lungs of the mice were lavaged immediately with PBS and protein content in the lavage fluid was measured using a BCA assay as a measure of pulmonary damage. No statistical difference was observed between groups. n=1 biological replicate with 6 mice per group.

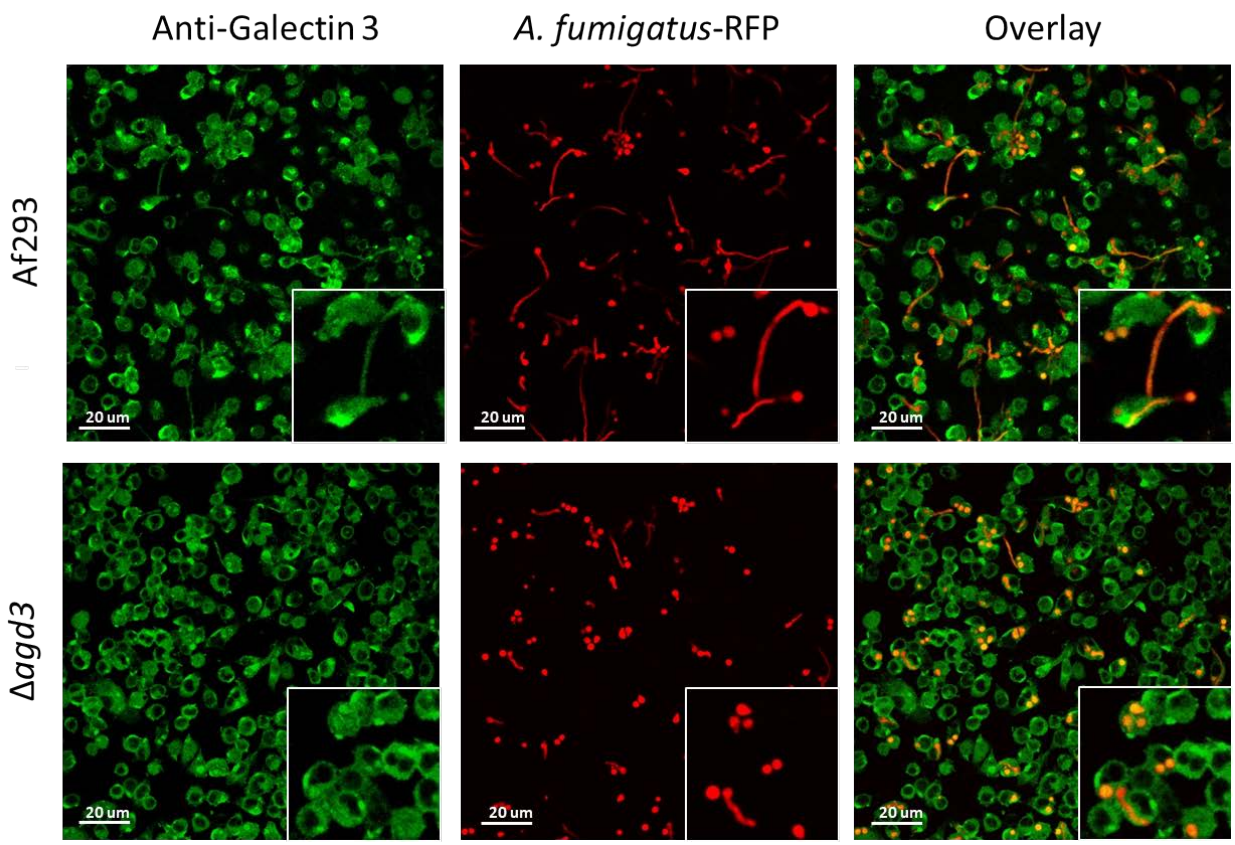


**Figure 7: Production of deacetylated GAG by *A. fumigatus* enhances fungal escape from macrophages.** Confocal micrographs of the indicated RFP-labeled *A. fumigatus* strains phagocytosed by MH-S macrophages. Conidia of the indicated RFP-expressing *A. fumigatus* strains were allowed to germinate for 4.5 hours before a further 4 hour co-culture with the MH-S macrophages on fibronectin-coated coverslips. After co-culture, coverslips were washed to remove extracellular fungi before fixing with 4% PFA. Macrophage cytoplasmic contents were labeled with anti-galectin 3 primary antibody and anti-rabbit secondary antibody conjugated to AlexaFluor 488.

# Chapter 5: Materials and methods

**Fungal strains and growth conditions:** *A. fumigatus* strains Af293 and Δ*akuB*$^{Ku80}$ (Ku80) (244) were used as the parent strains for construction of mutants. Strains were maintained on Yeast Extract-Peptone-Dextrose (YPD) agar (Difco) at 37°C and conidia harvested after 7 days by washing plates with phosphate buffered saline (PBS)+0.05% Tween 80 and then centrifuged to remove hyphal elements.

**Fungal culture supernatants:** Culture supernatants (CS) were prepared by inoculating $10^6$ conidia in 100ml of Brian media and incubated for 72 hours at 37°C shaking at 200rpm. Fungal biomass was removed by filtration with Miracloth (Millipore) and the CS were dialyzed for three days in 3500 MWCO tubing. Sodium azide was added to the dialysis water for the first overnight to sterilize the supernatants and the last 24 hours of dialysis were done with PBS at physiological pH in order to be compatible for culture with mammalian cells.

*Genetic manipulations*

**Transformations :** Transformations were performed using chemically protoplasted *A. fumigatus* strains as previously described (246). Briefly, β-D-glucanase from *Trichoderma harzianum* (Sigma) at a concentration of 48 mg/ml and 50U chitinase from *Streptomyces griseus* (Sigma) were used to digest fungal cell walls over a period of three hours. After digestion, protoplasts were collected by centrifugation and transformed with the indicated constructs then suspended in molten Aspergillus minimal medium (AMM) agar osmotically stabilized with 22 g/L sorbitol containing 150 µg/ml phleomycin, 250 µg/ml hygromycin or 1 µg/ml pyrithiamine as a selection marker and incubated at room temperature for 3 days to allow regeneration of cell walls. Isolated fungal colonies were used for single spore purification.

**Construction of the Δ*ega3*$^{CRISPR}$ mutant:** To construct the Δ*ega3*$^{CRISPR}$ mutant, a transient CRISPR-Cas9 gene deletion system has been used (294, 295). The Cas9 expression cassette was amplified from plasmid pFC331 (295), using primers Cas9-F and Cas9-R (**Table 1**). Two 20 bp protospacer sequences were designed within the 5' and 3' end of the coding sequence of the target gene (**Table 1**). The sgRNA expression cassette was constructed by single-junction fusion PCR. First, two DNA fragments were amplified from plasmid pFC334 (295), using paired primers sgRNA-F, Ega3-sgRNA-ss-R and sgRNA-R, Ega3-sgRNA-ss-F (**Table 1**). Then, the sgRNA expression cassette was amplified by fusion PCR from the two DNA fragments, using primers sgRNA-F and sgRNA-R (**Table 1**). The hygromycin resistance (HygR) repair template was amplified from plasmid pVG2.2-hph (296) using paired primers Hyg-F and Hyg-R, which had about a 50 bp homology region to the upstream 5' protospacer and the downstream 3' protospacer. The HygR repair template (5 µg) were mixed with Cas9 cassette (1 µg) and the two sgRNA cassette (1 µg each), and used for protoplast transformation. Hygromycin resistant clones were screened for the deletion of target gene by colony PCR using primers Ega3-Screen-F and Ega3-Screen-R (**Table**

**1**). The positive clones were also confirmed for lack of integration of Cas9 or synthetic gRNA, using paired primers Cas9-Screen-F, Cas9-Screen-R and sg-Screen-F, sg-Screen-R (**Table 1**).

**Construction of the Δ*ega3::ega3*$^{\text{CRISPR}}$ strain:** Complementation of the Δ*ega3*$^{\text{CRISPR}}$ strain was done at the native locus by using CRISPR/Cas9 to introduce an *ega3* allele with a silent mutation to differentiate it from *ega3* from Af293. This was done by making two cuts with sgRNAs targeted to either side of the hygromycin cassette that had been used to disrupt *ega3* and supplying the silently mutated *ega3* allele as well as a separate phleomycin resistance cassette as a repair template and ectopically-inserted selection marker respectively. The two sgRNAs were made in two steps. For step one, two independent PCRs were done: one with the primers Ega3-sgRNA(1/2)::pSNR52 and sgRNA-cassette-fwd using plasmid pSNR52 (sgRNA cassette) (PCR 1) and one with the primers Ega3-sgRNA(1/2)::scaffold and sgRNA-cassette-rev-low also using pSNR52 as a template (PCR 2). A fusion PCR was then performed using the products of the two previous PCR reactions and the nested primers sgRNA-cassette-Fwd-int and sgRNA-cassette-Rev-int to generate a construct containing the sgRNA promoter, target sequence, sgRNA scaffold and terminator. The Cas9 cassette was amplified with primers Cas9-Fwd and Cas9-Rev using pSR426 as a template. The repair template was made using a fusion PCR strategy to perform site-directed mutagenesis to code for two silent mutations in *ega3.* To do this, two PCRs were performed using Af293 gDNA as a template. PCR 1 was done with primers Ext5 and Point-Mutant-Rev, and PCR 2 was done with primers Ext3 and Point-Mutant-Fwd. The point mutations induced were 309C>A (Ile>Ile) and 312C> T (Asp>Asp). A nested PCR was then done with the products of the two previous reactions and the primers Ext5-nested and Ext3-nested. The phleomycin cassette for ectopic insertion was amplified using the primers Ble Pr7 and Ble Tr7. The sgRNA cassette, Cas9 cassette, repair template and resistance marker were all used to co- transform protoplasts as described above. Correct insertion of the *ega3* allele was verified using the primers Ega3 Ext1 and Ega3 Last, and verification of expression of *ega3* was done by RT-qPCR with the primers Ega3 RTII Fwd and Ega3 RTII Rev.

**Construction of the Δ*ega3*$^{\text{Ku80}}$ strain:** The constructs for transformation were generated by fusion PCR, where flanking sequences upstream and downstream were fused to overlapping halves of the phleomycin resistance (*ble*) cassette. The templates for the fusion constructs were generated by PCR from Af293 gDNA using the primers Ega3 P1/Ega3 P2 (upstream flanking sequence), Ega3 P3/Ega3 P4 far (downstream flanking sequence), and from the *ble* plasmid p402 using the primers Ble Pr7/Ble Tr7. The fragments for transformation were amplified by fusion PCR using the primers Ega3 P1/BL6 and LE8/Ega3 P4 far to generate the upstream and downstream halves respectively. Three µg total of the two PCR fragments were transformed into protoplasts of the Ku80 strain as described above. Correct insertion

of the marker was verified using the primers Ega3 ext 1 and BL6, and absence of *ega3* expression was confirmed using the primers Ega3 RTII fwd and Ega3 RTII rev.

**Construction of the Δ*ega3::*ega3$^{Ku80}$ strain:** The construct used to complement the Δ*ega3*$^{Ku80}$ strain was synthesized by Bio Basic Canada, Inc. Fragments of approximately 1Kb homologous to the upstream and downstream sequences of the *akuB* (Ku80) gene were synthesized and inserted into pAN-7.1 at the BtrI and SbfI restriction sites respectively to create pAN-7.1::Ku80FS. The *ega3* locus was PCR amplified using the primers Ega3 Ext1 and Ega3 Ext4-far (**Table 1**) and blunt-end cloned into the vector pCR-Blunt II-TOPO and then subcloned into pAN-7.1::*akuB*FS at the StuI restriction site to generate pAN-7.1::Ku80FS-*ega3*. Correct insertion was verified by restriction digest using the enzymes SnaB1 and Hpa1 (New England Biolabs). This plasmid was then linearized by restriction digest with DraI (New England Biolabs) and used to transform the Δ*ega3*$^{Ku80}$ strain. Correct insertion at the Ku80 locus was verified using the primer pairs Ku80 Ext 4/Ega3 1st and Ku80 Ext 1/Ega3 Last.

**Construction of the Δ*ega3*$^{CRISPR}$::*agd3*$^{Tet\ on}$ strain:** The *agd3* ORF and terminator were PCR amplified using primers *agd3*-First and *agd3*TrRev. The resulting product was then blunt-end cloned into the vector pCR-Blunt II-TOPO. The *agd3* ORF-terminator fragment was then subcloned into the BS216 vector between the PmeI and Bsu361 restriction sites by Bio Basic Canada, Inc. to create BS216::*agd3*. This plasmid was used to transform the Δ*ega3*$^{CRISPR}$ strain as previously described (246).

**Gene expression studies:** Expression of the GAG cluster genes *uge3*, *gtb3*, *sph3*, *agd3*, and *ega3* in the Δ*ega3*$^{CRISPR}$ and Δ*ega3*$^{Ku80}$ mutants as well as their respective *ega3* or *agd3* complemented strains were compared to their Af293 or Ku80 parent strains. Primer pairs spanned exon-exon junctions where applicable. The indicated strains were grown for 18h at 37°C in liquid shaking conditions in YPD or AMM (pH 6.5) media. Mycelia were collected by filtration and RNA was extracted by crushing under liquid nitrogen and purified on a column (Nucleospin RNA Plant, Macherey-Nagel) according to the manufacturer‘s instructions. cDNA was amplified with random hexamers using the Quantitect Reverse Transcription kit (Qiagen) and subsequently used for quantitative reverse transcription (RT-qPCR) using the SsoAdvanced Universal SYBR® Green Supermix (BioRad), performed using an Applied Biosystems 7300 Real Time PCR System thermocycler.

**Ega3 protein modeling:** The amino acid sequence for Ega3 (Afu3g07890) was obtained from www.fungidb.org and submitted to the Phyre2 server for alignment with known sequences for structure determination (238). The resulting .pdb file was loaded into PyMol 2 (Schrödinger LLC) for structure visualization. The same amino acid sequence was also submitted to the TMHMM server (237) for

prediction of the orientation of the N and C termini for Ega3 in relation to the inside and outside for the cell.

*Biochemical assays*

**Enzyme fingerprinting:** CS from 3 day old cultures of *A. fumigatus* Af293 were filtered through Miracloth (Millipore) prior to ethanol precipitation. The precipitate was then washed with 70% (v/v) ethanol twice, 150 mM NaCl, and then water. The precipitate was then freeze-dried. One milligram of precipitated secreted GAG was resuspended in 500 µl of PBS containing 1 µM $Ega3^{46-318}$. After incubating for 1 h, the sample was dried, reduced and then propionylated. Reduction was performed incubating the oligosaccharides in 10 mg/ml sodium borohydride in 1 M ammonium hydroxide overnight at room temperature. The reaction was then quenched with 30% acetic acid prior to the propionylation reaction. Oligosaccharides were resuspended in methanol/pyridine/propionic anhydride (10:2:3) for 1 h at room temperature. Reduced and propionylated oligosaccharides were then purified using the Hypercarb Hypersep SPE cartridge (Chromatographic Specialties Inc) and eluted with 50% (v/v) acetonitrile (ACN). Dried elute was resuspended in 0.2% trifluoroacetic acid (TFA) and spotted on a MALDI-TOF plate in a ratio of 1:1 (v/v) with 5 mg/ml 2,5-dihydroxybenzoic acid matrix reconstituted in ACN, 0.2% (v/v) TFA (70:30, v/v). Spectra were recorded on a Bruker UltrafleXtreme in positive reflector mode and an accumulation of 5000 laser shots (201).

**Extracellular vesicle (EV) isolation:** The protocol used in this thesis was developed from an established protocol for exosome isolation from *L. amazonensis* (297). *A. fumigatus* Af293 was grown for 72 hours at 37°C at an inoculation density of $1x10^6$ conidia/ml in Brian synthetic medium (pH 5.4) shaking at 200 rpm. Biomass was filtered out using a 0.22 µm pore filter. The filtrate was centrifuged at 100,000x*g* for 1 hour at 4°C in an ultracentrifuge (Optima XPN-90, Beckman Coulter Life Sciences) with a swing rotor (SW32.Ti) in thin-walled open-top polypropylene 16x102 nm tubes (Beckman Coulter). The supernatant was decanted and the pellets were pooled and resuspended in exosome buffer (137 mM NaCl, 20 mM Hepes pH 7.5) and ultracentrifuged once more. The pellet was then resuspended in the remaining exosome buffer (approximately 0.5 ml) and stored at -80°C until further use. The quantity of EVs was estimated using a commercial Micro BCA kit (Pierce). EV size and morphology were determined using nanoparticle tracking analysis with an LM-10 particle tracker (Nanosight) as well as negative staining with uranyl acetate and transmission electron microscopy with a FEI Tecnai 12 120 kV transmission electron microscope as previously described (297).

**Membrane fractionation:** Hyphae were harvested by filtration and re-suspended in 40 ml of lysis buffer (50 mM HEPES pH 7.5, 300 mM NaCl, 1 mM TCEP, 5% (v/v) glycerol, and protease inhibitor cocktail

for fungal and yeast extracts (Bioshop, product #PIC007.1)), and lysed by homogenization with a Polytron® PT 2500 E homogenizer (Kinematica). Cellular debris was removed by centrifugation at 20,000 x g for 30 min, and the supernatant was further centrifuged at 200,000 x g for 60 min in an Optima XPN-90 ultracentrifuge (Beckman Coulter Life Sciences) to pellet the membranes.

**Protein identification:** EV or membrane fraction samples were loaded onto a single stacking gel band to remove lipids, detergents and salts. The single gel band containing all proteins was reduced with DTT, alkylated with iodoacetic acid and digested with trypsin. Two micrograms of extracted peptides were re-solubilized in 0.1% aqueous formic acid and loaded onto a Thermo Acclaim Pepmap (Thermo, 75uM ID X 2cm C18 3uM beads) precolumn and then onto an Acclaim Pepmap Easyspray (Thermo, 75uM X 15cm with 2uM C18 beads) analytical column separation using a Dionex Ultimate 3000 uHPLC at 250 nl/min with a gradient of 2-35% organic (0.1% formic acid in acetonitrile) over 3 hours. Peptides were analyzed using a Thermo Orbitrap Fusion mass spectrometer operating at 120,000 resolution (FWHM in MS1) with HCD sequencing (15,000 resolution) at top speed for all peptides with a charge of 2+ or greater. The raw data were converted into .mgf format (Mascot generic format) for searching using the Mascot 2.6.2 search engine (Matrix Science) against A_fumigatus_Af293 predicted sequences. The database search results were loaded onto Scaffold Q+ Scaffold_4.9.0 (Proteome Sciences) for statistical treatment and data visualization.

**Western blotting:** 48 hour shaking cultures of the *ega3* null mutant and parental and complemented strains grown in YPD (Difco) at 37°C were harvested by filtration and ground under liquid nitrogen. Crushed biomass was resuspended in 1M Tris pH 7.5 supplemented with 10 µl protease inhibitors for fungal and yeast extracts (Bioshop product #PIC007.1) and 500 µl of 2% Triton X and incubated for 1 hour on a Nutator at 4°C. The slurry was frozen and then lyophilized overnight in a Labconco FreeZone 4.5L freeze drier. Proteins were extracted by cold acetone precipitation. Lyophilized samples were suspended in cold 80% acetone and incubated at -20°C for one hour. Proteins were pelleted by centrifuging for 10 minutes at 4°C at 10,000 rpm in a Sorvall RC 5B Plus high-speed centrifuge. The pellet was washed again with cold 80% acetone for 1 hour at -20°C and then centrifuged again. After drying, 50 mg of protein pellet were resuspended in Laemmli buffer and loaded onto an SDS-PAGE gel and separated according to size. Protein bands were transferred to a nitrocellulose membrane and then blocked in TBS with 5% (w/v) skim milk powder overnight at 4°C. Blocked membranes were incubated with a polyclonal rabbit anti-Ega3 primary antibody, produced by Cedarlane® as previously described (298) and kindly gifted by Dr. P. Lynne Howell, for three hours at room temperature. Detection was done using a donkey anti-rabbit secondary antibody conjugated to HRP (Cedarlane, product #711-035-152) and

ECL (Immobilon, Millipore-Sigma) was used for chemiluminescent signal, detected using a FluorChem SP gel doc (Alpha Innotech).

**Biofilm adherence:** The *ega3* null mutants and their parent and complemented strains were seeded onto a round-bottom 96 well tissue culture-treated plate at a concentration of $1x10^4$ conidia/ml in a volume of 100µl Brian medium and incubated for 18-20 hours at 37°C. Recombinant Agd3 was added at the time of inoculation as required. After incubation the non-adherent biomass was aspirated and then the plate was washed once with distilled water. After washing, the remaining biomass was stained with 0.1% crystal violet for 10 minutes. Next, the plate was washed again with distilled water. The biomass was destained with 100% ethanol which was transferred to a clean plate for optical density reading at 600nm in an Asys UVM340 spectrophotometer (Biochrom), and the results used to estimate residual adherent biomass.

*Confocal Microscopy*

**SBA staining:** Conidia of the Δ*ega3*$^{CRISPR}$ strain and its parent and complemented strains were allowed to germinate for 12 hours in white Roswell Park Memorial Institute (RPMI) medium (Wisent) ± 500 nM rAgd3 at 37°C + 5% $CO_2$. Staining was done as previously described, with the minor alteration that no counterstain was used (200). Images were acquired using a Zeiss LSM780 confocal microscope and processed using Fiji software by ImageJ (299).

**Fungal viability staining:** Conidia of *A. fumigatus* Af293 and the Δ*ega3*$^{CRISPR}$ and Δ*ega3*::*agd3*$^{Tet\ on}$ strains were grown for 18 hours in YPD ± 20 µg/ml doxycycline at a density of $1x10^6$ conidia/ml at 37°C shaking at 200 rpm. A sample of mycelium was taken for each condition and stained with the FUN1 fungal viability dye (InvitrogenTM catalog # F7030) according to manufacturer instructions. Ethanol-killed Af293 served as a non-viable control. Images were acquired using a Zeiss LSM780 confocal microscope, and image processing was done using Zen Black software (Zeiss).

**Confocal imaging of phagolysosomal escape:** 12mm coverslips were coated with fibronectin in HBSS in 24 well plates and then seeded with $2x10^5$ MH-S macrophage cells/well in DMEM+10% FBS overnight at 37°C in 5% $C0_2$. The next day, $10^7$ conidia of GFP-expressing *A. fumigatus* strain Af293 and the Δ*agd3* mutant strain were incubated in 20 ml Sabouraud broth for 4.5 hours shaking at 37°C to obtain swollen conidia. Next, cells were washed with DMEM+10% FBS and then 200 µl fungal culture and 800 µl DMEM+10% FBS (total volume 1 ml) was added to the cells. Cells and fungus were co-incubated for 4 hours and then washed with PBS and fixed in 4% paraformaldehyde for 15 minutes. After fixation cells were washed three times with PBS+1% BSA and then left in PBS overnight. The next day, cells were permeabilized with 0.05% triton X100 in 5% goat serum. Coverslips were then washed three times and

incubated with anti-galectin-3 antibody for 1 hour at room temperature to label the cytoplasm of the MH-S cells. Then, after three more washes, the anti-rabbit AlexaFluor 488 secondary antibody was added for 1 hour at room temperature. The coverslips were then washed three more times and mounted on slides for confocal imaging using a Leica TCS SP8 confocal microscope using the 40X objective. Z-stacked images were obtained and overlaid on each other using Leica image processing software.

*Detection of mono- and polysaccharides*

**Monosaccharide composition of culture supernatants:** CS of the Δ*ega3*$^{CRISPR}$and Δ*ega3*$^{Ku80}$ strains and their respective parent and complemented strains were grown for 72 hours in Brian medium at an inoculation density of 1x10$^4$ conidia/ml shaking at 200 rpm at 37$^o$C. After 72 hours, the resulting biomass was filtered out using Miracloth and the CS was dialyzed for 3 days using 3500 MWCO in distilled water that was changed three times each day. Following dialysis, the CS were frozen and then lyophilized in a FreeZone 4.5L lyophilizer (Labconco). Once dry, 0.5mg of each lyophilized CS were prepared for gas chromatography-mass spectrometry as previously described (300).

**Deacetylated GAG detection:** High-binding 96 well plates (source) were coated for 1 hour at 25$^o$C with culture filtrates from 72 hour cultures of the Δ*ega3*$^{CRISPR}$ and Δ*ega3*$^{Ku80}$ mutants and their respective parent and complemented strains grown in Brain media, with media alone used as a negative control. Recombinant Agd3 or Ega3, kindly produced and provided by the lab of Dr. P. Lynne Howell, was included during coating where indicated. After coating wells were washed three times with PBS+0.5% Tween 20 and following washing, adherent GAG was detected by incubation with biotinylated soybean agglutinin (SBA) (Vector Laboratories product #B-1015-5) at a concentration of 30 nM and avidin-HRP diluted 1:700 for an additional hour. Next, the plate was washed three times and TMB substrate (Millipore Sigma) was added for 10 minutes and then stopped with 2N $H_2SO_4$. Absorbance at 450nm was read on a NanoQuant Infinite® M200 Pro plate reader (Tecan).

*Mutation characterizations*

**Characterization of *agd3* deletion in the Δ*ega3*$^{CRISPR}$ strain:** The primers Agd3 881F and Ega3 End ORF Rev (**Table 1**) were used to amplify the 3` end of the *agd3* gene from genomic DNA extracted from the Af293 and the Δ*ega3*$^{CRISPR}$ strains. The product was run on a 1% agarose gel and stained with 1X SYBR green and visualized on an Fluor Chem SP gel doc (Alpha Innotec).

**Uge3 mutation identification:** Genomic DNA was extracted from protoplasts of the Ku80 and Δ*ega3*$^{Ku80}$ strains using the phenol-chloroform method in order to avoid DNA fragmentation. Briefly, strains were chemically protoplasted using lysing enzymes from *Trichoderma harzianum* (Sigma) as previously

described. Protoplasts were then pelleted and lysed using a lysis buffer (400mM TRIS-HCl, 60mM EDTA, 1% w/v SDS pH 8). DNA was extracted by phenol-chloroform extraction. Recovery of high molecular weight DNA was verified using a 0.8% agarose gel stained with SYBR™ Safe DNA gel stain. DNA samples were then used for PacBio Single Molecule Real-Time (SMRT) sequencing at Génome Québec Innovation Centre (Montréal QC). Sequence analysis was done using BLAST® (National Center for Biotechnology Information, Bethesda MD) and Integrated Genomics Viewer software (Broad Institute, Cambridge MA). Homology modeling was performed using the I-TASSER (247) and Phyre2 (238) web servers. Analysis of amino acid motifs was done using BLAST (301). All structural figures were generated using PyMol (The PyMol Molecular Graphics System, Version 1.2 Schrödinger, LLC).

*Comparison of fungal growth*

**Tube assays:** The Af293 and Δ*ega3*$^{CRISPR}$::*agd3*$^{Tet\ on}$ strains were inoculated in 20ml of YPD±0.6M KCl±20µg/ml doxycycline at a concentration of $5x10^5$ conidia/ml and grown for 18 hours shaking at 200rpm at 37°C. After 18 hours the amount of fungal biomass was visually assessed.

**Plate assays:** A previously developed protocol was used with slight modifications (284). Briefly, $2x10^6$ conidia/ml in 100µl 2X concentrated YPD±40µg/ml doxycycline were plated in a 96 well plate and then 100µl 0.1% Tween 80 was added to all wells (to keep a biofilm from forming at the surface) of a flat bottom 96 well plate. The plate was then loaded into a NanoQuant Infinite® M200 Pro plate reader (Tecan) and the optical density at 405nm measured hourly for 48 hours at 37°C.

*Fungal and mammalian cell damage*

**ATP assay:** Cultures of the Af293, Δ*ega3*$^{CRISPR}$ and Δ*ega3*$^{CRISPR}$::*agd3*$^{Tet\ on}$ strains were grown for 18 hours in YPD media at a concentration of $5x10^5$ conidia/ml at 37°C shaking at 200rpm. A 10µl sample of supernatant was taken from each culture and used in the ATP Determination Kit (Invitrogen) according to manufacturer instructions.

**Chromium release assay:** Damage to A549 pulmonary epithelial cells was measured as previously described (149). A549 cells were grown to confluence in 24 well tissue culture plates and incubated with 3 µCi of [$^{51}$Cr] for 24 hours at 37°C/5% $CO_2$. Cells were washed with HBSS to remove unincorporated [$^{51}$Cr] and then infected with $5x10^5$ conidia in the presence of either 40% dialyzed fungal culture supernatants or 40% dialyzed Brian media in serum free DF12K medium and incubated for 24 hours. The supernatant and cell pellets lysed with 6N NaOH were collected and the content of [$^{51}$Cr] was counted in a gamma counter for each fraction. Damage was determined by calculation using the following formula: (experimental release spontaneous release)/(total incorporation spontaneous release) x100 (302).

**BMDM differentiation:** Bone marrow derived macrophages (BMDMs) were differentiated from bone marrow aseptically harvested from femurs of healthy C57/Bl6 mice. Femurs were flushed and bone marrow was plated with BMDM differentiation media supplemented with 50 ng/ml recombinant murine macrophage colony-stimulating factor (M-CSF, PeproTech product #315-02) (day 0). BMDM differentiation medium was composed of RPMI 1640 medium (Wisent) supplemented with 10% FBS (Wisent), 10mM HEPES (Wisent), 1mM sodium pyruvate (Gibco), 1% essential and non-essential amino acids (Wisent), and 5% penicillin-streptomycin solution (Wisent). The medium was then balanced to physiological pH with 5N NaOH. Cells were fed with more BMDM differentiation media and M-CSF on day 3. For experiments, cells were harvested and counted on day 7 and used immediately.

**Propidium iodide (PI) staining:** PI staining was performed to assess cell death and membrane integrity of BMDMs in the presence of deacetylated GAG. After differentiation**,** BMDMs were seeded in 96 well flat bottom plates at a density of 200,000 cells/well and grown overnight. The next day, media was aspirated and dialyzed CS from the Af293, Δ*agd3* or Δ*gtb3* strains at a final concentration of 20% in BMDM media was added to the cells. 1 µM staurosporine (Sigma) was used as a positive control for induction of apoptotic cell death. Wells with dialyzed Brian media and wells without PI were also used as controls. PI fluorescence signal was read every hour for six hours and then every hour from 23-30 hours in a NanoQuant Infinite® M200 Pro plate reader (Tecan).

**NK and T cell isolation**: Peripheral blood mononuclear cells (PBMCs) were isolated from leukoreduction system (LRS) chambers, a byproduct of platelet donations from healthy individuals. LRS chambers were provided by the Institute for Transfusion Medicine and Haemotherapy of the University Hospital Wuerzburg. PBMCs were obtained by ficoll-Histopaque-density centrifugation. For that, peripheral heparinized blood from LRS chambers was transferred into a 50 ml centrifugation tube and diluted with HBSS buffer (Sigma Aldrich) supplemented with 2 mM EDTA (Sigma Aldrich) and 1% FCS (Sigma Aldrich) to a volume of 50 ml. The diluted blood sample was divided into two x 25ml and added to 50 ml centrifugation tubes containing 14 ml Histopaque separating solution each (Sigma Aldrich, density 1.077 g/ml). For isolation of PBMCs, the tubes were centrifuged at 800 x g for 20 min (RT) at the lowest acceleration and brake settings. The PBMC layer was carefully transferred to a fresh 50 ml tube using a sterile pasteur pipette. The cells were washed two times with 50 ml HBSS buffer and centrifuged at 120 x g for 15 min (RT) at the lowest acceleration and brake settings. After the last washing step, the PBMCs were counted with a cell viability analyzer.

The isolation of NK cells or T cells from freshly isolated PBMCs was performed by depletion of all other cell types with magnetically labeled antibodies using the human NK cell isolation kit or the human Pan T

cell isolation kit from Miltenyi Biotec. NK and Pan T cell isolation was performed following the manufacturer's instructions. Isolated NK or T cells were centrifuged at 300 xg and cultured at a concentration of 1 x $10^6$ cells/ml in RPMI (Gibco, Thermo Fisher Scientific) supplemented with 10% FCS if not stated otherwise. NK cells were stimulated overnight with 1000 U/ml IL-2 (Proleukin® S, Novartis). Cells were harvested by carefully pipetting up and down the cell suspension several times. After a centrifugation step, cells were resuspended at a cell concentration of 1 x $10^6$ cell/ml in fresh medium.

**NK/ T cell damage assay:** To analyze the ability of *A. fumigatus* derived culture supernatants to induce NK and T cell damage, T cell and pre-stimulated NK cell cultures were washed and adjusted to 2 x $10^6$ cells/ml. 100 µl of the NK or T cell suspension was seeded in a flat bottom 96-well plate and stimulated with equal volumes of either Af293-, *Δagd3*-, or *Δgtb3* mutant-derived supernatants (5X) diluted in RPMI. As negative control, cells were incubated with Brian medium, in which the different *A. fumigatus* strains were grown. Staurosporin (1 µM, Sigma Aldrich) served as positive control. The cell cultures were incubated at 37 °C, 5 % CO2 for 1 h, 6 h or 24 h. Flow cytometry was used to investigate the influence of CS derived from the Af293, Δ*agd3* and Δ*gtb3* strains on NK and T cell damage, as detailed below.

**Flow cytometry (surface and annexin v/ propidium iodide staining):** Cultured cells were harvested and transferred to FACS tubes. Samples were washed with 1 ml of pre-cooled HBSS buffer supplemented with 1 % FCS and 2 mM EDTA (FACS buffer) before a centrifugation step was performed. All centrifugation steps concerning the preparation of flow cytometric probes were performed at 1800 rpm for 5 min. For analysis of surface proteins, 50 µl of an antibody mix in FACS buffer was prepared. A complete list of surface markers and their applied dilutions can be found in **Table 2**. After incubation of the cell suspension with the surface staining solution for 15 min at 4 °C in the dark, the cells were washed with 2 ml of FACS buffer to wash away unbound surface antibodies. To investigate the toxic capacity of *A. fumigatus*-derived supernatants on NK and T cells, annexin V/propidium iodide (PI) staining was performed. Annexin V and PI (**Table 2**) were diluted in 1X annexin binding buffer (BD Bioscience) and cells were resuspended at a concentration of 2x$10^5$ cells in 100 µl of the annexin v/PI staining solution, incubated for 15 min at RT in the dark, and analyzed by flow cytometry immediately. NK cells were gated into CD3-/CD56+ cells and T cells into CD3+/CD56- cells. Their purity was consistently over 95 %. Flow cytometric analysis was performed on a MACSQuant Analyzer 10 (Miltenyi Biotec), and data were analyzed by Kaluza (Beckman Coulter) software. **Figure 1** illustrates the gating strategy which was applied. Lymphocytes were separated from other leukocytes in the forward/side scatter setting and cell aggregates were removed in the forward height vs. area setting. The viability dye was used to exclude dead cells. NK cells were gated into and T cells into CD3+/CD56- cells. Thereafter, the cell population

was separated in either CD3-/CD56+ NK cells or CD3+/CD56- cells T cells which were further analyzed for expression of the activation marker CD69. To distinguish apoptosis and necrosis, annexin V was plotted against PI.

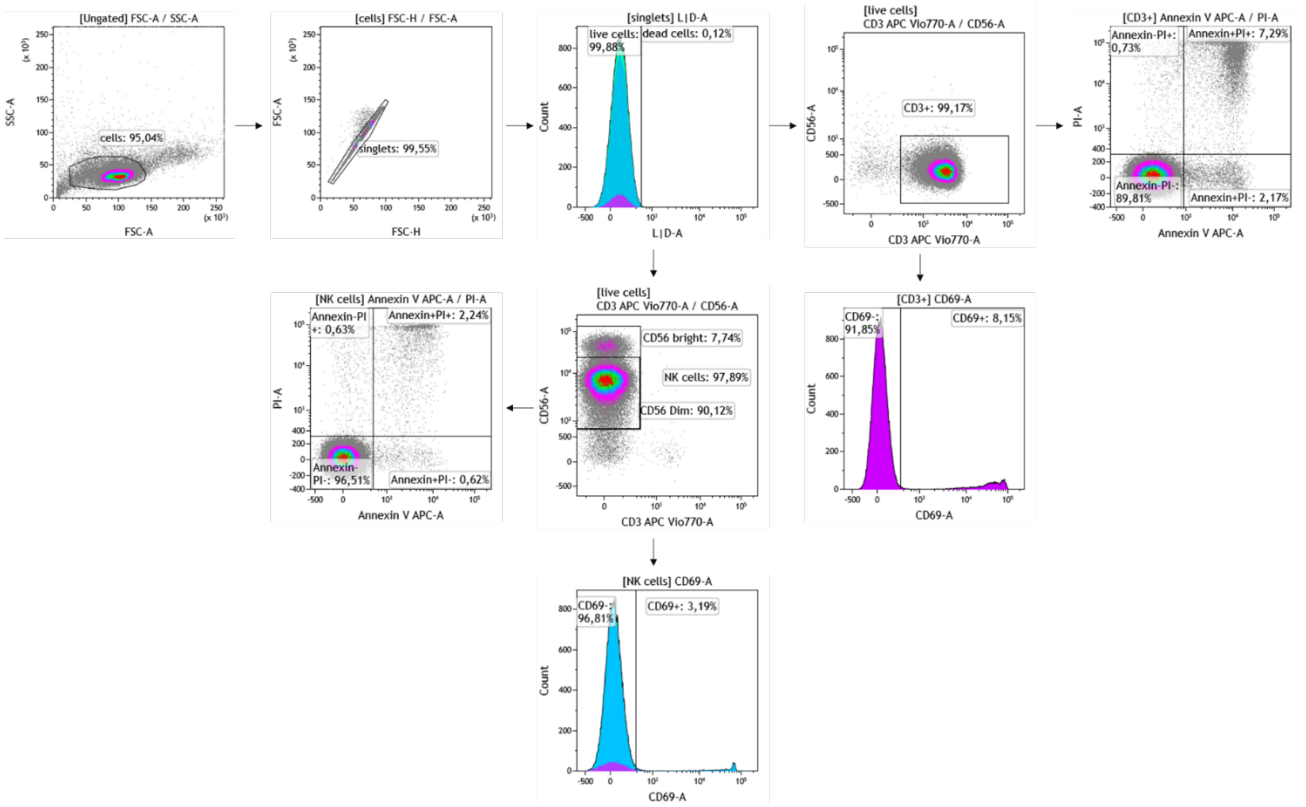


**Figure 1:** Gating-strategy for flow cytometry analysis of NK and T cells stimulated with *Aspergillus fumigatus*-derived supernatants. Lymphocytes were selected according to their forward and side scattering. CD3-CD56+ NK cells and CD3+CD56- T cells are further characterized regarding their annexin V/PI expression.

**MALDI-MS imaging:** Lungs from healthy 9 week old Balb/c mice were removed and inflated with dialyzed culture supernatants of Af293 (deacetylated GAG) or Δ*agd3* strain (fully acetylated GAG). 5 µg/ml LPS (eBioscience product # 501122025) and DMEM (Wisent) were used as positive and negative controls for inflammation, respectively. Inflated lungs were incubated in DMEM for 1 hour at 37°C. After 1 hour, lungs were injected with a 1% solution of low melting point agarose (Promega) to maintain inflation and then flash frozen on dry ice and stored at -80°C. Frozen lungs were then cryosectioned to obtain 20 µM cross-sectional slices using a Leica CM3050 S cryostat. The slices were mounted on MALDI imaging slides and covered uniformly sprayed with 26 passes of DAN matrix at 10mg/ml in 67% ACN using an HTX TM Sprayer™ spray coater (HTX Technologies). Tissue samples were analyzed in

positive reflectron mode with a pixel resolution at 100µm, 500 shots/pixel using a Bruker UltrafleXtreme MALDI-TOF mass spectrometer. The intensity of ions at m/z= 725.58 (sphingomyelin) and 732.57 (phosphatidylcholine), markers of inflammation and healthy tissue respectively, were used to label the pixels.Quantification of pixel intensity for sphingomyelin was done using SCiLS software (Bruker) with total ion current (TIC) normalization.

**Protoplast viability assay:** To determine the effect of deacetylated GAG synthesis on the cell membrane of *A. fumigatus* in the absence of a cell wall, protoplasts of Δ*ega3*$^{CRISPR}$::*agd3*$^{Tet\ on}$ and its parent strain Δ*ega3*$^{CRISPR}$ were made as previously described (246). In conditions where doxycycline was used, it was present at all stages of the experiment except for initial growth of the fungus to harvest conidia. Protoplasts were counted with a Countess II FL cell counter (Life Technologies) and approximately 200 protoplasts per condition were plated on osmotically stable medium in order to recover their cell walls. Colonies were counted as soon as they became visible.

**Protein content of culture supernatants:** 6-8 week old female Balb/c mice were immunosuppressed with anti-Ly6G antibody (Cedarlane) two days prior to infection. Mice were then intratracheally inoculated with $5x10^6$ conidia in 50 µl of PBS-0.05% Tween 80. After 24 hours, the mice were sacrificed and lungs were lavaged twice with 1 ml PBS. The lavage fluid was then assayed for protein concentration by bicinchoninic assay (Pierce) according to manufacturer instructions.

**Ethics statement:** The above animal experiments were carried out in accordance with the Institutional Animal Care and Use Committee (IACUC) of the McGill University Health Centre under Animal Use Protocols 7609 and 7674.

**Table 1.** Primers used in the study, all in 5'-3' direction.

| | |
|---|---|
| **Agd3 881F** | CTAGTCGACGGCTTCCTCAC |
| **Agd3 RTII fwd** | CGGCCAAGTACTCGATTTTCC |
| **Agd3 RTII rev** | AGGAAGTTCTCGGACATCTCTT |
| **BL6** | GTCCACGAACTTCCGGGA |
| **Ble Pr7** | TCTGGTAAAAGATTCACGAGATAGTACCTTCT |
| **Ble Tr7** | AAGCAAGGTTTTCAGTATAATGTTACATGCGTAC |
| **Cas9-F** | CGAGACAGCAGAATCACCGC |
| **Cas9-Fwd** | CACACCAGCCTTTCCACTTC |
| **Cas9-R** | GTATTGGGATGAATTTTGTATGCAC |
| **Cas9-Rev** | GTACCGGCCGCAAATTAAAG |

| | |
|---|---|
| **Cas9-Screen-F** | ATGGACAAGAAGTATAGCATCG |
| **Cas9-Screen-R** | GGAGTCAGACCAAGTGACAAC |
| **Ega3 1st** | ATGGATTCCCTTGGAAAAGGC |
| **Ega3 End ORF Rev** | GAACAATTGGGTGGAATATTGT |
| **Ega3 Ext1** | ACTGGATTACCCCTTTACTTG |
| **Ega3 Ext4-far** | AATCCAAAACGACCTATGGC |
| **Ega3-Hyg-F** | GGACAGATCATTGTTGGTCTTATCCCCCTTGGGATACTCGAT GTGAAACATTGACCAAGAATCTATTGCATC |
| **Ega3-Hyg-R** | TTCGCACCGCCATATATTGACACTTGCGCCGTGCCCACTATC TTATCTCAAGTGTGCTGGAATTCGCCCTTC |
| **Ega3 Last** | TTAACAATATTCCACCCAATTGTTCAG |
| **Ega3 P1** | AATGGAAGGGAAGGAGTGTTT |
| **Ega3 P2** | GGTGACAAGTGAACAGGATGA |
| **Ega3 P3** | TCCGAATCGAGTAAGCCAGA |
| **Ega3 P4 far** | GCCGACCTACCAATGCTCT |
| **Ega3 RTII fwd** | GGACTCGATCAGCTTTGTGAA |
| **Ega3 RTII rev** | TGACACTCCACTGCATGTTTT |
| **Ega3-Screen-F** | ACTGCTCGTTGACACTCCAC |
| **Ega3-Screen-R** | TCGACGCTGAGATCTACGAC |
| **Ega3-sgRNA1::pSNR52** | GGTGGTCCATGATTTCCAGCGATCATTTATCTTTCACTGCGG AGAAGTTTC |
| **Ega3-sgRNA2::pSNR52** | CGTTCTTCTGACTGGCCGTGGATCATTTATCTTTCACTGCGG AGAAGTTTC |
| **Ega3-sgRNA1::scaffold** | GCTGGAAATCATGGACCACCGTTTTAGAGCTAGAAATAGCA AGTTAAAATAAGGC |
| **Ega3-sgRNA2::scaffold** | CACGGCCAGTCAGAAGAACGGTTTTAGAGCTAGAAATAGCA AGTTAAAATAAGGC |
| **Ext3** | AGACTGGTTCCCTGCTATCCA |
| **Ext5** | CAGAAAGTTGTCAATGGGCAGTA |
| **Gtb3 RT antisense** | GCGACTGGTACCATTTGCGA |
| **Gtb3 RT sense** | ATTCCTGGTGGCAATTTGTCCT |
| **Ku80 ext1** | CACTCACCCTCAAAGCCATT |
| **Ku80 ext4** | TATGCCTGTCTCGAT |

| | |
|---|---|
| **LE8** | TCCGAATCGAGTAAGCCAGA |
| **Point-Mutant-Fwd** | GATCTACGACATAGATCTGTTCATCAAC |
| **Point-Mutant-Rev** | GTTGATGAACAGATCTATGTCGTAGATC |
| **sgRNA-cassette-fwd** | GAGAAGGTTTTGGGACGCTC |
| **sgRNA-cassette-Fwd-int** | CGAAGGCTTTAATTTGCGGC |
| **sgRNA-cassette-Rev-int** | CGAGTCAGTGAGCGAGGAA |
| **sgRNA-cassette-rev-low** | CGTTACCGCCTTTGAGTGAG |
| **sgRNA-F** | GCGTAAGCTCCCTAATTGGC |
| **sgRNA-R** | GAGCCAAGAGCGGATTCCTC |
| **sgRNA-ss-F1** | AGTAAGCTCGTCGGATACTCGATGTGAAACACGTTTTAGAG CTAGAAATAGCAAGT |
| **sgRNA-ssF2** | TGCCCACTATCTTATCTCATGACGAGCTTACTCGTTTCGTCCT CACGG |
| **sgRNA-ss-R1** | GTGTTTCACATCGAGTATCCGACGAGCTTACTCGTTTCGTCC TCACGG |
| **sgRNA-ssR2** | AGTAAGCTCGTCATGAGATAAGATAGTGGGCAGTTTTAGAG CTAGAAATAGCAAGT |
| **sg-Screen-F** | TTGGCCCATCCGGCATCTGTA |
| **sg-Screen-R** | CTCTGCTAAGCTATTCTTCTGC |
| **Sph3 RTII fwd** | CCGGATCATTACGTGGTTCAC |
| **Sph3 RTII rev** | CTCCATGGCGTTCCTGAAAG |
| **Tef1 RTII fwd** | AAGTATGAGGTCACTGTCATCGAT |
| **Tef1 RTII rev** | ATACCAGCCTCGAACTCACC |
| **Tef1RT-F** | GTGACTCCAAGAACGATCC |
| **Tef1RT-R** | AGAACTTGCAAGCAATGTGG |
| **Uge RTII fwd** | TCGACAATCTCAGCAACTCCT |
| **Uge RTII rev** | GAAGTTCCTTGAGAGCAGCAG |

**Table 2:** Antibodies/stains used for flow cytometry.

| Antibody | Fluorochrome | Dilution | Clone | Manufacturer |
|---|---|---|---|---|
| Viability 405/452 | PB450/VioBlue | 1:100 | - | Miltenyi Biotec |
| CD56 | FITC | 1:100 | REA196 | Miltenyi Biotec |
| CD69 | PE | 1:10 | - | BD Pharmingen |
| Propidium Iodide | - | 1:50 | - | BD Pharmingen |
| Annexin V | APC | 1:50 | - | BD Pharmingen |
| CD3 | APC-Vio770 | 1:100 | REA613 | Miltenyi Biotec |

# Chapter 6: General discussion

In this work we demonstrate that Ega3 is a membrane-bound GH that specifically hydrolyzes deacetylated (cationic) GAG. Although it was originally predicted that Ega3 would play a role in biosynthesis like the other genes in the GAG cluster, our findings show that Ega3 is actually dispensible for biofilm formation and instead serves to protect the fungal cell membrane from damage by cationic GAG. We have also shown that the cationic charge of GAG may play a role in virulence by directly damaging host cell membranes and/or facilitating phagolysosomal escape by *A. fumigatus* (**Figure 1**).

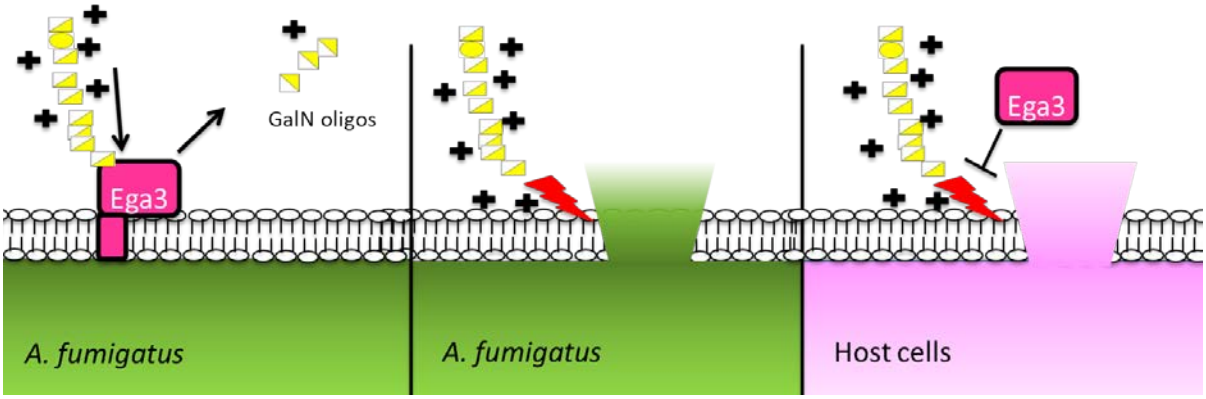


**Figure 1:** Model of fungal and host cell membrane protection by Ega3.

We had initially predicted that Ega3 played a role in the biosynthesis of GAG, since every other gene from the GAG biosynthetic cluster had been characterized as necessary for production or maturation of GAG. Ega3 was found to be specific for deacetylated GAG, which is generated within the outer cell wall (197, 199, 201). Since Ega3 is a membrane-bound GH, it was not obvious how it would be able to come into contact with its substrate in the outer cell wall. Recent studies have demonstrated that in fungi such as *C. neoformans* and *S. cerevisiae*, extracellular vesicles (EVs) are involved in synthesis of the capsule and cell wall, respectively (213, 214). In *C. neoformans*, the polysaccharide GXM is transported in EVs for incorporation into the capsule, while *S. cerevisiae* EVs carry chitin and β-glucan synthases that were shown to participate in cell wall repair (213, 214). We hypothesized that Ega3 could be transported in EV membranes to the outer cell wall to hydrolyze deacetylated GAG, or act on GAG that is packaged within EVs. While subsequent studies on EVs produced by *A. fumigatus* protoplasts have presented evidence that under some conditions Ega3 and GAG may be packaged in EVs, the GH domain of Ega3 is predicted to face the extracellular space, making it unlikely to hydrolyze GAG within the EV (201, 230, 303). However, our proteomic studies of *A. fumigatus* EVs failed to identify Ega3. Proteins associated with other fungal EVs were present, suggesting that the lack of Ega3 was not due to deficiencies in our EV isolation and protein identification protocols (208, 211). Interestingly, multiple GEL proteins were found, suggesting a possible role for *A. fumigatus* EVs in modification of β-glucans, which agrees with

the work on EVs produced by *A. fumigatus* protoplasts (230, 304). However, our data suggests that EVs are not involved in bridging the gap between Ega3 and GAG. These findings raise another question, however: if GAG were enclosed in EVs for its transport to the outer cell wall, as has been suggested (230), why would Ega3 be necessary for protection of the plasma membrane? Perhaps Ega3 normally protects subcellular membranes as GAG transits through the cell during synthesis and/or protects the outer membrane from mislocalized GAG which is deacetylated by Agd3 as the enzyme transits to its location in the cell wall. Co-localization studies of GAG and Agd3 will be helpful in distinguishing these possibilities, possibly using immunogold staining in conjunction with transmission electron microscopy. In this work, we have produced several lines of evidence to suggest that *ega3* is a conditionally essential gene. Many unsuccessful attempts in our lab and collaborating labs were made to disrupt *ega3* in both a wild-type and nonhomologous end joining-deficient mutant. In the Af293 wild-type strain and in the Ku80 strain which is often used as a parent strain to minimize ectopic insertions and non-homologous end joining in *A. fumigatus*, a clean disruption of *ega3* could not be achieved. All transformations resulted in either the absence of viable clones, ectopic insertion of the drug resistance marker, or duplication of *ega3* (244). We now hypothesize that clean *ega3* null mutants may have resulted from these transformations but were missed due to a growth defect like the one demonstrated in the Δ*ega3*$^{CRISPR}$ strain and that the faster-growing transformants with an intact *ega3* allele appeared first, and that any *ega3* null transformants simply were not given enough time to grow into visible colonies. In any case, after changes in our approach to disrupting *ega3* by using CRISPR/Cas9 in Af293 and using different homologous sequences for the split marker approach in the Ku80 strain, two Δ*ega3* strains were finally made, but upon further analysis we found that both mutants lacked the ability to make deacetylated GAG. The second line of evidence supporting the conditional essentiality of *ega3* for normal growth was revealed when introduction of a tetracycline-inducible *agd3* allele into the Δ*ega3*$^{CRISPR}$ strain resulted in a growth defect in this strain when *agd3* expression was induced. This observation supports a model where deacetylated GAG production is harmful to *A. fumigatus* in the absence of Ega3. Of note, introduction of the tetracycline-inducible *agd3* allele in Af293 did not result in any growth defect despite a clear increase in *agd3* expression upon addition of Dox. Similar findings of a conditionally essential carbohydrate degrading enzyme have been reported in *P. aeruginosa* in which alginate lyase is required to clear misdirected alginate from the periplasmic space to prevent rupture of the cell (305). Other examples of conditionally essential GH exist in fungi, two of which are found in *Schizosaccharomyces pombe*: Exg1, a GH5 family protein essential for septum formation and consequently vegetative growth, and Gas4p, a GH72 family protein which is essential for ascospore viability and proper cell wall assembly in ascospores (306, 307). In the latter example however, Gas4p was shown to exhibit glucanosyltransferase activity rather than hydrolytic activity in the cell wall, suggesting its primary role was to link β-glucan

units rather than cleaving them (307). In other deacetylated polysaccharide biosynthetic systems such as poly-β(1,6)-*N*-acetylglucosamine (PNAG) in *Escherichia coli* and Pel in *P. aeruginosa*, the polysaccharide deacetylase and GH specific for hydrolysis of the deacetylated polysaccharide are two domains of the same protein (PgaB and PelA, respectively), possibly suggesting the biological importance of the two enzymes staying in close proximity (270, 308). It is unknown whether deletion of only the GH portion of PgaB or PelA would have deleterious effect on the organism.

The Δ*ega3*$^{Ku80}$ strain did not undergo the same genetic complementation experiments as the Δ*ega3*$^{CRISPR}$ strain, although the secondary mutation in *uge3* is predicted to have a negative effect on binding of UDP-galactose or -GalNAc, the substrates for Uge3 (198). A small inversion was found in the *uge3* sequence found after sequencing the entire Δ*ega3*$^{Ku80}$ strain's genome. To determine the effects of this mutation on GAG synthesis, a *uge3* allele with the same mutation would have to be constructed and introduced into the Δ*uge3* strain to see if GAG production is restored and to what degree. There is still a question as to whether there are other factors at play, however. Despite repeated attempts, disruption of *ega3* has still not been successfully done in Δ*uge3* or Δ*agd3* backgrounds. This observation raises the possibility that another factor besides deacetylated GAG requires the presence of Ega3 and has also been silenced in the two Δ*ega3* strains that were produced. However, no other significant mutations besides the *uge3* inversion were identified in the genome sequencing of the Δ*ega3*$^{Ku80}$ mutant. To address this question, RNA sequencing or proteomics could be performed on the Δ*ega3*$^{Ku80}$ strain to determine if there is yet another secondary mutation that was not detected at the genomic level.

The findings of our inducible Agd3 expression studies strongly suggest that Ega3 is essential in the presence of deacetylated GAG. However, exogenous rAgd3 supplementation did not result in growth inhibition of Ega3-deficient *A. fumigatus*. If *ega3* is conditionally essential in the presence of deacetylated GAG, it would be expected that Agd3 supplementation would also have negative effects on the Δ*ega3*$^{CRISPR}$::*agd3*$^{Tet\ on}$ mutant. However, the strain appears to grow normally and form a biofilm due to the presence of cationic GAG. This discrepancy may indicate may indicate that once GAG has reached the outer cell wall, where it can be deacetylated by exogenous rAgd3, it may not be able to reach the plasma membrane, and that other layers of the cell wall (the inner fibrillar layer composed of β-glucan and chitin) prevent this interaction from occurring (309). This finding would suggest that Ega3 is important to protect the plasma membrane from "mislocalized" deacetylated GAG resulting from inappropriate early deacetylation by Agd3 as it transits to the outer cell wall. Additionally, we hypothesize that the cell wall protects the plasma membrane from the harmful of effects of deacetylated GAG to the plasma membrane in the Δ*ega3*$^{CRISPR}$ strain resulting in growth inhibition rather than fungal cell death.

Our data suggests that cationic GAG could injure fungal membranes in the absence of Ega3. The closely related fungal species *Neurospora crassa* produces a cationic homopolymer of N-acetyl galactosamine that, like GAG, is partially deacetylated outside of the cell (197, 282, 310). Adsorption of this polymer to *N. crassa* conidia caused efflux of radioactively labeled metabolites (281). We hypothesized that a similar process could take place in *A. fumigatus*, and that Ega3 protects the cell membrane by hydrolyzing GAG to dissipate the positive charge. It is probable that hydrolysis of the polymer would decrease its ability to damage the plasma membrane, since cytotoxicity of cationic polymers is directly proportional to polymer molecular weight (273). This observation fits with our data showing that Ega3 specifically hydrolyzes deacetylated GAG and is found in the membrane fraction. In an attempt to observe the effect of native deacetylated GAG production on the cell membrane in the absence of Ega3, we tried expressing *agd3* in protoplasts of the Δ*ega3*$^{\text{CRISPR}}$::*agd3*$^{\text{Tet on}}$ mutant. In doing this experiment, we hoped to show that production of deacetylated GAG would be lethal due to lysis of the protoplasts. To our surprise, while their growth was slowed, the viability of the protoplasts was not significantly affected, although *agd3* expression was repressed despite the addition of doxycycline to the protoplasting solutions. This trait was heritable, as conidia produced after protoplast regeneration had lost the ability to overexpress *agd3*. This observation supports our other evidence that *agd3* expression is indeed damaging to the fungal cell membrane in the absence of *ega3* and also highlights the dramatic genomic plasticity of *A. fumigatus*. In parallel, we exposed the Δ*ega3*$^{\text{CRISPR}}$::*agd3*$^{\text{Tet on}}$ strain to high salt concentration, which was deleterious to its growth. This finding is consistent with the mutant exhibiting reduced tolerance to osmotic stress, pointing to perturbation of the membrane. We were able to provide evidence that this perturbation caused leakage of the cytosol by testing for ATP released into the media of Δ*ega3*$^{\text{CRISPR}}$::*agd3*$^{\text{Tet on}}$ strain during *agd3* expression, which was significantly elevated compared to ATP release in the absence of *agd3* expression. This technique had previously been used to test for decreased cellular viability due to membrane permeability in *E. coli* and provided an alternative to use of radioactive materials (311). The results of this experiment strongly suggest that cationic GAG can disrupt cellular membranes to an extent that causes impaired growth due to loss of cytosolic contents in a similar fashion to the polygalactosamine polymer of *N. crassa*. Although human exposure to *N. crassa* is very high in some settings, no infection has ever been reported and the fungus is poorly adapted to survival in a mammalian host (312). Therefore, while studies have been done on the chemistry and production of its partially deacetylated polygalactosamine polymer, no studies have explored the cytotoxicity of this polymer beyond its effects on *N. crassa* conidia (281, 282, 310).

GAG is a virulence factor that interacts with the host in a variety of ways, most of which have been explored only *in vitro*. GAG largely mediates host-pathogen interactions through its adhesive properties, protects the fungus from immune recognition and attack, and can induce non-protective anti-

inflammatory signals (149, 181, 186). Despite all of these different interactions with the host, no mammalian receptor for GAG has been found (138, 313). This observation begs the question of whether some intrinsic quality of GAG is dictating these interactions. Previous work suggests that the cationic charge of GAG is responsible for its adhesiveness, specifically the positive charge imparted by protonated GalN residues (197). The studies of *N. crassa* polygalactosamine previously and our findings suggest that fungal exopolysaccharides can be directly toxic to the fungi that produce them. Other polycations have also been shown to be directly cytotoxic to mammalian cells through acidic hydrolysis of phosphodiester bonds (276). Another possibility that was suggested for the galactosamine polymer of *N. crassa* is that GAG binds to the negatively charged phosphate heads of membrane lipids, thereby distorting the membrane and allowing cytoplasmic contents to leak out (282). The acid hydrolysis hypothesis could easily be tested using nuclear magnetic resonance imaging of lipids released due to deacetylated GAG exposure as done in similar studies (276). With our evidence thus far, we hypothesized that GAG would likely also have direct cytotoxic effects on mammalian cells due to its cationic charge. Cytosolic efflux was demonstrated in A549 pulmonary epithelial cells with the use of radioactive chromium upon exposure to deacetylated GAG-containing fungal culture supernatants. In this experiment fully acetylated GAG did not cause cytosolic efflux, and addition of Ega3 to wild-type culture supernatants prevented cell damage, mirroring the observations in the Δ*ega3*$^{\text{CRISPR}}$::*agd3*$^{\text{Tet on}}$ strain. This finding not only lends support to our hypothesis that Ega3 acts as an antitoxin *in situ* but also suggests a new potential role for GAG as a virulence factor during infection. Cell viability was not measured in this experiment but upon repeating the same conditions using BMDMs, we were able to show that exposure to deacetylated GAG can be lethal to mammalian cells as shown with propidium iodide staining, which stains DNA of cells whose membranes have been compromised (287). We hypothesize that GAG is lethal (rather than inhibitory, as seen in *A. fumigatus*) to mammalian cells due to the absence of a protective cell wall.

GAG induces apoptosis in neutrophils in a mechanism that involves a receptor-ligand interaction with natural killer (NK) cells (185). In the referenced study, purified GAG did not induce neutrophil apoptosis directly. However, it has been demonstrated that polycations induce necrosis in mouse fibroblasts and apoptosis in various cell lines (272, 285). Perhaps the conditions were not conducive to cytotoxicity in the aforementioned GAG study, since preparation of GAG for these experiments differed from our method and may not have had the same proportion of GalN (181, 185). The data presented in this thesis is consistent with necrotic cell death caused by GAG. In addition to the cell injury and death experiments, we have also shown that deacetylated GAG induces either apoptosis or necrosis in human NK and T cells. There is some ambiguity in these results since annexin V staining can indicate either mode of cell death. If the cytotoxicity is really due to the polycationic properties of GAG, it would be expected that the cells die of necrosis due to irreparable membrane damage (288). Programmed cell death

pathways could be ruled out by exposing the cells to a pan-caspase inhibitor either prior to or during exposure to the culture supernatants. Other studies have demonstrated that polycation-induced apoptosis is triggered through mitochondrial events which can be detected in assays for mitochondrial function, such as the MTT colorimetric assay (273). These experiments could also be performed in the future, though it seems unlikely that a large molecule such as GAG would diffuse passively through the cell membrane and cause death through the mitochondria. On the other hand, it is possible that this interaction could occur *in vivo* in host cells after uptake of GAG-containing *A. fumigatus* EVs by host cells. Macrophages can take up EVs from both *C. neoformans* and *A. fumigatus*, and there is evidence that GXM within *C. neoformans* EVs can reduce nitric oxide production by the macrophages (224, 229). Taken together, it is possible that GAG could act intracellularly to induce apoptosis, however the fact that soluble Ega3 can protect cells from secreted GAG suggests that this mechanism is not at play in our experiments.

*A. fumigatus* can escape host macrophages after being phagocytosed by inhibiting phagosome acidification and eventually growing too large to be contained by the macrophage. Initially, melanin protects the conidia from lysosomal acidification of the phagosome through a mechanism that has yet to be characterized, but seems to involve inhibition of host vacuolar ATPase, which pumps protons into the phagolysosome for acidification (292, 314, 315). Two mechanisms for physical escape from the phagolysosome have been proposed: growth of the organism until the phagolysosome can no longer stay intact through inadequate incorporation of donor membranes or fusion of the phagolysosomal membrane with the plasma membrane as the organelle enlarges, releasing the fungus to exit through the plasma membrane without causing lysis (evidenced by a lack of lactate dehydrogenase release and antibody staining of the fungus within the macrophage) (316-318). No mechanism has been proposed for how the macrophage plasma membrane remains intact in the latter situation (318). *A. fumigatus* produces several lipases and phospholipases including phospholipase D which contributes to virulence of the fungus, however deletion of the *pld* gene coding for this phospholipase was associated with decreased uptake of the fungus by A549 epithelial cells which was thought to explain decrease in virulence of the Δ*pld* strain (319, 320). A putative lipase was also found on the surface of *A. fumigatus* conidia, however its role in virulence or otherwise has not been investigated (321, 322). In this work we present a possible alternate mechanism for phagolysosomal escape by *A. fumigatus*. As deacetylated GAG is able to disrupt cell membranes, it is possible that GAG-mediated disruption of phagolysosomal membranes could allow escape from this organelle, leading to unrestrained intracellular growth. We have shown strong preliminary evidence for this hypothesis, as wild-type *A. fumigatus* is able to grow within the phagosome and escape the cell whereas a deacetylase deficient (though still polymer producing) strain remains largely confined to the phagosome. Synthetic polycations used for DNA delivery into cells can have

similar effects on cellular organelles, mediated by their positive charge (323). The polycation PEI has been hypothesized to act as a "proton sponge" in the endolysosome, creating a so-called charge gradient that induces the influx of chloride ions leading to swelling and bursting of the endolysosome (323). It is possible that the GalN residues of GAG can play a similar role and contribute to the prevention of not only membrane rupture but of phagosomal acidification after germination. The Δ*agd3* strain has no GalN residues to protonate, which fits with its inability to escape the phagosome. Other interesting methods of phagosomal escape are seen with *C. albicans* and *C. neoformans.* The yeast *C. albicans* can undergo a switch to hyphal morphology in macrophages, and by continuing to grow by apical extension it can escape the phagolysosome once it can no longer keep up with growth of the organism by fusion of lysosomal membranes (316). Hyphal growth is likely not the mechanism employed by *A. fumgiatus,* as the germination rates of the wild-type and deacetylase-deficient strains are equal despite their differences in phagolysosomal escape. A similar mechanism for phagosomal escape was observed in *C. neoformans* by continued binary fission. It was proposed that the growing capsule was able to dilute the lysosomal components and prevent harm to the yeast cell, and GXM-containing vesicles were found in the cytoplasm (324). GXM is a negatively charged polysaccharide, therefore it is unlikely to act as a proton sponge the way that polycations have been proposed to do (325). Perhaps this observation points to a novel mechanism of phagosomal escape in *A. fumigatus.* Additionally, since *A. fumigatus* is an opportunistic pathogen, these defense mechanisms likely did not evolve for protection against host immune systems (7). Since *A. fumigatus* is an inhabitant of the soil, it is possible that deacetylated GAG production is among the mechanisms, including prevention of phagocytosis by amoebae by DHN melanin, that it employs to protect itself from soil amoebae. Consistent with this hypothesis, *A. fumigatus* conidia are also able to survive after being phagocytosed by amoeba and germinate, lysing the cell (326).

In addition to *A. fumigatus,* many pathogenic bacteria also synthesize cationic polymers that are important for biofilm formation, masking of PAMPs, and antibiotic resistance similar to GAG (286, 327-331). The best studied examples are polysaccharide intercellular adhesin (PIA) which is produced by multiple *Staphylococcus* species and composed of β-1,6-linked GlcNAc that is partially deacetylated, PNAG (mentioned above), and Pel which is produced by *P. aeruginosa,* which is a linear chain of dimeric repeats of α-1,4-linked Gal and GalNAc that is partially de-*N*-acetylated. (270, 332-335). The model of synthesis of PIA and PNAG are similar to that predicted for GAG where a transferase polymerizes the monosaccharides to the outside of the plasma membrane, after which the resulting polysaccharide is deacetylated to yield hexosamine residues interspersed throughout the polymer (270, 331, 336, 337). Deacetylation of these polysaccharides is required for biofilm formation as with GAG, and aids in repelling antimicrobial peptides (197, 270). It would therefore be worth studying these

polymers to determine whether they play a role in phagolysosomal escape and mediating toxic effects on host cells, given their similarities to GAG.

In this work we also utilize an innovative technique, matrix assisted laser desorption/ionization-time of flight (MALDI-TOF) imaging for assessing and mapping cellular injury in cross sections from mouse lungs. While this technique requires optimization, it could pave the way for some very useful studies in the future. The dynamics of *Aspergillus* lung infection could be visualized and elements from the host and fungus could be colocalized which could help direct the decisions for which antifungals to use and their mode of application, as well as possible immunotherapies that could be used to enhance the effects of those antifungals. The latter could potentially be done with proteomics studies which can be paired with MALDI-TOF by performing tandem mass spectrometry on the same lung sections concurrently to reveal which cellular pathways are being activated by the presence of the fungus. We attempted to perform this experiment but we were not able to identify many peptides. Further optimization of this technique is therefore required.

This work presents two different ways Ega3 could be used to treat invasive aspergillosis. On one hand, recombinant Ega3 could be used to digest GAG and prevent cellular injury and invasion, while also clearing the way for antifungals to reach their targets. Recombinant Ega3 has already shown excellent tolerability in mice at large doses, and glycoside hydrolases have potentiating effects when used in conjunction with antifungals (204). Advancing the preclinical development of these agents for ultimate use in human patients is ongoing. Alternatively, small molecule inhibitors could be tested for inhibition of Ega3 *in situ*, to use alone or as a combination therapy with another antifungal.

There remains much work that can be done to follow up on the findings from our studies. One important task will be to localize GAG in and on the hyphae at all stages of growth in order to pinpoint the stages where Ega3 is crucial for protection of the fungus. In order to fully characterize how exactly Ega3 detoxifies the cell membrane of *A. fumigatus*, it would be helpful to colocalize Ega3 and GAG as the fungus is actively producing the polysaccharide. This interaction could be observed by performing immunogold staining of the Ega3-GFP strain, with an anti-GFP antibody conjugated to a gold nanoparticle in conjunction with our anti-GAG antibody and corresponding anti-mouse secondary antibody conjugated to a gold nanoparticle of a different size. It would also be interesting to visualize the germlings of the Δ*ega3*$^{\text{CRISPR}}$::*agd3*$^{\text{Tet on}}$ strain exposed to doxycycline to visualize the cell lysis we hypothesize is behind the observed growth impairment. Determining the cytotoxic effects of GAG *in vivo* during infection will also be important, and may prove useful in finding new therapeutics. In order to determine how deacetylated GAG may or may not be aiding in phagolysosome escape by the fungus more studies will also need to be done. Some preliminary work has been done in optimizing loading of phagocytic host cells with fluorescent dextran with the goal of visualizing at what point the *A. fumigatus*

germlings lyse the phagoloysosome, and how it differs with deacetylated GAG and fully acetylated GAG. It would also be possible to better characterize the effects of deacetylated GAG on host cells during infection by taking a more reductionist approach and introducing only the deacetylated/fully acetylated GAG containing culture supernatants to the lungs of living mice and then assaying for protein concentration of the bronchoalveolar lavage fluid, as infection with the whole organism may have introduced too many variables, such as the reaction to uncloaked β-glucans in the Δ*agd3* mutant.

In conclusion, this work is the first of its kind to reveal that a microbial polysaccharide is directly toxic to both the microbe and the host and that the production of a glycoside hydrolase can serve as an antitoxin to protect the micro-organism from the toxic effects of the polysaccharide. We have also shown that GAG interacts with host cells with no need of a receptor, and potentially also plays a role in phagolysosomal escape. The identification of this new toxin/antitoxin system may open up new avenues in the treatment of *A. fumigatus* infections and also offer insights into the pathogenesis of other microorganisms that produce similar cationic exopolysaccharides.

## References


1. Sugui JA, Kwon-Chung KJ, Juvvadi PR, Latgé J-P, Steinbach WJ. Aspergillus fumigatus and related species. Cold Spring Harb Perspect Med. 2014;5(2):a019786-a.
2. International Symposium on A, Aspergillosis, Bossche Hvd, Mackenzie DWR, Cauwenbergh G. Aspergillus and aspergillosis. New York: Springer Science+Business Media; 1988. Available from: https://doi.org/10.1007/978-1-4899-3505-2.
3. Houbraken J, de Vries RP, Samson RA. Modern taxonomy of biotechnologically important Aspergillus and Penicillium species. Adv Appl Microbiol. 2014;86:199-249.
4. Tekaia F, Latgé JP. Aspergillus fumigatus: saprophyte or pathogen? Curr Opin Microbiol. 2005;8(4):385-92.
5. Liang Y, Pan L, Lin Y. Analysis of extracellular proteins of Aspergillus oryzae grown on soy sauce koji. Biosci Biotechnol Biochem. 2009;73(1):192-5.
6. Maschmeyer GD, Haas A, Cornely OA. Invasive Aspergillosis : Epidemiology, Diagnosis and Management in Immunocompromised Patients. Drugs. 2007;67(11):1567-601.
7. Latge JP. Aspergillus fumigatus and aspergillosis. Clin Microbiol Rev. 1999;12(2):310-50.
8. O'Gorman CM, Fuller H, Dyer PS. Discovery of a sexual cycle in the opportunistic fungal pathogen Aspergillus fumigatus. Nature. 2009;457(7228):471-4.
9. Oiartzabal-Arano E, Perez-de-Nanclares-Arregi E, Espeso EA, Etxebeste O. Apical control of conidiation in Aspergillus nidulans. Curr Genet. 2016;62(2):371-7.
10. Latge JP. The pathobiology of Aspergillus fumigatus. Trends Microbiol. 2001;9(8):382-9.
11. Rohde M, Schwienbacher M, Nikolaus T, Heesemann J, Ebel F. Detection of early phase specific surface appendages during germination of Aspergillus fumigatus conidia. FEMS Microbiol Lett. 2002;206(1):99-105.
12. Valsecchi I, Dupres V, Stephen-Victor E, Guijarro JI, Gibbons J, Beau R, et al. Role of Hydrophobins in Aspergillus fumigatus. J Fungi (Basel). 2017;4(1).
13. Bayry J, Beaussart A, Dufrêne YF, Sharma M, Bansal K, Kniemeyer O, et al. Surface structure characterization of Aspergillus fumigatus conidia mutated in the melanin synthesis pathway and their human cellular immune response. Infect Immun. 2014;82(8):3141-53.
14. Tsai HF, Wheeler MH, Chang YC, Kwon-Chung KJ. A developmentally regulated gene cluster involved in conidial pigment biosynthesis in Aspergillus fumigatus. J Bacteriol. 1999;181(20):6469-77.
15. d'Enfert C. Fungal Spore Germination: Insights from the Molecular Genetics of Aspergillus nidulansand Neurospora crassa. Fungal Genetics and Biology. 1997;21(2):163-72.
16. Rhodes JC. Aspergillus fumigatus: growth and virulence. Med Mycol. 2006;44 Suppl 1:S77-81.
17. Upadhyay SK, Mahajan L, Ramjee S, Singh Y, Basir SF, Madan T. Identification and characterization of a laminin-binding protein of Aspergillus fumigatus: extracellular thaumatin domain protein (AfCalAp). J Med Microbiol. 2009;58(Pt 6):714-22.
18. Momany M, Taylor I. Landmarks in the early duplication cycles of Aspergillus fumigatus and Aspergillus nidulans: polarity, germ tube emergence and septation. Microbiology. 2000;146 Pt 12:3279-84.
19. Fiddy C, Trinci AP. Mitosis, septation, branching and the duplication cycle in Aspergillus nidulans. J Gen Microbiol. 1976;97(2):169-84.
20. Cramer RA, Jr., Perfect BZ, Pinchai N, Park S, Perlin DS, Asfaw YG, et al. Calcineurin target CrzA regulates conidial germination, hyphal growth, and pathogenesis of Aspergillus fumigatus. Eukaryot Cell. 2008;7(7):1085-97.
21. Oh KB, Nishiyama T, Sakai E, Matsuoka H, Kurata H. Flow sensing in mycelial fungi. J Biotechnol. 1997;58(3):197-204.

22. Hope WW, Walsh TJ, Denning DW. Laboratory diagnosis of invasive aspergillosis. Lancet Infect Dis. 2005;5(10):609-22.
23. Sheppard DC, Doedt T, Chiang LY, Kim HS, Chen D, Nierman WC, et al. The Aspergillus fumigatus StuA protein governs the up-regulation of a discrete transcriptional program during the acquisition of developmental competence. Mol Biol Cell. 2005;16(12):5866-79.
24. Park HS, Yu JH. Developmental regulators in Aspergillus fumigatus. J Microbiol. 2016;54(3):223-31.
25. Timberlake WE. Temporal and spatial controls of Aspergillus development. Curr Opin Genet Dev. 1991;1(3):351-7.
26. Gravelat FN, Ejzykowicz DE, Chiang LY, Chabot JC, Urb M, Macdonald KD, et al. Aspergillus fumigatus MedA governs adherence, host cell interactions and virulence. Cell Microbiol. 2010;12(4):473-88.
27. Schneider T, Gerrits B, Gassmann R, Schmid E, Gessner MO, Richter A, et al. Proteome analysis of fungal and bacterial involvement in leaf litter decomposition. Proteomics. 2010;10(9):1819-30.
28. Abad A, Fernández-Molina JV, Bikandi J, Ramírez A, Margareto J, Sendino J, et al. What makes Aspergillus fumigatus a successful pathogen? Genes and molecules involved in invasive aspergillosis. Rev Iberoam Micol. 2010;27(4):155-82.
29. Saykhedkar S, Ray A, Ayoubi-Canaan P, Hartson SD, Prade R, Mort AJ. A time course analysis of the extracellular proteome of Aspergillus nidulans growing on sorghum stover. Biotechnol Biofuels. 2012;5(1):52.
30. Kwon-Chung KJ, Sugui JA. Aspergillus fumigatus--what makes the species a ubiquitous human fungal pathogen? PLoS Pathog. 2013;9(12):e1003743.
31. Noble R, Roberts SJ. Eradication of plant pathogens and nematodes during composting: a review. Plant Pathology. 2004;53(5):548-68.
32. Sugui JA, Losada L, Wang W, Varga J, Ngamskulrungroj P, Abu-Asab M, et al. Identification and characterization of an Aspergillus fumigatus "supermater" pair. mBio. 2011;2(6).
33. Jensen HL. THE FUNGUS FLORA OF THE SOIL. Soil Science. 1931;31(2):123.
34. Moreno-González G, Ricart de Mesones A, Tazi-Mezalek R, Marron-Moya MT, Rosell A, Mañez R. Invasive Pulmonary Aspergillosis with Disseminated Infection in Immunocompetent Patient. Can Respir J. 2016;2016:7984032.
35. Dagenais TR, Keller NP. Pathogenesis of Aspergillus fumigatus in Invasive Aspergillosis. Clin Microbiol Rev. 2009;22(3):447-65.
36. Liu X, Yang J, Ma W. Primary cutaneous aspergillosis caused by Aspergillus.fumigatus in an immunocompetent patient: A case report. Medicine (Baltimore). 2017;96(48):e8916.
37. Schweer KE, Bangard C, Hekmat K, Cornely OA. Chronic pulmonary aspergillosis. Mycoses. 2014;57(5):257-70.
38. Geiser DM, Klich MA, Frisvad JC, Peterson SW, Varga J, Samson RA. The current status of species recognition and identification in Aspergillus. Stud Mycol. 2007;59:1-10.
39. Hedayati MT, Pasqualotto AC, Warn PA, Bowyer P, Denning DW. Aspergillus flavus: human pathogen, allergen and mycotoxin producer. Microbiology (Reading). 2007;153(Pt 6):1677-92.
40. Fianchi L, Picardi M, Cudillo L, Corvatta L, Mele L, Trapè G, et al. Aspergillus niger infection in patients with haematological diseases: a report of eight cases. Mycoses. 2004;47(3-4):163-7.
41. Henriet SS, Verweij PE, Warris A. Aspergillus nidulans and chronic granulomatous disease: a unique host-pathogen interaction. J Infect Dis. 2012;206(7):1128-37.
42. Iwen PC, Rupp ME, Langnas AN, Reed EC, Hinrichs SH. Invasive pulmonary aspergillosis due to Aspergillus terreus: 12-year experience and review of the literature. Clin Infect Dis. 1998;26(5):1092-7.
43. Sales-Campos H, Tonani L, Cardoso CR, Kress MR. The immune interplay between the host and the pathogen in Aspergillus fumigatus lung infection. Biomed Res Int. 2013;2013:693023.

44. Cowley AC, Thornton DJ, Denning DW, Horsley A. Aspergillosis and the role of mucins in cystic fibrosis. Pediatr Pulmonol. 2017;52(4):548-55.
45. Bustamante-Marin XM, Ostrowski LE. Cilia and Mucociliary Clearance. Cold Spring Harb Perspect Biol. 2017;9(4).
46. Bruns S, Kniemeyer O, Hasenberg M, Aimanianda V, Nietzsche S, Thywissen A, et al. Production of extracellular traps against Aspergillus fumigatus in vitro and in infected lung tissue is dependent on invading neutrophils and influenced by hydrophobin RodA. PLoS Pathog. 2010;6(4):e1000873.
47. Gerson SL, Talbot GH, Hurwitz S, Strom BL, Lusk EJ, Cassileth PA. Prolonged granulocytopenia: the major risk factor for invasive pulmonary aspergillosis in patients with acute leukemia. Ann Intern Med. 1984;100(3):345-51.
48. Minari A, Husni R, Avery RK, Longworth DL, DeCamp M, Bertin M, et al. The incidence of invasive aspergillosis among solid organ transplant recipients and implications for prophylaxis in lung transplants. Transpl Infect Dis. 2002;4(4):195-200.
49. Margalit A, Kavanagh K. The innate immune response to Aspergillus fumigatus at the alveolar surface. FEMS Microbiol Rev. 2015;39(5):670-87.
50. Robson GD, Huang J, Wortman J, Archer DB. A preliminary analysis of the process of protein secretion and the diversity of putative secreted hydrolases encoded in Aspergillus fumigatus: insights from the genome. Med Mycol. 2005;43 Suppl 1:S41-7.
51. Kamai Y, Lossinsky AS, Liu H, Sheppard DC, Filler SG. Polarized response of endothelial cells to invasion by Aspergillus fumigatus. Cell Microbiol. 2009;11(1):170-82.
52. Dragonetti G, Criscuolo M, Fianchi L, Pagano L. Invasive aspergillosis in acute myeloid leukemia: Are we making progress in reducing mortality? Med Mycol. 2017;55(1):82-6.
53. Tejerina EE, Abril E, Padilla R, Rodríguez Ruíz C, Ballen A, Frutos-Vivar F, et al. Invasive aspergillosis in critically ill patients: An autopsy study. Mycoses. 2019;62(8):673-9.
54. Kousha M, Tadi R, Soubani AO. Pulmonary aspergillosis: a clinical review. Eur Respir Rev. 2011;20(121):156-74.
55. Walsh TJ, Anaissie EJ, Denning DW, Herbrecht R, Kontoyiannis DP, Marr KA, et al. Treatment of aspergillosis: clinical practice guidelines of the Infectious Diseases Society of America. Clin Infect Dis. 2008;46(3):327-60.
56. Kanj A, Abdallah N, Soubani AO. The spectrum of pulmonary aspergillosis. Respir Med. 2018;141:121-31.
57. Denning DW, Cadranel J, Beigelman-Aubry C, Ader F, Chakrabarti A, Blot S, et al. Chronic pulmonary aspergillosis: rationale and clinical guidelines for diagnosis and management. Eur Respir J. 2016;47(1):45-68.
58. Graham KG, Nasir A. Chronic Cavitary Pulmonary Aspergillosis: A Case Report and Review of the Literature. Am J Case Rep. 2019;20:1220-4.
59. Godet C, Philippe B, Laurent F, Cadranel J. Chronic pulmonary aspergillosis: an update on diagnosis and treatment. Respiration. 2014;88(2):162-74.
60. Patterson TF, Thompson GR, 3rd, Denning DW, Fishman JA, Hadley S, Herbrecht R, et al. Executive Summary: Practice Guidelines for the Diagnosis and Management of Aspergillosis: 2016 Update by the Infectious Diseases Society of America. Clin Infect Dis. 2016;63(4):433-42.
61. El-Baba F, Gao Y, Soubani AO. Pulmonary Aspergillosis: What the Generalist Needs to Know. Am J Med. 2020;133(6):668-74.
62. Muldoon EG, Sharman A, Page I, Bishop P, Denning DW. Aspergillus nodules; another presentation of Chronic Pulmonary Aspergillosis. BMC Pulm Med. 2016;16(1):123.
63. Kosmidis C, Denning DW. The clinical spectrum of pulmonary aspergillosis. Thorax. 2015;70(3):270-7.

64. Shah A, Panjabi C. Allergic Bronchopulmonary Aspergillosis: A Perplexing Clinical Entity. Allergy Asthma Immunol Res. 2016;8(4):282-97.
65. Del Donno M, Bittesnich D, Chetta A, Olivieri D, Lopez-Vidriero MT. The effect of inflammation on mucociliary clearance in asthma: an overview. Chest. 2000;118(4):1142-9.
66. Robinson M, Bye PT. Mucociliary clearance in cystic fibrosis. Pediatr Pulmonol. 2002;33(4):293-306.
67. Moss RB. Pathophysiology and immunology of allergic bronchopulmonary aspergillosis. Med Mycol. 2005;43 Suppl 1:S203-6.
68. Agarwal R, Chakrabarti A, Shah A, Gupta D, Meis JF, Guleria R, et al. Allergic bronchopulmonary aspergillosis: review of literature and proposal of new diagnostic and classification criteria. Clin Exp Allergy. 2013;43(8):850-73.
69. Laoudi Y, Paolini JB, Grimfed A, Just J. Nebulised corticosteroid and amphotericin B: an alternative treatment for ABPA? Eur Respir J. 2008;31(4):908-9.
70. Segal BH, Barnhart LA, Anderson VL, Walsh TJ, Malech HL, Holland SM. Posaconazole as salvage therapy in patients with chronic granulomatous disease and invasive filamentous fungal infection. Clin Infect Dis. 2005;40(11):1684-8.
71. Zotchev SB. Polyene macrolide antibiotics and their applications in human therapy. Curr Med Chem. 2003;10(3):211-23.
72. Posch W, Blatzer M, Wilflingseder D, Lass-Flörl C. Aspergillus terreus: Novel lessons learned on amphotericin B resistance. Med Mycol. 2018;56(suppl_1):73-82.
73. Bates DW, Su L, Yu DT, Chertow GM, Seger DL, Gomes DR, et al. Mortality and costs of acute renal failure associated with amphotericin B therapy. Clin Infect Dis. 2001;32(5):686-93.
74. Patterson TF. Treatment of invasive aspergillosis: Polyenes, echinocandins, or azoles? Med Mycol. 2006;44(Supplement_1):S357-s62.
75. Herbrecht R, Denning DW, Patterson TF, Bennett JE, Greene RE, Oestmann JW, et al. Voriconazole versus amphotericin B for primary therapy of invasive aspergillosis. N Engl J Med. 2002;347(6):408-15.
76. Martino R. Efficacy, safety and cost-effectiveness of Amphotericin B Lipid Complex (ABLC): a review of the literature. Curr Med Res Opin. 2004;20(4):485-504.
77. Leenders AC, Daenen S, Jansen RL, Hop WC, Lowenberg B, Wijermans PW, et al. Liposomal amphotericin B compared with amphotericin B deoxycholate in the treatment of documented and suspected neutropenia-associated invasive fungal infections. Br J Haematol. 1998;103(1):205-12.
78. Bowden R, Chandrasekar P, White MH, Li X, Pietrelli L, Gurwith M, et al. A double-blind, randomized, controlled trial of amphotericin B colloidal dispersion versus amphotericin B for treatment of invasive aspergillosis in immunocompromised patients. Clin Infect Dis. 2002;35(4):359-66.
79. Zonios DI, Bennett JE. Update on azole antifungals. Semin Respir Crit Care Med. 2008;29(2):198-210.
80. Schutze GE. Oral azole drugs as systemic antifungal therapy. N Engl J Med. 1994;330(24):1759-60.
81. Troke P, Schwartz S, Ruhnke M, Ribaud P, Corey L, Driscoll T, et al., editors. Voriconazole (VRC) therapy (Rx) in 86 patients (pts) with CNS aspergillosis (CNSA): a retrospective analysis. 43rd Interscience Conference on Antimicrobial Agents and Chemotherapy Chicago, IL; 2003.
82. Andes DR, Ghannoum MA, Mukherjee PK, Kovanda LL, Lu Q, Jones ME, et al. Outcomes by MIC Values for Patients Treated with Isavuconazole or Voriconazole for Invasive Aspergillosis in the Phase 3 SECURE and VITAL Trials. Antimicrob Agents Chemother. 2019;63(1).
83. Cornely OA, Maertens J, Winston DJ, Perfect J, Ullmann AJ, Walsh TJ, et al. Posaconazole vs. fluconazole or itraconazole prophylaxis in patients with neutropenia. N Engl J Med. 2007;356(4):348-59.

84. Chowdhary A, Kathuria S, Xu J, Meis JF. Emergence of azole-resistant aspergillus fumigatus strains due to agricultural azole use creates an increasing threat to human health. PLoS Pathog. 2013;9(10):e1003633.
85. Howard SJ, Cerar D, Anderson MJ, Albarrag A, Fisher MC, Pasqualotto AC, et al. Frequency and evolution of Azole resistance in Aspergillus fumigatus associated with treatment failure. Emerg Infect Dis. 2009;15(7):1068-76.
86. Snelders E, Huis In 't Veld RA, Rijs AJ, Kema GH, Melchers WJ, Verweij PE. Possible environmental origin of resistance of Aspergillus fumigatus to medical triazoles. Appl Environ Microbiol. 2009;75(12):4053-7.
87. Aruanno M, Glampedakis E, Lamoth F. Echinocandins for the Treatment of Invasive Aspergillosis: from Laboratory to Bedside. Antimicrob Agents Chemother. 2019;63(8).
88. Fortwendel JR, Juvvadi PR, Perfect BZ, Rogg LE, Perfect JR, Steinbach WJ. Transcriptional regulation of chitin synthases by calcineurin controls paradoxical growth of Aspergillus fumigatus in response to caspofungin. Antimicrob Agents Chemother. 2010;54(4):1555-63.
89. Brown GD. Dectin-1: a signalling non-TLR pattern-recognition receptor. Nat Rev Immunol. 2006;6(1):33-43.
90. Lamaris GA, Lewis RE, Chamilos G, May GS, Safdar A, Walsh TJ, et al. Caspofungin-mediated beta-glucan unmasking and enhancement of human polymorphonuclear neutrophil activity against Aspergillus and non-Aspergillus hyphae. J Infect Dis. 2008;198(2):186-92.
91. Segal BH, Walsh TJ. Current approaches to diagnosis and treatment of invasive aspergillosis. Am J Respir Crit Care Med. 2006;173(7):707-17.
92. Jiménez-Ortigosa C, Moore C, Denning DW, Perlin DS. Emergence of Echinocandin Resistance Due to a Point Mutation in the fks1 Gene of Aspergillus fumigatus in a Patient with Chronic Pulmonary Aspergillosis. Antimicrob Agents Chemother. 2017;61(12).
93. Denning DW. Chronic forms of pulmonary aspergillosis. Clin Microbiol Infect. 2001;7 Suppl 2:25-31.
94. Farid S, Mohamed S, Devbhandari M, Kneale M, Richardson M, Soon SY, et al. Results of surgery for chronic pulmonary Aspergillosis, optimal antifungal therapy and proposed high risk factors for recurrence--a National Centre's experience. J Cardiothorac Surg. 2013;8:180.
95. Alastruey-Izquierdo A, Cadranel J, Flick H, Godet C, Hennequin C, Hoenigl M, et al. Treatment of Chronic Pulmonary Aspergillosis: Current Standards and Future Perspectives. Respiration. 2018;96(2):159-70.
96. Puerta-Alcalde P, Garcia-Vidal C. Changing Epidemiology of Invasive Fungal Disease in Allogeneic Hematopoietic Stem Cell Transplantation. J Fungi (Basel). 2021;7(10).
97. McCormick A, Loeffler J, Ebel F. Aspergillus fumigatus: contours of an opportunistic human pathogen. Cell Microbiol. 2010;12(11):1535-43.
98. Hohl TM, Feldmesser M. Aspergillus fumigatus: principles of pathogenesis and host defense. Eukaryot Cell. 2007;6(11):1953-63.
99. Paris S, Debeaupuis JP, Crameri R, Carey M, Charlès F, Prévost MC, et al. Conidial hydrophobins of Aspergillus fumigatus. Appl Environ Microbiol. 2003;69(3):1581-8.
100. Aimanianda V, Bayry J, Bozza S, Kniemeyer O, Perruccio K, Elluru SR, et al. Surface hydrophobin prevents immune recognition of airborne fungal spores. Nature. 2009;460(7259):1117-21.
101. Bayry J, Aimanianda V, Guijarro JI, Sunde M, Latgé JP. Hydrophobins--unique fungal proteins. PLoS Pathog. 2012;8(5):e1002700.
102. Jensen BG, Andersen MR, Pedersen MH, Frisvad JC, Søndergaard I. Hydrophobins from Aspergillus species cannot be clearly divided into two classes. BMC Res Notes. 2010;3:344.
103. Sunde M, Kwan AH, Templeton MD, Beever RE, Mackay JP. Structural analysis of hydrophobins. Micron. 2008;39(7):773-84.

104. Askew DS. Aspergillus fumigatus: virulence genes in a street-smart mold. Curr Opin Microbiol. 2008;11(4):331-7.
105. Langfelder K, Streibel M, Jahn B, Haase G, Brakhage AA. Biosynthesis of fungal melanins and their importance for human pathogenic fungi. Fungal Genet Biol. 2003;38(2):143-58.
106. Tsai HF, Chang YC, Washburn RG, Wheeler MH, Kwon-Chung KJ. The developmentally regulated alb1 gene of Aspergillus fumigatus: its role in modulation of conidial morphology and virulence. J Bacteriol. 1998;180(12):3031-8.
107. Stappers MHT, Clark AE, Aimanianda V, Bidula S, Reid DM, Asamaphan P, et al. Recognition of DHN-melanin by a C-type lectin receptor is required for immunity to Aspergillus. Nature. 2018;555(7696):382-6.
108. Tone K, Stappers MHT, Willment JA, Brown GD. C-type lectin receptors of the Dectin-1 cluster: Physiological roles and involvement in disease. Eur J Immunol. 2019;49(12):2127-33.
109. Tone K, Stappers MHT, Hatinguais R, Dambuza IM, Salazar F, Wallace C, et al. MelLec Exacerbates the Pathogenesis of Aspergillus fumigatus-Induced Allergic Inflammation in Mice. Front Immunol. 2021;12:675702.
110. Boettner D, Huebner N, Rhodes JC, Askew DS. Molecular cloning of Aspergillus fumigatus CgrA, the ortholog of a conserved fungal nucleolar protein. Med Mycol. 2001;39(6):517-21.
111. Bhabhra R, Miley MD, Mylonakis E, Boettner D, Fortwendel J, Panepinto JC, et al. Disruption of the Aspergillus fumigatus gene encoding nucleolar protein CgrA impairs thermotolerant growth and reduces virulence. Infect Immun. 2004;72(8):4731-40.
112. Rementeria A, López-Molina N, Ludwig A, Vivanco AB, Bikandi J, Pontón J, et al. Genes and molecules involved in Aspergillus fumigatus virulence. Rev Iberoam Micol. 2005;22(1):1-23.
113. Kolattukudy PE, Lee JD, Rogers LM, Zimmerman P, Ceselski S, Fox B, et al. Evidence for possible involvement of an elastolytic serine protease in aspergillosis. Infect Immun. 1993;61(6):2357-68.
114. Blanco JL, Hontecillas R, Bouza E, Blanco I, Pelaez T, Muñoz P, et al. Correlation between the elastase activity index and invasiveness of clinical isolates of Aspergillus fumigatus. J Clin Microbiol. 2002;40(5):1811-3.
115. Kogan TV, Jadoun J, Mittelman L, Hirschberg K, Osherov N. Involvement of secreted Aspergillus fumigatus proteases in disruption of the actin fiber cytoskeleton and loss of focal adhesion sites in infected A549 lung pneumocytes. J Infect Dis. 2004;189(11):1965-73.
116. Hissen AH, Chow JM, Pinto LJ, Moore MM. Survival of Aspergillus fumigatus in serum involves removal of iron from transferrin: the role of siderophores. Infect Immun. 2004;72(3):1402-8.
117. Schrettl M, Bignell E, Kragl C, Joechl C, Rogers T, Arst HN, Jr., et al. Siderophore biosynthesis but not reductive iron assimilation is essential for Aspergillus fumigatus virulence. J Exp Med. 2004;200(9):1213-9.
118. Willger SD, Puttikamonkul S, Kim KH, Burritt JB, Grahl N, Metzler LJ, et al. A sterol-regulatory element binding protein is required for cell polarity, hypoxia adaptation, azole drug resistance, and virulence in Aspergillus fumigatus. PLoS Pathog. 2008;4(11):e1000200.
119. Willger SD, Grahl N, Cramer RA, Jr. Aspergillus fumigatus metabolism: clues to mechanisms of in vivo fungal growth and virulence. Med Mycol. 2009;47 Suppl 1(Suppl 1):S72-9.
120. Chung D, Barker BM, Carey CC, Merriman B, Werner ER, Lechner BE, et al. ChIP-seq and in vivo transcriptome analyses of the Aspergillus fumigatus SREBP SrbA reveals a new regulator of the fungal hypoxia response and virulence. PLoS Pathog. 2014;10(11):e1004487.
121. Kowalski CH, Beattie SR, Fuller KK, McGurk EA, Tang YW, Hohl TM, et al. Heterogeneity among Isolates Reveals that Fitness in Low Oxygen Correlates with Aspergillus fumigatus Virulence. mBio. 2016;7(5).

122. Vaknin Y, Hillmann F, Iannitti R, Ben Baruch N, Sandovsky-Losica H, Shadkchan Y, et al. Identification and Characterization of a Novel Aspergillus fumigatus Rhomboid Family Putative Protease, RbdA, Involved in Hypoxia Sensing and Virulence. Infect Immun. 2016;84(6):1866-78.
123. Kroll K, Shekhova E, Mattern DJ, Thywissen A, Jacobsen ID, Strassburger M, et al. The hypoxia-induced dehydrogenase HorA is required for coenzyme Q10 biosynthesis, azole sensitivity and virulence of Aspergillus fumigatus. Mol Microbiol. 2016;101(1):92-108.
124. Hemmann S, Menz G, Ismail C, Blaser K, Crameri R. Skin test reactivity to 2 recombinant Aspergillus fumigatus allergens in A fumigatus-sensitized asthmatic subjects allows diagnostic separation of allergic bronchopulmonary aspergillosis from fungal sensitization. J Allergy Clin Immunol. 1999;104(3 Pt 1):601-7.
125. Chaudhary N, Marr KA. Impact of Aspergillus fumigatus in allergic airway diseases. Clin Transl Allergy. 2011;1(1):4.
126. Nierman WC, Pain A, Anderson MJ, Wortman JR, Kim HS, Arroyo J, et al. Genomic sequence of the pathogenic and allergenic filamentous fungus Aspergillus fumigatus. Nature. 2005;438(7071):1151-6.
127. Kurup VP, Kumar A, Kenealy WR, Greenberger PA. Aspergillus ribotoxins react with IgE and IgG antibodies of patients with allergic bronchopulmonary aspergillosis. J Lab Clin Med. 1994;123(5):749-56.
128. Keller N, Bok J, Chung D, Perrin RM, Keats Shwab E. LaeA, a global regulator of Aspergillus toxins. Med Mycol. 2006;44(Supplement_1):S83-s5.
129. Guruceaga X, Perez-Cuesta U, Abad-Diaz de Cerio A, Gonzalez O, Alonso RM, Hernando FL, et al. Fumagillin, a Mycotoxin of Aspergillus fumigatus: Biosynthesis, Biological Activities, Detection, and Applications. Toxins (Basel). 2019;12(1).
130. Gayathri L, Akbarsha MA, Ruckmani K. In vitro study on aspects of molecular mechanisms underlying invasive aspergillosis caused by gliotoxin and fumagillin, alone and in combination. Sci Rep. 2020;10(1):14473.
131. Fallon JP, Reeves EP, Kavanagh K. Inhibition of neutrophil function following exposure to the Aspergillus fumigatus toxin fumagillin. J Med Microbiol. 2010;59(Pt 6):625-33.
132. Zbidah M, Lupescu A, Jilani K, Lang F. Stimulation of suicidal erythrocyte death by fumagillin. Basic Clin Pharmacol Toxicol. 2013;112(5):346-51.
133. Guruceaga X, Ezpeleta G, Mayayo E, Sueiro-Olivares M, Abad-Diaz-De-Cerio A, Aguirre Urízar JM, et al. A possible role for fumagillin in cellular damage during host infection by Aspergillus fumigatus. Virulence. 2018;9(1):1548-61.
134. Stanzani M, Orciuolo E, Lewis R, Kontoyiannis DP, Martins SL, St John LS, et al. Aspergillus fumigatus suppresses the human cellular immune response via gliotoxin-mediated apoptosis of monocytes. Blood. 2005;105(6):2258-65.
135. Ben-Ami R, Lewis RE, Leventakos K, Kontoyiannis DP. Aspergillus fumigatus inhibits angiogenesis through the production of gliotoxin and other secondary metabolites. Blood. 2009;114(26):5393-9.
136. Kroll M, Arenzana-Seisdedos F, Bachelerie F, Thomas D, Friguet B, Conconi M. The secondary fungal metabolite gliotoxin targets proteolytic activities of the proteasome. Chem Biol. 1999;6(10):689-98.
137. Kwon-Chung KJ, Sugui JA. What do we know about the role of gliotoxin in the pathobiology of Aspergillus fumigatus? Med Mycol. 2009;47 Suppl 1(Suppl 1):S97-103.
138. Zacharias CA, Sheppard DC. The role of Aspergillus fumigatus polysaccharides in host-pathogen interactions. Curr Opin Microbiol. 2019;52:20-6.
139. Bernard M, Latgé JP. Aspergillus fumigatus cell wall: composition and biosynthesis. Med Mycol. 2001;39 Suppl 1:9-17.

140. Latgé JP, Beauvais A, Chamilos G. The Cell Wall of the Human Fungal Pathogen Aspergillus fumigatus: Biosynthesis, Organization, Immune Response, and Virulence. Annu Rev Microbiol. 2017;71:99-116.
141. Da Silva CA, Chalouni C, Williams A, Hartl D, Lee CG, Elias JA. Chitin is a size-dependent regulator of macrophage TNF and IL-10 production. J Immunol. 2009;182(6):3573-82.
142. Becker KL, Aimanianda V, Wang X, Gresnigt MS, Ammerdorffer A, Jacobs CW, et al. Aspergillus Cell Wall Chitin Induces Anti- and Proinflammatory Cytokines in Human PBMCs via the Fc-γ Receptor/Syk/PI3K Pathway. mBio. 2016;7(3).
143. García-Rodriguez LJ, Trilla JA, Castro C, Valdivieso MH, Durán A, Roncero C. Characterization of the chitin biosynthesis process as a compensatory mechanism in the fks1 mutant of Saccharomyces cerevisiae. FEBS Lett. 2000;478(1-2):84-8.
144. Kapteyn JC, Hoyer LL, Hecht JE, Müller WH, Andel A, Verkleij AJ, et al. The cell wall architecture of Candida albicans wild-type cells and cell wall-defective mutants. Mol Microbiol. 2000;35(3):601-11.
145. Kurtz MB, Heath IB, Marrinan J, Dreikorn S, Onishi J, Douglas C. Morphological effects of lipopeptides against Aspergillus fumigatus correlate with activities against (1,3)-beta-D-glucan synthase. Antimicrob Agents Chemother. 1994;38(7):1480-9.
146. Dichtl K, Samantaray S, Aimanianda V, Zhu Z, Prévost MC, Latgé JP, et al. Aspergillus fumigatus devoid of cell wall β-1,3-glucan is viable, massively sheds galactomannan and is killed by septum formation inhibitors. Mol Microbiol. 2015;95(3):458-71.
147. Carrion SDJ, Leal SM, Ghannoum MA, Aimanianda V, Latge JP, Pearlman E. The RodA Hydrophobin on Aspergillus fumigatus Spores Masks Dectin-1 and Dectin-2-Dependent Responses and Enhances Fungal Survival in vivo. Journal of Immunology. 2013:2581-8.
148. Steele C, Rapaka RR, Metz A, Pop SM, Williams DL, Gordon S, et al. The beta-glucan receptor dectin-1 recognizes specific morphologies of Aspergillus fumigatus. PLoS Pathog. 2005;1(4):e42.
149. Gravelat FN, Beauvais A, Liu H, Lee MJ, Snarr BD, Chen D, et al. Aspergillus galactosaminogalactan mediates adherence to host constituents and conceals hyphal beta-glucan from the immune system. PLoS Pathog. 2013;9(8):e1003575.
150. Balloy V, Chignard M. The innate immune response to Aspergillus fumigatus. Microbes Infect. 2009;11(12):919-27.
151. Werner JL, Metz AE, Horn D, Schoeb TR, Hewitt MM, Schwiebert LM, et al. Requisite role for the dectin-1 beta-glucan receptor in pulmonary defense against Aspergillus fumigatus. J Immunol. 2009;182(8):4938-46.
152. Li X, Cullere X, Nishi H, Saggu G, Durand E, Mansour MK, et al. PKC-δ activation in neutrophils promotes fungal clearance. J Leukoc Biol. 2016;100(3):581-8.
153. Rogers NC, Slack EC, Edwards AD, Nolte MA, Schulz O, Schweighoffer E, et al. Syk-Dependent Cytokine Induction by Dectin-1 Reveals a Novel Pattern Recognition Pathway for C Type Lectins. 2005;22(4):507-17.
154. Werner JL, Gessner MA, Lilly LM, Nelson MP, Metz AE, Dunaway CW, et al. Neutrophils Produce Interleukin 17A (IL-17A) in a Dectin-1 and IL-23-Dependent Manner during Invasive Fungal Infection. Infection and Immunity. 2011:3966-77.
155. Khan NS, Kasperkovitz PV, Timmons AK, Mansour MK, Tam JM, Seward MW, et al. Dectin-1 Controls TLR-9 Trafficking To Phagosomes Containing B-1,3 Glucan. 2016;196.
156. Beauvais A, Bozza S, Kniemeyer O, Formosa C, Balloy V, Henry C, et al. Deletion of the α-(1,3)-glucan synthase genes induces a restructuring of the conidial cell wall responsible for the avirulence of Aspergillus fumigatus. PLoS Pathog. 2013;9(11):e1003716.
157. Bozza S, Clavaud C, Giovannini G, Fontaine T, Beauvais A, Sarfati J, et al. Immune sensing of Aspergillus fumigatus proteins, glycolipids, and polysaccharides and the impact on Th immunity and vaccination. J Immunol. 2009;183(4):2407-14.

158. Rinaudo M. Chitin and chitosan: Properties and applications. Progress in Polymer Science. 2006;31(7):603-32.
159. O'Dea EM, Amarsaikhan N, Li H, Downey J, Steele E, Van Dyken SJ, et al. Eosinophils are recruited in response to chitin exposure and enhance Th2-mediated immune pathology in Aspergillus fumigatus infection. Infect Immun. 2014;82(8):3199-205.
160. Da Silva CA, Hartl D, Liu W, Lee CG, Elias JA. TLR-2 and IL-17A in chitin-induced macrophage activation and acute inflammation. J Immunol. 2008;181(6):4279-86.
161. Hohl TM, Van Epps HL, Rivera A, Morgan LA, Chen PL, Feldmesser M, et al. Aspergillus fumigatus triggers inflammatory responses by stage-specific beta-glucan display. PLoS Pathog. 2005;1(3):e30.
162. Garth JM, Mackel JJ, Reeder KM, Blackburn JP, Dunaway CW, Yu Z, et al. Acidic Mammalian Chitinase Negatively Affects Immune Responses during Acute and Chronic Aspergillus fumigatus Exposure. Infect Immun. 2018;86(7).
163. Thomsen T, Schlosser A, Holmskov U, Sorensen GL. Ficolins and FIBCD1: soluble and membrane bound pattern recognition molecules with acetyl group selectivity. Mol Immunol. 2011;48(4):369-81.
164. Jensen K, Lund KP, Christensen KB, Holm AT, Dubey LK, Moeller JB, et al. M-ficolin is present in Aspergillus fumigatus infected lung and modulates epithelial cell immune responses elicited by fungal cell wall polysaccharides. Virulence. 2017;8(8):1870-9.
165. Gastebois A, Clavaud C, Aimanianda V, Latgé JP. Aspergillus fumigatus: cell wall polysaccharides, their biosynthesis and organization. Future Microbiol. 2009;4(5):583-95.
166. Latgé JP, Kobayashi H, Debeaupuis JP, Diaquin M, Sarfati J, Wieruszeski JM, et al. Chemical and immunological characterization of the extracellular galactomannan of Aspergillus fumigatus. Infect Immun. 1994;62(12):5424-33.
167. Leitao EA, Bittencourt VC, Haido RM, Valente AP, Peter-Katalinic J, Letzel M, et al. Beta-galactofuranose-containing O-linked oligosaccharides present in the cell wall peptidogalactomannan of Aspergillus fumigatus contain immunodominant epitopes. Glycobiology. 2003;13(10):681-92.
168. Kudoh A, Okawa Y, Shibata N. Significant structural change in both O- and N-linked carbohydrate moieties of the antigenic galactomannan from Aspergillus fumigatus grown under different culture conditions. Glycobiology. 2015;25(1):74-87.
169. Katafuchi Y, Li Q, Tanaka Y, Shinozuka S, Kawamitsu Y, Izumi M, et al. GfsA is a β1,5-galactofuranosyltransferase involved in the biosynthesis of the galactofuran side chain of fungal-type galactomannan in Aspergillus fumigatus. Glycobiology. 2017;27(6):568-81.
170. Serrano-Gomez D, Dominguez-Soto A, Ancochea J, Jiminez-Heffernan JA, Leal JA, Corbi AL. Dendritic Cell-Specific Intercellular Adhesion Molecule 3-Grabbing Nonintegrin Mediates Binding and Internalization of Aspergillus fumigatus Conidia by Dendritic Cells and Macrophages. Journal of Immunology. 2004:5635-43.
171. Mezger M, Kneitz S, Wozniok I, Kurzai O, Einsele H, Loeffler J. Proinflammatory Response of Immature Human Dendritic Cells is Mediated by Dectin-1 after Exposure to Aspergillus fumigatus Germ Tubes. 2008;197(6):924–31.
172. Neth O, Jack DL, Dodds AW, Holzel H, Klein NJ, Turner MW. Mannose-binding lectin binds to a range of clinically relevant microorganisms and promotes complement deposition. Infect Immun. 2000;68(2):688-93.
173. Feinberg H, Jégouzo SAF, Rex MJ, Drickamer K, Weis WI, Taylor ME. Mechanism of pathogen recognition by human dectin-2. J Biol Chem. 2017;292(32):13402-14.
174. Sun H, Xu XY, Tian XL, Shao HT, Wu XD, Wang Q, et al. Activation of NF-κB and respiratory burst following Aspergillus fumigatus stimulation of macrophages. Immunobiology. 2014;219(1):25-36.
175. Loures FV, Röhm M, Lee CK, Santos E, Wang JP, Specht CA, et al. Recognition of Aspergillus fumigatus hyphae by human plasmacytoid dendritic cells is mediated by dectin-2 and results in formation of extracellular traps. PLoS Pathog. 2015;11(2):e1004643.

176. Dumestre-Pérard C, Lamy B, Aldebert D, Lemaire-Vieille C, Grillot R, Brion JP, et al. Aspergillus conidia activate the complement by the mannan-binding lectin C2 bypass mechanism. J Immunol. 2008;181(10):7100-5.
177. Kaur S, Gupta VK, Thiel S, Sarma PU, Madan T. Protective role of mannan-binding lectin in a murine model of invasive pulmonary aspergillosis. Clin Exp Immunol. 2007;148(2):382-9.
178. Clemons KV, Martinez M, Tong AJ, Stevens DA. Resistance of MBL gene-knockout mice to experimental systemic aspergillosis. Immunol Lett. 2010;128(2):105-7.
179. Hogaboam CM, Takahashi K, Ezekowitz RA, Kunkel SL, Schuh JM. Mannose-binding lectin deficiency alters the development of fungal asthma: effects on airway response, inflammation, and cytokine profile. J Leukoc Biol. 2004;75(5):805-14.
180. Briard B, Muszkieta L, Latgé JP, Fontaine T. Galactosaminogalactan of Aspergillus fumigatus, a bioactive fungal polymer. Mycologia. 2016;108(3):572-80.
181. Lee MJ, Liu H, Barker BM, Snarr BD, Gravelat FN, Al Abdallah Q, et al. The Fungal Exopolysaccharide Galactosaminogalactan Mediates Virulence by Enhancing Resistance to Neutrophil Extracellular Traps. PLoS Pathog. 2015;11(10):e1005187.
182. Beaussart A, El-Kirat-Chatel S, Fontaine T, Latgé JP, Dufrêne YF. Nanoscale biophysical properties of the cell surface galactosaminogalactan from the fungal pathogen Aspergillus fumigatus. Nanoscale. 2015;7(36):14996-5004.
183. Briard B, Fontaine T, Samir P, Place DE, Muszkieta L, Malireddi RKS, et al. Galactosaminogalactan activates the inflammasome to provide host protection. Nature. 2020;588(7839):688-92.
184. Fontaine T, Delangle A, Simenel C, Coddeville B, van Vliet SJ, van Kooyk Y, et al. Galactosaminogalactan, a new immunosuppressive polysaccharide of Aspergillus fumigatus. PLoS Pathog. 2011;7(11):e1002372.
185. Robinet P, Baychelier F, Fontaine T, Picard C, Debre P, Vieillard V, et al. A polysaccharide virulence factor of a human fungal pathogen induces neutrophil apoptosis via NK cells. J Immunol. 2014;192(11):5332-42.
186. Gresnigt MS, Bozza S, Becker KL, Joosten LA, Abdollahi-Roodsaz S, van der Berg WB, et al. A polysaccharide virulence factor from Aspergillus fumigatus elicits anti-inflammatory effects through induction of Interleukin-1 receptor antagonist. PLoS Pathog. 2014;10(3):e1003936.
187. Rambach G, Blum G, Latgé JP, Fontaine T, Heinekamp T, Hagleitner M, et al. Identification of Aspergillus fumigatus Surface Components That Mediate Interaction of Conidia and Hyphae With Human Platelets. J Infect Dis. 2015;212(7):1140-9.
188. Stanzani M, Sassi C, Lewis RE, Tolomelli G, Bazzocchi A, Cavo M, et al. High resolution computed tomography angiography improves the radiographic diagnosis of invasive mold disease in patients with hematological malignancies. Clin Infect Dis. 2015;60(11):1603-10.
189. Latgé JP. The cell wall: a carbohydrate armour for the fungal cell. Mol Microbiol. 2007;66(2):279-90.
190. Bowman SM, Free SJ. The structure and synthesis of the fungal cell wall. Bioessays. 2006;28(8):799-808.
191. Roncero C. The genetic complexity of chitin synthesis in fungi. Curr Genet. 2002;41(6):367-78.
192. Mellado E, Aufauvre-Brown A, Gow NA, Holden DW. The Aspergillus fumigatus chsC and chsG genes encode class III chitin synthases with different functions. Mol Microbiol. 1996;20(3):667-79.
193. Lee MJ, Sheppard DC. Recent advances in the understanding of the Aspergillus fumigatus cell wall. J Microbiol. 2016;54(3):232-42.
194. Latgé JP, Mouyna I, Tekaia F, Beauvais A, Debeaupuis JP, Nierman W. Specific molecular features in the organization and biosynthesis of the cell wall of Aspergillus fumigatus. Med Mycol. 2005;43 Suppl 1:S15-22.

195. Henry C, Latgé JP, Beauvais A. α1,3 glucans are dispensable in Aspergillus fumigatus. Eukaryot Cell. 2012;11(1):26-9.
196. Fontaine T, Latgé JP. Galactomannan Produced by Aspergillus fumigatus: An Update on the Structure, Biosynthesis and Biological Functions of an Emblematic Fungal Biomarker. J Fungi (Basel). 2020;6(4).
197. Lee MJ, Geller AM, Bamford NC, Liu H, Gravelat FN, Snarr BD, et al. Deacetylation of Fungal Exopolysaccharide Mediates Adhesion and Biofilm Formation. mBio. 2016;7(2):e00252-16.
198. Lee MJ, Gravelat FN, Cerone RP, Baptista SD, Campoli PV, Choe SI, et al. Overlapping and distinct roles of Aspergillus fumigatus UDP-glucose 4-epimerases in galactose metabolism and the synthesis of galactose-containing cell wall polysaccharides. J Biol Chem. 2014;289(3):1243-56.
199. Bamford NC, Le Mauff F, Van Loon JC, Ostapska H, Snarr BD, Zhang Y, et al. Structural and biochemical characterization of the exopolysaccharide deacetylase Agd3 required for Aspergillus fumigatus biofilm formation. Nat Commun. 2020;11(1):2450.
200. Bamford NC, Snarr BD, Gravelat FN, Little DJ, Lee MJ, Zacharias CA, et al. Sph3 Is a Glycoside Hydrolase Required for the Biosynthesis of Galactosaminogalactan in Aspergillus fumigatus. J Biol Chem. 2015;290(46):27438-50.
201. Bamford NC, Le Mauff F, Subramanian AS, Yip P, Millan C, Zhang Y, et al. Ega3 from the fungal pathogen Aspergillus fumigatus is an endo-alpha-1,4-galactosaminidase that disrupts microbial biofilms. J Biol Chem. 2019;294(37):13833-49.
202. Le Mauff F, Bamford NC, Alnabelseya N, Zhang Y, Baker P, Robinson H, et al. Molecular mechanism of Aspergillus fumigatus biofilm disruption by fungal and bacterial glycoside hydrolases. J Biol Chem. 2019;294(28):10760-72.
203. Franklin MJ, Nivens DE, Weadge JT, Howell PL. Biosynthesis of the Pseudomonas aeruginosa Extracellular Polysaccharides, Alginate, Pel, and Psl. Front Microbiol. 2011;2:167.
204. Ostapska H, Raju D, Lehoux M, Lacdao I, Gilbert S, Sivarajah P, et al. Preclinical Evaluation of Recombinant Microbial Glycoside Hydrolases in the Prevention of Experimental Invasive Aspergillosis. mBio. 2021;12(5):e0244621.
205. Snarr BD, Baker P, Bamford NC, Sato Y, Liu H, Lehoux M, et al. Microbial glycoside hydrolases as antibiofilm agents with cross-kingdom activity. Proc Natl Acad Sci U S A. 2017;114(27):7124-9.
206. Takeo K, Uesaka I, Uehira K, Nishiura M. Fine structure of Cryptococcus neoformans grown in vitro as observed by freeze-etching. J Bacteriol. 1973;113(3):1442-8.
207. Takeo K, Uesaka I, Uehira K, Nishiura M. Fine structure of Cryptococcus neoformans grown in vivo as observed by freeze-etching. J Bacteriol. 1973;113(3):1449-54.
208. Rodrigues ML, Nakayasu ES, Oliveira DL, Nimrichter L, Nosanchuk JD, Almeida IC, et al. Extracellular vesicles produced by Cryptococcus neoformans contain protein components associated with virulence. Eukaryot Cell. 2008;7(1):58-67.
209. Pegtel DM, Gould SJ. Exosomes. Annu Rev Biochem. 2019;88:487-514.
210. Oliveira DL, Rizzo J, Joffe LS, Godinho RM, Rodrigues ML. Where do they come from and where do they go: candidates for regulating extracellular vesicle formation in fungi. Int J Mol Sci. 2013;14(5):9581-603.
211. Rodrigues ML, Nakayasu ES, Almeida IC, Nimrichter L. The impact of proteomics on the understanding of functions and biogenesis of fungal extracellular vesicles. J Proteomics. 2014;97:177-86.
212. Zamith-Miranda D, Peres da Silva R, Couvillion SP, Bredeweg EL, Burnet MC, Coelho C, et al. Omics Approaches for Understanding Biogenesis, Composition and Functions of Fungal Extracellular Vesicles. Front Genet. 2021;12:648524.
213. Zhao K, Bleackley M, Chisanga D, Gangoda L, Fonseka P, Liem M, et al. Extracellular vesicles secreted by Saccharomyces cerevisiae are involved in cell wall remodelling. Commun Biol. 2019;2:305.

214. Rodrigues ML, Nimrichter L, Oliveira DL, Frases S, Miranda K, Zaragoza O, et al. Vesicular polysaccharide export in Cryptococcus neoformans is a eukaryotic solution to the problem of fungal trans-cell wall transport. Eukaryot Cell. 2007;6(1):48-59.
215. Rodrigues ML, Godinho RM, Zamith-Miranda D, Nimrichter L. Traveling into Outer Space: Unanswered Questions about Fungal Extracellular Vesicles. PLoS Pathog. 2015;11(12):e1005240.
216. Cherniak R, Sundstrom JB. Polysaccharide antigens of the capsule of Cryptococcus neoformans. Infect Immun. 1994;62(5):1507-12.
217. Zaragoza O, Rodrigues ML, De Jesus M, Frases S, Dadachova E, Casadevall A. The capsule of the fungal pathogen Cryptococcus neoformans. Advances in applied microbiology. 2009;68:133-216.
218. Yoneda A, Doering TL. A eukaryotic capsular polysaccharide is synthesized intracellularly and secreted via exocytosis. Mol Biol Cell. 2006;17(12):5131-40.
219. Doering TL. How sweet it is! Cell wall biogenesis and polysaccharide capsule formation in Cryptococcus neoformans. Annu Rev Microbiol. 2009;63:223-47.
220. Bose I, Reese AJ, Ory JJ, Janbon G, Doering TL. A yeast under cover: the capsule of Cryptococcus neoformans. Eukaryot Cell. 2003;2(4):655-63.
221. Albuquerque PC, Cordero RJ, Fonseca FL, Peres da Silva R, Ramos CL, Miranda KR, et al. A Paracoccidioides brasiliensis glycan shares serologic and functional properties with cryptococcal glucuronoxylomannan. Fungal Genet Biol. 2012;49(11):943-54.
222. Zarnowski R, Sanchez H, Covelli AS, Dominguez E, Jaromin A, Bernhardt J, et al. Candida albicans biofilm-induced vesicles confer drug resistance through matrix biogenesis. PLoS Biol. 2018;16(10):e2006872.
223. Monari C, Bistoni F, Vecchiarelli A. Glucuronoxylomannan exhibits potent immunosuppressive properties. FEMS Yeast Res. 2006;6(4):537-42.
224. Oliveira DL, Freire-de-Lima CG, Nosanchuk JD, Casadevall A, Rodrigues ML, Nimrichter L. Extracellular vesicles from Cryptococcus neoformans modulate macrophage functions. Infect Immun. 2010;78(4):1601-9.
225. Huang SH, Wu CH, Chang YC, Kwon-Chung KJ, Brown RJ, Jong A. Cryptococcus neoformans-derived microvesicles enhance the pathogenesis of fungal brain infection. PLoS One. 2012;7(11):e48570.
226. Bielska E, May RC. Extracellular vesicles of human pathogenic fungi. Curr Opin Microbiol. 2019;52:90-9.
227. Gehrmann U, Qazi KR, Johansson C, Hultenby K, Karlsson M, Lundeberg L, et al. Nanovesicles from Malassezia sympodialis and host exosomes induce cytokine responses--novel mechanisms for host-microbe interactions in atopic eczema. PLoS One. 2011;6(7):e21480.
228. Brauer VS, Pessoni AM, Bitencourt TA, de Paula RG, de Oliveira Rocha L, Goldman GH, et al. Extracellular Vesicles from Aspergillus flavus Induce M1 Polarization In Vitro. mSphere. 2020;5(3).
229. Souza JAM, Baltazar LM, Carregal VM, Gouveia-Eufrasio L, de Oliveira AG, Dias WG, et al. Characterization of Aspergillus fumigatus Extracellular Vesicles and Their Effects on Macrophages and Neutrophils Functions. Front Microbiol. 2019;10:2008.
230. Rizzo J, Chaze T, Miranda K, Roberson RW, Gorgette O, Nimrichter L, et al. Characterization of Extracellular Vesicles Produced by Aspergillus fumigatus Protoplasts. mSphere. 2020;5(4).
231. Bitencourt TA, Hatanaka O, Pessoni AM, Freitas MS, Trentin G, Santos P, et al. Fungal Extracellular Vesicles Are Involved in Intraspecies Intracellular Communication. mBio. 2022;13(1):e0327221.
232. Jenks JD, Hoenigl M. Point-of-care diagnostics for invasive aspergillosis: nearing the finish line. Expert Rev Mol Diagn. 2020;20(10):1009-17.
233. Lestrade PP, Bentvelsen RG, Schauwvlieghe A, Schalekamp S, van der Velden W, Kuiper EJ, et al. Voriconazole Resistance and Mortality in Invasive Aspergillosis: A Multicenter Retrospective Cohort Study. Clin Infect Dis. 2019;68(9):1463-71.

234. Yousefian S, Dastan F, Marjani M, Tabarsi P, Barati S, Shahsavari N, et al. Determination of Voriconazole Plasma Concentration by HPLC Technique and Evaluating Its Association with Clinical Outcome and Adverse Effects in Patients with Invasive Aspergillosis. Can J Infect Dis Med Microbiol. 2021;2021:5497427.
235. Reissig JL, Lai WH, Glasgow JE. An endogalactosaminidase from Streptomyces griseus. Can J Biochem. 1975;53(12):1237-49.
236. Lombard V, Golaconda Ramulu H, Drula E, Coutinho PM, Henrissat B. The carbohydrate-active enzymes database (CAZy) in 2013. Nucleic Acids Res. 2014;42(Database issue):D490-5.
237. Krogh A, Larsson B, von Heijne G, Sonnhammer EL. Predicting transmembrane protein topology with a hidden Markov model: application to complete genomes. J Mol Biol. 2001;305(3):567-80.
238. Kelley LA, Mezulis S, Yates CM, Wass MN, Sternberg MJ. The Phyre2 web portal for protein modeling, prediction and analysis. Nat Protoc. 2015;10(6):845-58.
239. Dessau MA, Modis Y. Protein crystallization for X-ray crystallography. J Vis Exp. 2011(47).
240. Gil-Bona A, Llama-Palacios A, Parra CM, Vivanco F, Nombela C, Monteoliva L, et al. Proteomics unravels extracellular vesicles as carriers of classical cytoplasmic proteins in Candida albicans. J Proteome Res. 2015;14(1):142-53.
241. Hassani K, Shio MT, Martel C, Faubert D, Olivier M. Absence of metalloprotease GP63 alters the protein content of Leishmania exosomes. PLoS One. 2014;9(4):e95007.
242. Oliveira DL, Nakayasu ES, Joffe LS, Guimarães AJ, Sobreira TJ, Nosanchuk JD, et al. Characterization of yeast extracellular vesicles: evidence for the participation of different pathways of cellular traffic in vesicle biogenesis. PLoS One. 2010;5(6):e11113.
243. Mouyna I, Morelle W, Vai M, Monod M, Léchenne B, Fontaine T, et al. Deletion of GEL2 encoding for a beta(1-3)glucanosyltransferase affects morphogenesis and virulence in Aspergillus fumigatus. Mol Microbiol. 2005;56(6):1675-88.
244. da Silva Ferreira ME, Kress MR, Savoldi M, Goldman MH, Härtl A, Heinekamp T, et al. The akuB(KU80) mutant deficient for nonhomologous end joining is a powerful tool for analyzing pathogenicity in Aspergillus fumigatus. Eukaryot Cell. 2006;5(1):207-11.
245. Bertuzzi M, van Rhijn N, Krappmann S, Bowyer P, Bromley MJ, Bignell EM. On the lineage of Aspergillus fumigatus isolates in common laboratory use. Med Mycol. 2021;59(1):7-13.
246. Gravelat FN, Askew DS, Sheppard DC. Targeted gene deletion in Aspergillus fumigatus using the hygromycin-resistance split-marker approach. Methods Mol Biol. 2012;845:119-30.
247. Yang J, Yan R, Roy A, Xu D, Poisson J, Zhang Y. The I-TASSER Suite: protein structure and function prediction. Nat Methods. 2015;12(1):7-8.
248. Thoden JB, Wohlers TM, Fridovich-Keil JL, Holden HM. Crystallographic evidence for Tyr 157 functioning as the active site base in human UDP-galactose 4-epimerase. Biochemistry. 2000;39(19):5691-701.
249. Seo MD, Won HS, Kim JH, Mishig-Ochir T, Lee BJ. Antimicrobial peptides for therapeutic applications: a review. Molecules. 2012;17(10):12276-86.
250. Kościuczuk EM, Lisowski P, Jarczak J, Strzałkowska N, Jóźwik A, Horbańczuk J, et al. Cathelicidins: family of antimicrobial peptides. A review. Mol Biol Rep. 2012;39(12):10957-70.
251. Zasloff M. Antimicrobial peptides of multicellular organisms. Nature. 2002;415(6870):389-95.
252. Bahar AA, Ren D. Antimicrobial peptides. Pharmaceuticals (Basel). 2013;6(12):1543-75.
253. Lipke PN, Ovalle R. Cell wall architecture in yeast: new structure and new challenges. J Bacteriol. 1998;180(15):3735-40.
254. Swidergall M, Ernst JF. Interplay between Candida albicans and the antimicrobial peptide armory. Eukaryot Cell. 2014;13(8):950-7.
255. Hwang B, Hwang JS, Lee J, Kim JK, Kim SR, Kim Y, et al. Induction of yeast apoptosis by an antimicrobial peptide, Papiliocin. Biochem Biophys Res Commun. 2011;408(1):89-93.

256. Fry DE. Antimicrobial Peptides. Surg Infect (Larchmt). 2018;19(8):804-11.
257. Lupetti A, Paulusma-Annema A, Welling MM, Dogterom-Ballering H, Brouwer CP, Senesi S, et al. Synergistic activity of the N-terminal peptide of human lactoferrin and fluconazole against Candida species. Antimicrob Agents Chemother. 2003;47(1):262-7.
258. Kirkpatrick CH, Green I, Rich RR, Schade AL. Inhibition of growth of Candida albicans by iron-unsaturated lactoferrin: relation to host-defense mechanisms in chronic mucocutaneous candidiasis. J Infect Dis. 1971;124(6):539-44.
259. Nikawa H, Samaranayake LP, Tenovuo J, Pang KM, Hamada T. The fungicidal effect of human lactoferrin on Candida albicans and Candida krusei. Arch Oral Biol. 1993;38(12):1057-63.
260. Lupetti A, van Dissel JT, Brouwer CP, Nibbering PH. Human antimicrobial peptides' antifungal activity against Aspergillus fumigatus. Eur J Clin Microbiol Infect Dis. 2008;27(11):1125-9.
261. Zarember KA, Sugui JA, Chang YC, Kwon-Chung KJ, Gallin JI. Human polymorphonuclear leukocytes inhibit Aspergillus fumigatus conidial growth by lactoferrin-mediated iron depletion. J Immunol. 2007;178(10):6367-73.
262. Kavanagh K, Dowd S. Histatins: antimicrobial peptides with therapeutic potential. J Pharm Pharmacol. 2004;56(3):285-9.
263. Helmerhorst EJ, Breeuwer P, van't Hof W, Walgreen-Weterings E, Oomen LC, Veerman EC, et al. The cellular target of histatin 5 on Candida albicans is the energized mitochondrion. J Biol Chem. 1999;274(11):7286-91.
264. Helmerhorst EJ, Troxler RF, Oppenheim FG. The human salivary peptide histatin 5 exerts its antifungal activity through the formation of reactive oxygen species. Proc Natl Acad Sci U S A. 2001;98(25):14637-42.
265. Helmerhorst EJ, Reijnders IM, van't Hof W, Simoons-Smit I, Veerman EC, Amerongen AV. Amphotericin B- and fluconazole-resistant Candida spp., Aspergillus fumigatus, and other newly emerging pathogenic fungi are susceptible to basic antifungal peptides. Antimicrob Agents Chemother. 1999;43(3):702-4.
266. van't Hof W, Reijnders IM, Helmerhorst EJ, Walgreen-Weterings E, Simoons-Smit IM, Veerman EC, et al. Synergistic effects of low doses of histatin 5 and its analogues on amphotericin B anti-mycotic activity. Antonie Van Leeuwenhoek. 2000;78(2):163-9.
267. Luo XL, Li JX, Huang HR, Duan JL, Dai RX, Tao RJ, et al. LL37 Inhibits Aspergillus fumigatus Infection via Directly Binding to the Fungus and Preventing Excessive Inflammation. Front Immunol. 2019;10:283.
268. Sheehan G, Bergsson G, McElvaney NG, Reeves EP, Kavanagh K. The Human Cathelicidin Antimicrobial Peptide LL-37 Promotes the Growth of the Pulmonary Pathogen Aspergillus fumigatus. Infect Immun. 2018;86(7).
269. Ballard E, Yucel R, Melchers WJG, Brown AJP, Verweij PE, Warris A. Antifungal Activity of Antimicrobial Peptides and Proteins against Aspergillus fumigatus. J Fungi (Basel). 2020;6(2).
270. Ostapska H, Howell PL, Sheppard DC. Deacetylated microbial biofilm exopolysaccharides: It pays to be positive. PLoS Pathog. 2018;14(12):e1007411.
271. Thomas M, Klibanov AM. Non-viral gene therapy: polycation-mediated DNA delivery. Appl Microbiol Biotechnol. 2003;62(1):27-34.
272. Fischer D, Li Y, Ahlemeyer B, Krieglstein J, Kissel T. In vitro cytotoxicity testing of polycations: influence of polymer structure on cell viability and hemolysis. Biomaterials. 2003;24(7):1121-31.
273. Hunter AC. Molecular hurdles in polyfectin design and mechanistic background to polycation induced cytotoxicity. Adv Drug Deliv Rev. 2006;58(14):1523-31.
274. Quinton PM, Philpott CW. A role for anionic sites in epithelial architecture. Effects of cationic polymers on cell membrane structure. J Cell Biol. 1973;56(3):787-96.

275. Monnery BD, Wright M, Cavill R, Hoogenboom R, Shaunak S, Steinke JHG, et al. Cytotoxicity of polycations: Relationship of molecular weight and the hydrolytic theory of the mechanism of toxicity. Int J Pharm. 2017;521(1-2):249-58.
276. Baciu M, Sebai SC, Ces O, Mulet X, Clarke JA, Shearman GC, et al. Degradative transport of cationic amphiphilic drugs across phospholipid bilayers. Philos Trans A Math Phys Eng Sci. 2006;364(1847):2597-614.
277. Khattak S, Wahid F, Liu LP, Jia SR, Chu LQ, Xie YY, et al. Applications of cellulose and chitin/chitosan derivatives and composites as antibacterial materials: current state and perspectives. Appl Microbiol Biotechnol. 2019;103(5):1989-2006.
278. Goy RC, Britto Dd, Assis OB. A review of the antimicrobial activity of chitosan. Polímeros. 2009;19:241-7.
279. Patel SKS, Kim JH, Kalia VC, Lee JK. Antimicrobial Activity of Amino-Derivatized Cationic Polysaccharides. Indian J Microbiol. 2019;59(1):96-9.
280. Chethan PD, Vishalakshi B, Sathish L, Ananda K, Poojary B. Preparation of substituted quaternized arylfuran chitosan derivatives and their antimicrobial activity. Int J Biol Macromol. 2013;59:158-64.
281. Jensen JW, Debusk RM, Debusk AG. Induction of cellular efflux by a galactosamine polymer from Neurospora crassa. J Gen Microbiol. 1984;130(3):557-65.
282. Glasgow JE, Reissig JL. Interaction of galactosaminoglycan with Neurospora conidia. J Bacteriol. 1974;120(2):759-66.
283. Vogt K, Bhabhra R, Rhodes JC, Askew DS. Doxycycline-regulated gene expression in the opportunistic fungal pathogen Aspergillus fumigatus. BMC Microbiol. 2005;5:1.
284. Meletiadis J, Meis JF, Mouton JW, Verweij PE. Analysis of growth characteristics of filamentous fungi in different nutrient media. J Clin Microbiol. 2001;39(2):478-84.
285. Hunter AC, Moghimi SM. Cationic carriers of genetic material and cell death: a mitochondrial tale. Biochim Biophys Acta. 2010;1797(6-7):1203-9.
286. Speth C, Rambach G, Lass-Flörl C, Howell PL, Sheppard DC. Galactosaminogalactan (GAG) and its multiple roles in Aspergillus pathogenesis. Virulence. 2019;10(1):976-83.
287. Brana C, Benham C, Sundstrom L. A method for characterising cell death in vitro by combining propidium iodide staining with immunohistochemistry. Brain research protocols. 2002;10(2):109-14.
288. Parhamifar L, Larsen AK, Hunter AC, Andresen TL, Moghimi SM. Polycation cytotoxicity: a delicate matter for nucleic acid therapy—focus on polyethylenimine. Soft Matter. 2010;6(17):4001-9.
289. Aichler M, Walch A. MALDI Imaging mass spectrometry: current frontiers and perspectives in pathology research and practice. Lab Invest. 2015;95(4):422-31.
290. Zheng Y, Gardner SE, Clarke MC. Cell death, damage-associated molecular patterns, and sterile inflammation in cardiovascular disease. Arterioscler Thromb Vasc Biol. 2011;31(12):2781-6.
291. Nixon GF. Sphingolipids in inflammation: pathological implications and potential therapeutic targets. Br J Pharmacol. 2009;158(4):982-93.
292. Gilbert AS, Wheeler RT, May RC. Fungal Pathogens: Survival and Replication within Macrophages. Cold Spring Harb Perspect Med. 2014;5(7):a019661.
293. Thywißen A, Heinekamp T, Dahse HM, Schmaler-Ripcke J, Nietzsche S, Zipfel PF, et al. Conidial Dihydroxynaphthalene Melanin of the Human Pathogenic Fungus Aspergillus fumigatus Interferes with the Host Endocytosis Pathway. Front Microbiol. 2011;2:96.
294. Min K, Ichikawa Y, Woolford CA, Mitchell AP. Candida albicans Gene Deletion with a Transient CRISPR-Cas9 System. mSphere. 2016;1(3).
295. Nødvig CS, Nielsen JB, Kogle ME, Mortensen UH. A CRISPR-Cas9 System for Genetic Engineering of Filamentous Fungi. PLoS One. 2015;10(7):e0133085.

296. Macheleidt J, Scherlach K, Neuwirth T, Schmidt-Heck W, Straßburger M, Spraker J, et al. Transcriptome analysis of cyclic AMP-dependent protein kinase A-regulated genes reveals the production of the novel natural compound fumipyrrole by Aspergillus fumigatus. Mol Microbiol. 2015;96(1):148-62.
297. da Silva Lira Filho A, Fajardo EF, Chang KP, Clément P, Olivier M. Leishmania Exosomes/Extracellular Vesicles Containing GP63 Are Essential for Enhance Cutaneous Leishmaniasis Development Upon Co-Inoculation of Leishmania amazonensis and Its Exosomes. Front Cell Infect Microbiol. 2021;11:709258.
298. Baker P, Whitfield GB, Hill PJ, Little DJ, Pestrak MJ, Robinson H, et al. Characterization of the Pseudomonas aeruginosa Glycoside Hydrolase PslG Reveals That Its Levels Are Critical for Psl Polysaccharide Biosynthesis and Biofilm Formation. J Biol Chem. 2015;290(47):28374-87.
299. Schindelin J, Arganda-Carreras I, Frise E, Kaynig V, Longair M, Pietzsch T, et al. Fiji: an open-source platform for biological-image analysis. Nat Methods. 2012;9(7):676-82.
300. Chen Y, Le Mauff F, Wang Y, Lu R, Sheppard DC, Lu L, et al. The Transcription Factor SomA Synchronously Regulates Biofilm Formation and Cell Wall Homeostasis in Aspergillus fumigatus. mBio. 2020;11(6).
301. Gish W, States DJ. Identification of protein coding regions by database similarity search. Nat Genet. 1993;3(3):266-72.
302. Lopes Bezerra LM, Filler SG. Interactions of Aspergillus fumigatus with endothelial cells: internalization, injury, and stimulation of tissue factor activity. Blood. 2004;103(6):2143-9.
303. Ceccarelli S, Visco V, Raffa S, Wakisaka N, Pagano JS, Torrisi MR. Epstein-Barr virus latent membrane protein 1 promotes concentration in multivesicular bodies of fibroblast growth factor 2 and its release through exosomes. Int J Cancer. 2007;121(7):1494-506.
304. Gastebois A, Fontaine T, Latgé JP, Mouyna I. beta(1-3)Glucanosyltransferase Gel4p is essential for Aspergillus fumigatus. Eukaryot Cell. 2010;9(8):1294-8.
305. Jain S, Ohman DE. Role of an alginate lyase for alginate transport in mucoid Pseudomonas aeruginosa. Infect Immun. 2005;73(10):6429-36.
306. Dueñas-Santero E, Martín-Cuadrado AB, Fontaine T, Latgé JP, del Rey F, Vázquez de Aldana C. Characterization of glycoside hydrolase family 5 proteins in Schizosaccharomyces pombe. Eukaryot Cell. 2010;9(11):1650-60.
307. De Medina-Redondo M, Arnáiz-Pita Y, Fontaine T, Del Rey F, Latgé JP, De Aldana CRV. The β-1, 3-glucanosyltransferase gas4p is essential for ascospore wall maturation and spore viability in Schizosaccharomyces pombe. Molecular microbiology. 2008;68(5):1283-99.
308. Little DJ, Pfoh R, Le Mauff F, Bamford NC, Notte C, Baker P, et al. PgaB orthologues contain a glycoside hydrolase domain that cleaves deacetylated poly-β(1,6)-N-acetylglucosamine and can disrupt bacterial biofilms. PLoS Pathog. 2018;14(4):e1006998.
309. Garcia-Rubio R, de Oliveira HC, Rivera J, Trevijano-Contador N. The Fungal Cell Wall: Candida, Cryptococcus, and Aspergillus Species. Front Microbiol. 2019;10:2993.
310. Jorge JA, de Almeida EM, de Lourdes Polizeli M, Terenzi HF. Changes in N-acetyl galactosaminoglycan deacetylase levels during growth of Neurospora crassa: effect of l-sorbose on enzyme production. Journal of Basic Microbiology: An International Journal on Biochemistry, Physiology, Genetics, Morphology, and Ecology of Microorganisms. 1999;39(5-6):337-44.
311. Ukuku DO, Geveke DJ, Cooke P, Zhang HQ. Membrane damage and viability loss of Escherichia coli K-12 in apple juice treated with radio frequency electric field. J Food Prot. 2008;71(4):684-90.
312. Perkins DD, Davis RH. Evidence for safety of Neurospora species for academic and commercial uses. Appl Environ Microbiol. 2000;66(12):5107-9.
313. Latgé JP. Tasting the fungal cell wall. Cell Microbiol. 2010;12(7):863-72.

314. Heinekamp T, Thywißen A, Macheleidt J, Keller S, Valiante V, Brakhage AA. Aspergillus fumigatus melanins: interference with the host endocytosis pathway and impact on virulence. Front Microbiol. 2012;3:440.
315. Kissing S, Hermsen C, Repnik U, Nesset CK, von Bargen K, Griffiths G, et al. Vacuolar ATPase in phagosome-lysosome fusion. J Biol Chem. 2015;290(22):14166-80.
316. Westman J, Walpole GFW, Kasper L, Xue BY, Elshafee O, Hube B, et al. Lysosome Fusion Maintains Phagosome Integrity during Fungal Infection. Cell Host Microbe. 2020;28(6):798-812.e6.
317. Seidel C, Moreno-Velásquez SD, Ben-Ghazzi N, Gago S, Read ND, Bowyer P. Phagolysosomal Survival Enables Non-lytic Hyphal Escape and Ramification Through Lung Epithelium During Aspergillus fumigatus Infection. Front Microbiol. 2020;11:1955.
318. Wasylnka JA, Moore MM. Aspergillus fumigatus conidia survive and germinate in acidic organelles of A549 epithelial cells. J Cell Sci. 2003;116(Pt 8):1579-87.
319. Chauhan N, Latge JP, Calderone R. Signalling and oxidant adaptation in Candida albicans and Aspergillus fumigatus. Nat Rev Microbiol. 2006;4(6):435-44.
320. Li X, Gao M, Han X, Tao S, Zheng D, Cheng Y, et al. Disruption of the phospholipase D gene attenuates the virulence of Aspergillus fumigatus. Infect Immun. 2012;80(1):429-40.
321. Heinekamp T, Schmidt H, Lapp K, Pähtz V, Shopova I, Köster-Eiserfunke N, et al. Interference of Aspergillus fumigatus with the immune response. Semin Immunopathol. 2015;37(2):141-52.
322. Croft CA, Culibrk L, Moore MM, Tebbutt SJ. Interactions of Aspergillus fumigatus Conidia with Airway Epithelial Cells: A Critical Review. Front Microbiol. 2016;7:472.
323. Cho YW, Kim JD, Park K. Polycation gene delivery systems: escape from endosomes to cytosol. J Pharm Pharmacol. 2003;55(6):721-34.
324. Tucker SC, Casadevall A. Replication of Cryptococcus neoformans in macrophages is accompanied by phagosomal permeabilization and accumulation of vesicles containing polysaccharide in the cytoplasm. Proc Natl Acad Sci U S A. 2002;99(5):3165-70.
325. Nimrichter L, Frases S, Cinelli LP, Viana NB, Nakouzi A, Travassos LR, et al. Self-aggregation of Cryptococcus neoformans capsular glucuronoxylomannan is dependent on divalent cations. Eukaryot Cell. 2007;6(8):1400-10.
326. Hillmann F, Novohradská S, Mattern DJ, Forberger T, Heinekamp T, Westermann M, et al. Virulence determinants of the human pathogenic fungus Aspergillus fumigatus protect against soil amoeba predation. Environ Microbiol. 2015;17(8):2858-69.
327. Cramton SE, Gerke C, Schnell NF, Nichols WW, Götz F. The intercellular adhesion (ica) locus is present in Staphylococcus aureus and is required for biofilm formation. Infect Immun. 1999;67(10):5427-33.
328. Wang X, Preston JF, 3rd, Romeo T. The pgaABCD locus of Escherichia coli promotes the synthesis of a polysaccharide adhesin required for biofilm formation. J Bacteriol. 2004;186(9):2724-34.
329. O'Gara JP. ica and beyond: biofilm mechanisms and regulation in Staphylococcus epidermidis and Staphylococcus aureus. FEMS microbiology letters. 2007;270(2):179-88.
330. Izano EA, Sadovskaya I, Vinogradov E, Mulks MH, Velliyagounder K, Ragunath C, et al. Poly-N-acetylglucosamine mediates biofilm formation and antibiotic resistance in Actinobacillus pleuropneumoniae. Microb Pathog. 2007;43(1):1-9.
331. Vuong C, Kocianova S, Voyich JM, Yao Y, Fischer ER, DeLeo FR, et al. A crucial role for exopolysaccharide modification in bacterial biofilm formation, immune evasion, and virulence. J Biol Chem. 2004;279(52):54881-6.
332. Rohde H, Frankenberger S, Zähringer U, Mack D. Structure, function and contribution of polysaccharide intercellular adhesin (PIA) to Staphylococcus epidermidis biofilm formation and pathogenesis of biomaterial-associated infections. Eur J Cell Biol. 2010;89(1):103-11.

333. Rohde H, Burandt EC, Siemssen N, Frommelt L, Burdelski C, Wurster S, et al. Polysaccharide intercellular adhesin or protein factors in biofilm accumulation of Staphylococcus epidermidis and Staphylococcus aureus isolated from prosthetic hip and knee joint infections. Biomaterials. 2007;28(9):1711-20.
334. Skurnik D, Cywes-Bentley C, Pier GB. The exceptionally broad-based potential of active and passive vaccination targeting the conserved microbial surface polysaccharide PNAG. Expert review of vaccines. 2016;15(8):1041-53.
335. Le Mauff F, Razvi E, Reichhardt C, Sivarajah P, Parsek MR, Howell PL, et al. The Pel polysaccharide is predominantly composed of a dimeric repeat of α-1,4 linked galactosamine and N-acetylgalactosamine. Commun Biol. 2022;5(1):502.
336. Little DJ, Poloczek J, Whitney JC, Robinson H, Nitz M, Howell PL. The structure- and metal-dependent activity of Escherichia coli PgaB provides insight into the partial de-N-acetylation of poly-β-1,6-N-acetyl-D-glucosamine. J Biol Chem. 2012;287(37):31126-37.
337. Colvin KM, Alnabelseya N, Baker P, Whitney JC, Howell PL, Parsek MR. PelA deacetylase activity is required for Pel polysaccharide synthesis in Pseudomonas aeruginosa. J Bacteriol. 2013;195(10):2329-39.